

APPENDIX C:

FLOOD SUSCEPTIBILITY MODEL BACK UP

- Extended analysis report
- 2018 Study Report
- 2018 Water Resources Research article

Flood Susceptibility Map of the Lower Connecticut River Valley Region: Extended Analysis

Introduction

In 2017 a flood mapping study was performed for the Lower Connecticut River Valley Region (LCRVR). Several methods were considered to estimate flood susceptibility. The final selected method involved a method called logistic regression, which is a statistical method that uses several variables (in our case flood risk factors) that allows the development of an equation to estimate the chance that a location will be inundated by a particular flood. The flood risk factors represent site characteristics that could potentially affect the region and for which sufficient data are available. Flood risk factors considered include elevation, slope, land curvature (concave, convex, or flat), distance to water body, land cover, vegetative density, surficial materials, soil drainage class, and percent impervious surface. The objective was to link each of the flood risk factors to the extent of a flood event that occurs once every 100 years. Due to the fact that the overall quality of recent satellite images, after flooding events, over the region was not sufficient for this analysis, it was decided to use the 100-year FEMA floodplain to estimate the extent of a typical 100-year flood.

The LCRVR in the initial phase of the study was not analyzed as one large region but was divided into three sub-regions (urban, rural, and coastal) to determine the differences in the contributions of each flood risk factor to flood susceptibility between an urban and a rural area and between inland vs. coastal areas; the expanded analysis discussed below assesses how the results change if the LCRVR is analyzed as one region. Flood risk factors within each sub-region in the original analysis were sampled at 4,000 randomly selected points from datasets having a 30-m resolution; the effect of using high-resolution datasets for the elevation and land cover flood risk factors is tested in the expanded analysis below. An equal number of these points were selected in locations that were within and outside of the FEMA 100-year floodplain for each sub-region. The data for each flood risk factor were selected from all locations using ArcGIS and associated with a '1' if the location was within the floodplain and a '0' otherwise. The resulting relationships between each flood risk factor and inundation due to a 100-year flood event were assessed by ingesting all sample data into a logistic regression. Logistic coefficients were obtained for each flood risk factor and used to develop an equation that estimates the chances of inundation. The magnitude of the coefficients indicates the relative strength of each flood risk factor's influence on flooding in a sub-region; positive coefficients mean that an increase in a particular flood risk factor increases flood susceptibility, while negative coefficients infer that an increase in a flood risk factor reduces flood susceptibility.

The overall results identified 'elevation' and 'distance to water' as having the most influence on flood susceptibility in the urban and coastal sub-regions, while 'distance to water' and 'surficial materials' dominate in the rural sub-region. The resulting equations for each sub-region were finally used to create an overall probability map of the LCRVR; no consideration was given to whether a particular flood risk factor was found to be significant when including it in the equation. Estimated probabilities were classified as either 0 – 20% ("very low risk"); 20 – 40% ("low risk"); 40 – 60% ("medium risk"); 60 – 80% ("high risk"); or 80 – 100% ("very high risk"). Several areas classified as "very high risk" and "high risk"

were found outside of the original FEMA 100-year floodplain and were found to contain various types of critical infrastructure previously thought to be safe from flooding due to a 100-year event.

The FEMA 100-year flood maps are limited to the sub-watersheds of greater than one square mile that FEMA chose to study with limited resources. Other limiting factors are the age of the underlying studies illustrated by the FEMA maps (often more than two decades old) and their focus on only areas where development existed or was imminently anticipated. FEMA's flood mapping is developed using physical models to perform hydrologic and hydraulic analysis of a statistical rainfall event with a one percent chance of being equaled or exceeded in any given year (referred to as the 100-year flood). In general terms, hydrologic analysis is the study of transforming rainfall amounts into quantity of runoff. Hydraulic analysis takes that quantity of water and uses a physical model to route it through existing terrain, while considering such factors as topography and vegetative density. This modeling is referred to as "detailed analysis." Some areas are studied by "approximate methods." In general, areas studied by approximate methods use a simplified hydrologic analysis methodology and route runoff quantity along best available topography alone.

The susceptibility maps from this study provided a less expensive method of covering all land area within the region. By using the statistical modeling methodology described in the associated report it was possible to identify the contribution of flood risk factors within the physically modeled FEMA 100-year floodplain and apply them to the entire study region to identify areas thought to be susceptible to flooding. As part of that study an ArcGIS map document file is available for the region's municipalities' future planning analysis containing the flood susceptibility, land use, and critical infrastructure datasets. An important disclaimer about the flood susceptibility map is that it was created for present-day conditions and is only to be used for planning purposes. It was not intended to replace the FEMA mapping for regulatory or flood insurance decisions.

Expanded Analysis

During the 2020 RiverCOG Hazard Mitigation Plan Update process, additional resources were provided to perform an expanded analysis to determine if certain changes in the flood mapping methodology would yield beneficial results for the final susceptibility mapping product. The expanded analysis documented here included the following steps:

1. Testing the significance of all flood risk factors to determine which, if any, should not be included in the final flood susceptibility model;
2. Perform one flood susceptibility analysis for the entire planning region and compare the results to the original sub-regional (urban, rural, and coastal) analyses;
3. Using higher-resolution elevation (LIDAR) data, assess any resulting changes in the contributions of all flood risk factors to flood susceptibility and the resulting flood susceptibility model; and
4. Using higher-resolution land cover data, assess any resulting change in the contributions of all flood risk factors to flood susceptibility and the resulting flood susceptibility model.

The technical results of the extended analysis are discussed below.

1. Testing the Significance of Flood Risk Factors

Previously all flood risk factors were included in the final flood susceptibility equation without considering whether they are significant or not. In order to explain the definition of significance, one needs to remember that when creating a flood model based on various flood risk factors, the model is based on any links that are found between each flood risk factor and locations of flooding. In essence, an attempt is made to correlate each flood risk factor with flooding in order to be able to predict where flooding can be expected. Flood risk factors that exhibit an apparently strong link with flooding will end up having very high (positive) or low (negative) coefficients in the model. The problem is that these apparent links may not be real; they may just have appeared at random due to the statistics used. For example, a correlation can almost be found between anything (e.g. taxes and the phase of the moon) if you search through the data long enough. For this reason, the reality (or significance) of the link between any flood risk factor and flood susceptibility needs to be estimated.

Significance is measured as the chance (we will refer to this as p) that the links between each flood risk factor and flooding is not real or essentially zero; such information is provided when performing the original logistic regression. If we look at the example of taxes and the phase of the moon, suppose that a very strong link is found in the data, but since there is no logical explanation for this, the significance of the link is tested and a value of $p = 0.99$ is found. This would mean that there is a 99% chance that the link is not real or that there is 1% chance that it is real. In order to say that a flood risk factor has a significant contribution, the value of p must be less than 0.05, which indicates a less than 5% chance that it does not (or a greater than 95% chance that it does) significantly impact flood susceptibility. The resulting values of p for all flood risk factors and sub-regions are shown in Table 1.1; any values there were found to be greater than 0.05 are highlighted in red.

Based on the results in Table 1.1, each flood risk factor for which p was greater than 0.05 has been eliminated from the appropriate sub-regional flood susceptibility analysis when developing the revised flood susceptibility map. For instance, the flood susceptibility model that is developed for the coastal sub-region (Column 1) now only considers the flood risk factors elevation (ELEV), slope (SLOPE), vegetative density (VEG), distance to water (DIST), soil drainage (SOIL), and surficial materials (GEO); land curvature (CURV), land cover (LAND), and percent impervious surface (IMP) were found to be insignificant and therefore were not included. The slightly revised coefficients for each significant flood risk factor and each sub-region are shown in Table A.1 of the Appendix.

Each revised sub-regional model was then used to construct a new flood susceptibility map for the entire LCRVR (Fig. 1.1). Due to the fact that the only difference between the current analysis and the analysis used in the 2017 study is the omission of flood risk factors that were found not to have a significant impact on flood extent, the current flood susceptibility map is very similar to the 2017 map. The major improvement is that the methodology used to create the current map is more defensible and thus the results are more robust.

Table 1.1: The probability (p) that the link identified between each flood risk factor and flood extent in the coastal, rural, and urban sub-regions is given. Values greater than 0.05 are highlighted in red.

Factor	Coastal	Rural	Urban
ELEV	0.00	0.00	0.00
CURV	0.55	0.00	0.00
SLOPE	0.00	0.00	0.00
VEG	0.00	0.00	0.08
LAND	0.08	0.00	0.00
DIST	0.00	0.00	0.00
SOIL	0.00	0.00	0.00
IMP	0.35	0.28	0.09
GEO	0.00	0.00	0.00

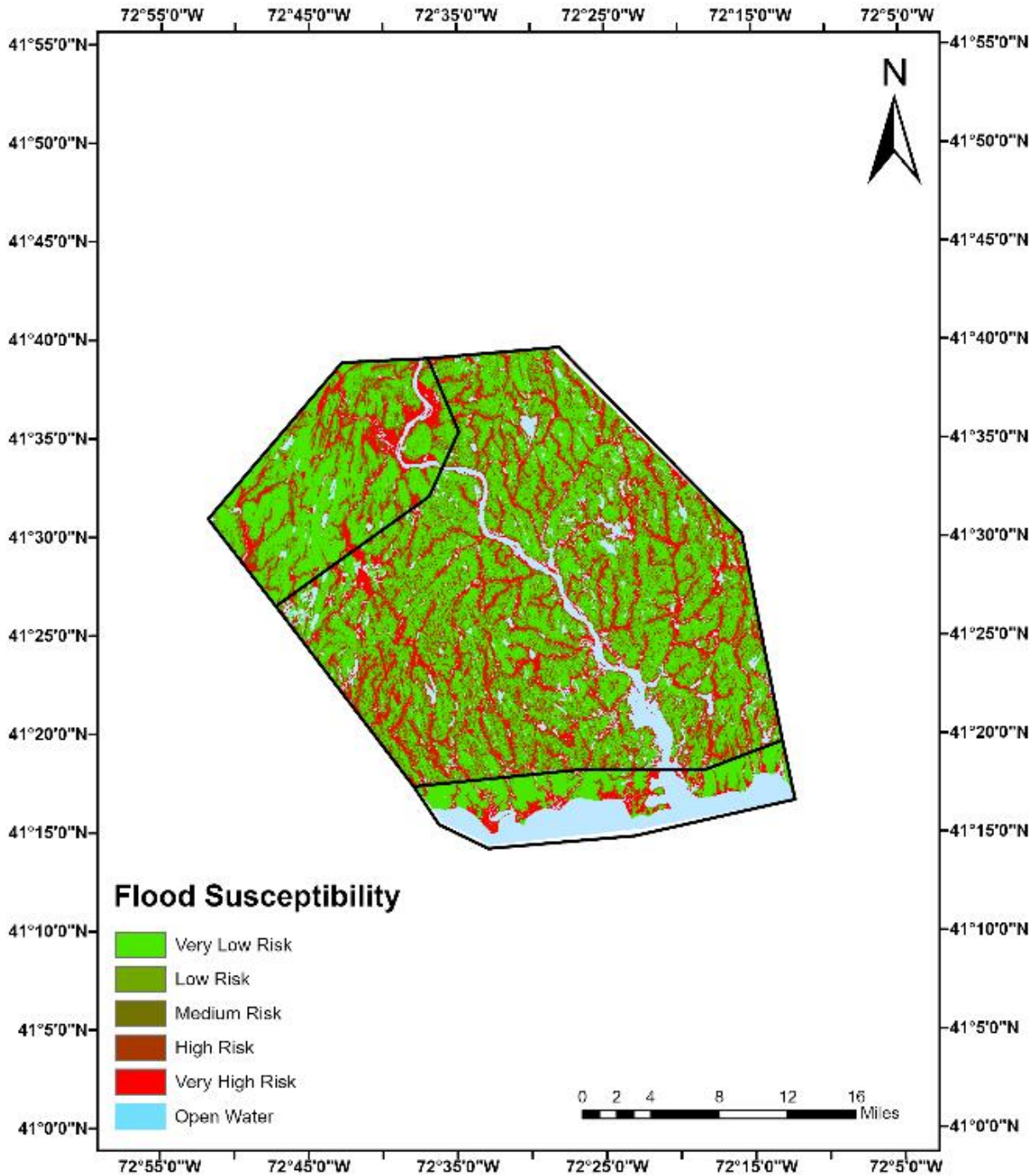


Figure 1.1: Flood susceptibility map of the LCRVR using separate flood models for the coastal, rural, and urban sub-regions. Insignificant flood risk factors as identified for each sub-region in red in Table 1.1 are omitted from the appropriate sub-region’s flood model. Flood susceptibility is classified as “very low risk” (0 – 20%), “low risk” (20 – 40%), “medium risk” (40 – 60%), “high risk” (60 – 80%), or “very high risk” (80 – 100%).

2. Regional vs. Sub-regional Analysis

The second task of this expanded analysis was to look at the effect of developing a flood susceptibility map based on an analysis of the LCRVR as a whole compared to the method used in the 2017 study, which was to develop separate flood susceptibility maps for three sub-regions (e.g. urban, coastal, and rural) within the LCRVR and then combine them to create one regional map. The reasoning for creating separate sub-regional models was to prevent flood risk factors that have a strong impact, for example, on flooding in the urban setting of Middletown, from having an influence on rural and coastal portions of the flood susceptibility map and likewise for the other sub-regions. There was also a desire to compare the flood risk factors that are most important to consider for an urban vs. rural setting, which may provide clues on the impact of urbanization on the mechanisms responsible for increased flood risk. The issue with combining the three sub-regional maps into one map is that unrealistic artifacts appeared at the boundaries of the sub-regions. Also the range of values displayed throughout the various sub-regions varied as can be seen in Fig. 1.1 above: the rural sub-region has much more widespread areas of dark green that indicate “low” risk whereas the coastal and urban sub-regions are more heavily dominated by bright green areas of “very low” risk; also there is no smooth transition between sub-regions.

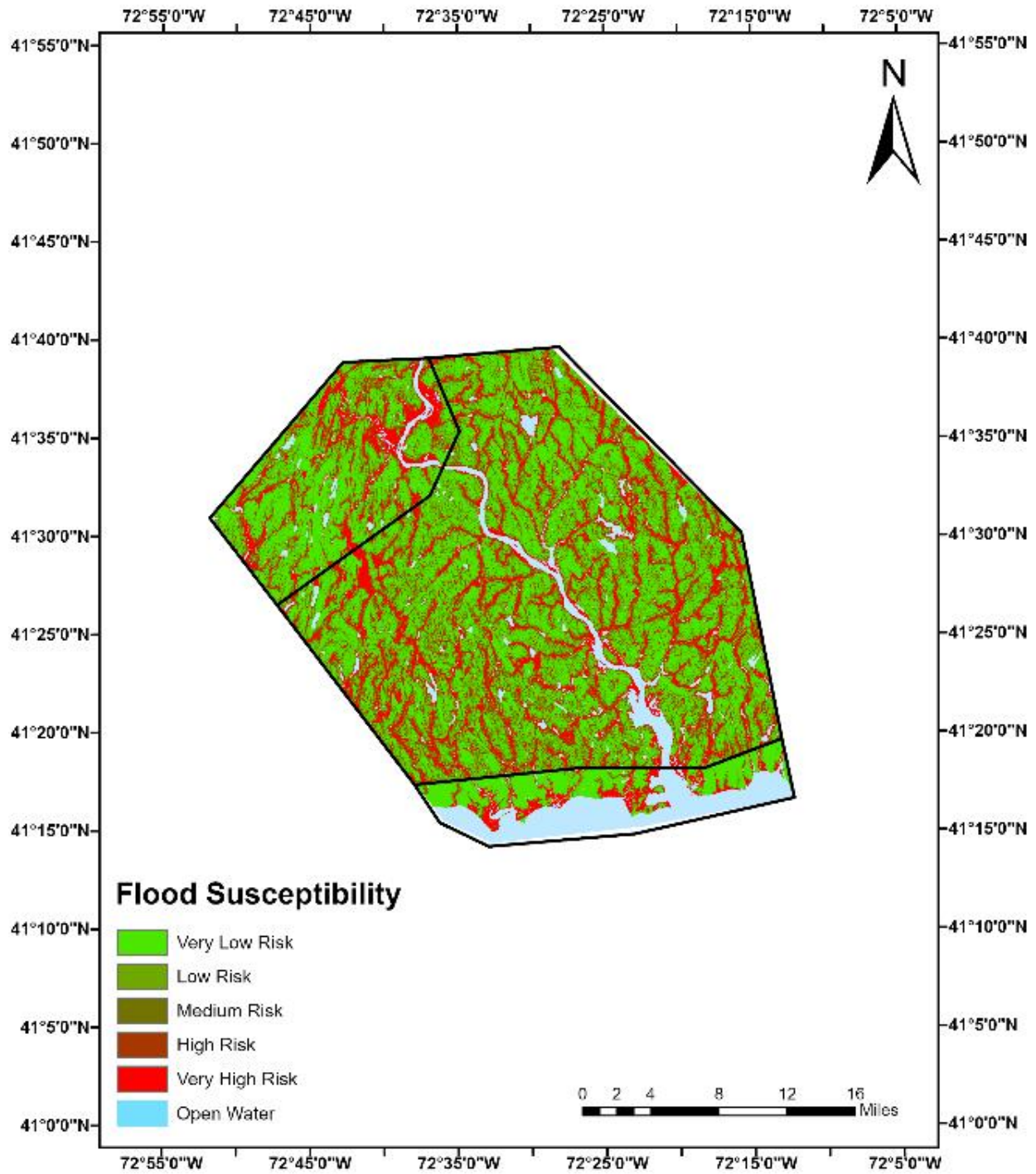
Based on the reasoning above, it was decided to create one flood susceptibility model for the entire LCRVR and then compare the resulting coefficients for each flood risk factor and the resulting flood susceptibility maps between the current analysis and the 2017 study results. In order to compare the results, the first step was to compute the average of the coefficients for each flood risk factor. It should be noted again, that in the original study each flood risk factor was divided into up to 10 classes or categories. For instance, elevation was split into 10 classes that were based on all elevation values throughout the LCRVR; classes were defined so that an equal number of values was included in each class. Therefore, when creating the flood model each elevation measurement is assigned a number between 1 to 10 depending on its raw value. Logistic coefficients are then estimated for each class; therefore, elevation would have ten coefficients, one for each class. These coefficients are then averaged and compared to the average value from the 2017 study as a percent change. The results of this comparison are shown in Table 2.1. Significant differences can be observed in the contributions of each flood risk factor to flooding, particularly regarding the land curvature (CURV), vegetative density (VEG), and soil drainage (SOIL) flood risk factors. Much of this change is again due to the fact that we created one model that takes into account the relationships between flooding and the flood risk factors throughout the entire LCRVR instead of limited the analysis to the smaller sub-regions.

Figure 2.1 compares the original flood susceptibility map from the 2017 study (Fig. 2.1a) and the revised flood susceptibility map when using the updated coefficients (essentially the updated logistic model) described above (Fig. 2.1b). The major change observed is that the previously described issue regarding the lack of smooth transitions between sub-regions (Fig. 2.1a) has been resolved, resulting in a much more realistic map (Fig. 2.1b). Also, flood susceptibility values in Fig. 2.1b overall seem to be less throughout the study region with the “very high” risk areas within Middletown and along the coast reduced in size. This is likely due to the fact that the regional model includes the rural sub-region, which is much larger than the other sub-regions and was found in 2017 to have substantially lower flood susceptibility overall compared to the other sub-regions; this will inevitably have an impact on the flood

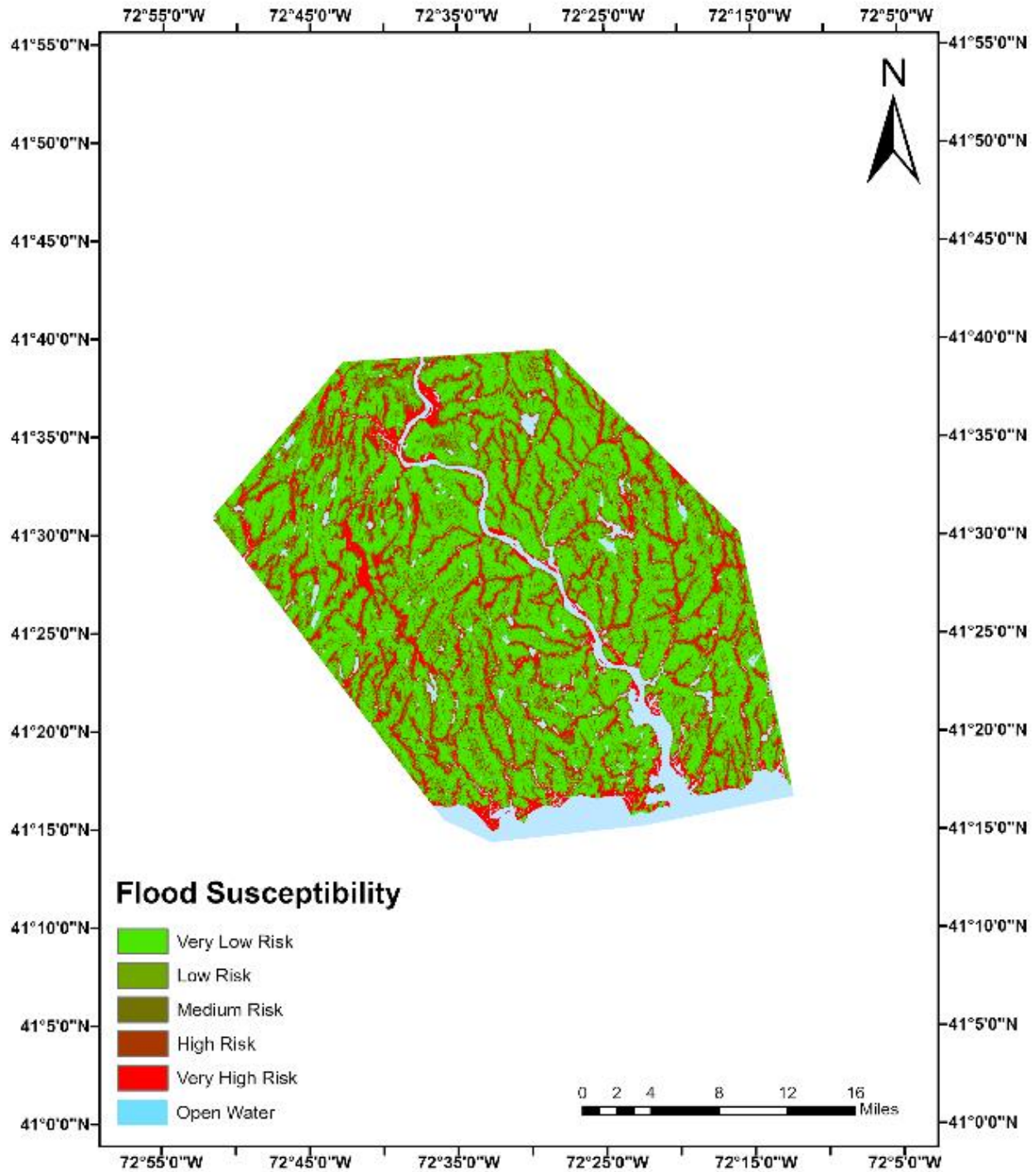
susceptibility values in what were previously the urban and coastal sub-regions and thus cause a reduction in the size of areas of “very high” flood risk.

Table 2.1: Differences between the average values of the regional flood risk factor coefficients computed in the current study and the sub-regional coefficients computed in the 2017 study.

Factor	Coastal	Rural	Urban
ELEV	77%	-54%	80%
CURV	437%	27%	-237%
SLOPE	-15%	-10%	38%
VEG	98%	118%	104%
LAND	-193%	74%	93%
DIST	50%	18%	-6%
SOIL	244%	151%	57%
IMP	-34%	40%	29%
GEO	69%	63%	-15%



(a)



(b)

Figure 2.1: Flood susceptibility maps from (a) the original 2017 study using separate flood models for each sub-region and (b) the current study using one flood model for the entire LCRVR. Flood susceptibility is classified as “very low risk” (0 – 20%), “low risk” (20 – 40%), “medium risk” (40 – 60%), “high risk” (60 – 80%), or “very high risk” (80 – 100%).

3. High-Resolution LIDAR Data

Task 3 of the expanded analysis involved incorporating the higher-resolution elevation (LIDAR) data into the flood susceptibility model and assessing any resulting changes in the contribution of each flood risk factor to flood susceptibility and the resulting flood susceptibility map. The 2017 flood susceptibility map utilized a lower-resolution 30-meter Digital Elevation Model (DEM) dataset to estimate the values of the elevation (ELEV), slope (SLOPE), and land curvature (CURV) flood risk factors at each point (or cell) throughout the LCRVR. The expanded analysis study tested the effect of using the higher-resolution 1-meter LIDAR data on the resulting contribution of each flood risk factor to flood susceptibility and on the revised flood susceptibility map. The specific dataset used was the 1-m Connecticut Statewide LiDAR DEM with 1.2cm point spacing, which was downloaded from the National Oceanic and Atmospheric Administration (NOAA), National Ocean Service (NOS, Office for Coastal Management (OCM), website. After incorporating the higher-resolution data, the updated contributions (or coefficients; shown in Table A.2 of the Appendix for the entire region (A) and for the coastal (C), rural (R), and urban (U) sub-regions) for each flood risk factor were averaged for each sub-region (similar to what was done in Section 2 above) and compared to the results of the 2017 study in terms of percent change (see Table 3.1). It can be seen that the higher resolution data has a substantial impact on almost all flood risk factors (excluding DIST), with maximum change observed in the coefficients for the CURV and SLOPE flood risk factors. The reason for these changes stems from the fact that the 1-m LIDAR data used to extract the ELEV, SLOPE, and CURV flood risk factor values and to estimate the resulting contributions of all flood risk factors to flood susceptibility is much more accurate than the previous 30-m DEM.

Figure 3.1 shows the resulting flood susceptibility map when using the 1-m LIDAR dataset to estimate the ELEV, SLOPE, and CURV flood risk factors. Since the current comparison still uses the sub-regional flood models (as opposed to the single regional model used above in Section 2), the artifact between sub-regions is still observed, especially between the rural and coastal sub-regions in the southern portion of the map. Even though the 1-m LIDAR dataset is much more accurate than the previously used 30-m DEM, the resulting flood susceptibility map in Fig. 3.1 is very similar to the original 2017 map (refer to Fig. 2.1a) except that the extent of areas of “very high” risk (bright red) are slightly reduced, especially within the vicinity of Middletown and along the coast, and that areas with “very low” risk (bright green) are more homogeneous.

Table 3.1: Differences between the average values of the sub-regional flood risk factor coefficients computed in the current study using the 1-m LIDAR dataset and the sub-regional coefficients computed in the 2017 study using the 30-m DEM dataset.

Factor	Coastal	Rural	Urban
ELEV	12%	39%	1%
CURV	131%	111%	91%
IMP	67%	188%	14%
DIST	5%	4%	3%
VEG	107%	28%	85%
LAND	3194%	56%	49%
GEO	122%	10%	17%
SOIL	53%	138%	23%
SLOPE	421%	1217%	432%

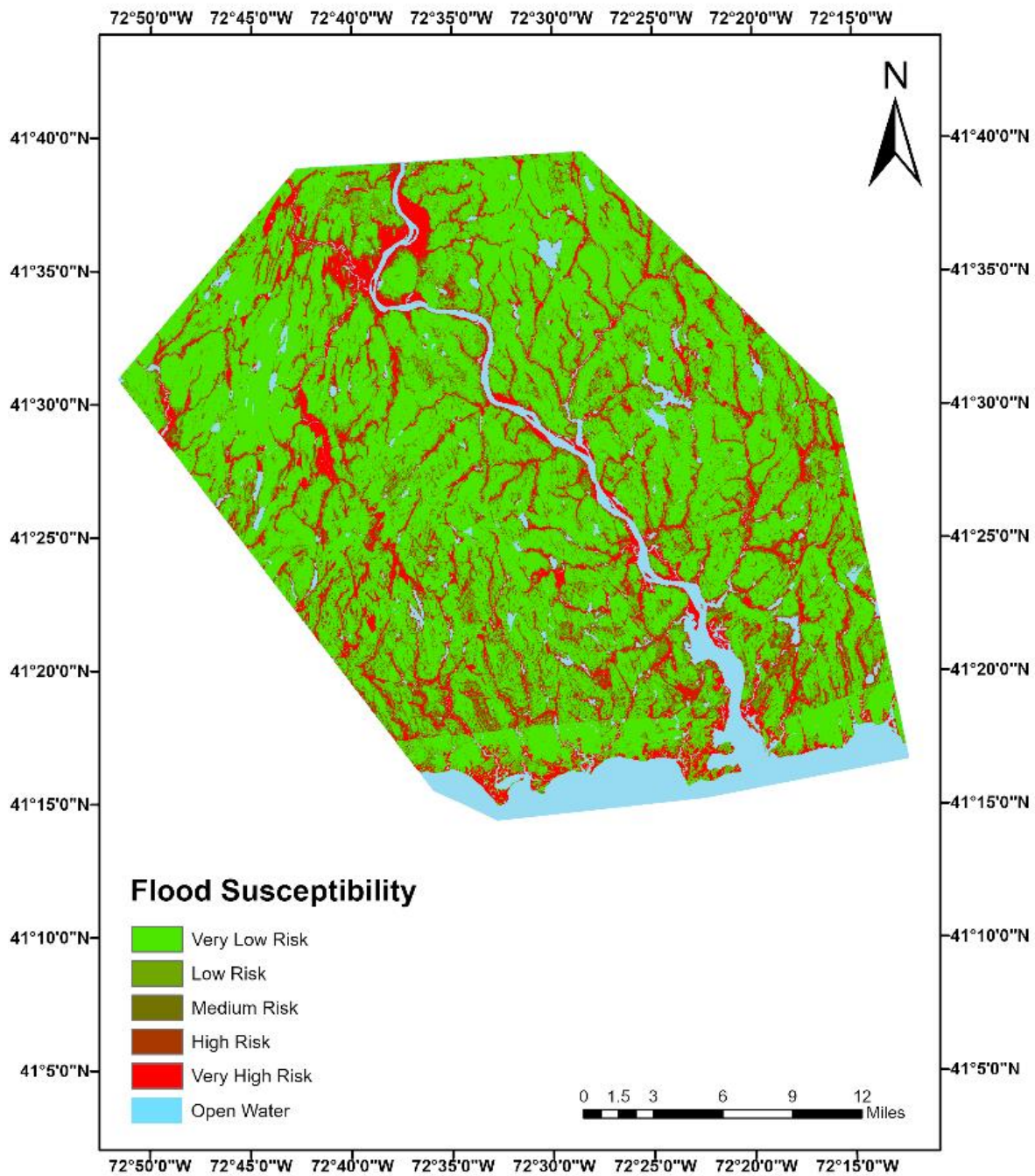


Figure 3.1: Flood susceptibility map using separate logistic models for the coastal, rural, and urban sub-regions and the higher-resolution 1-m LIDAR data. Flood susceptibility is classified as “very low risk” (0 – 20%), “low risk” (20 – 40%), “medium risk” (40 – 60%), “high risk” (60 – 80%), or “very high risk” (80 – 100%).

4. High-Resolution Land Cover Data

The next task involved incorporating higher-resolution land cover data into the flood susceptibility model and assessing any resulting changes in the contribution of each flood risk factor to flood susceptibility and the resulting flood susceptibility map. The 2017 flood susceptibility map utilized the lower-resolution 30-m National Land Cover Dataset (NLCD) to estimate the values of the land cover (LAND) flood risk factor at each point (or cell) throughout the LCRVR. The current study tested the effect of using higher-resolution 1-m land cover data on the resulting contribution of each flood risk factor to flood susceptibility and on the revised flood susceptibility map. The 1-m NOAA Land Cover data is based on data collected by The NOAA Office for Coastal Management Coastal Change Analysis Program (C-CAP), which is a contributing member of the Multi-Resolution Land Characteristics consortium; C-CAP products are included as the coastal expression of land cover within the National Land Cover Database. The classes within which the data are categorized are slightly different between the original 30-m NLCD and the 1-m NOAA datasets; the categories of both datasets that are included in the classes used in the current analysis are listed in Table A.3 of the Appendix. After incorporating the higher-resolution data, the updated contributions (or coefficients) for each flood risk factor were averaged for each sub-region (similar to what was done in Section 2 above) and compared to the results of the 2017 study in terms of percent change (see Table 4.1). It can be seen that the higher resolution data has a substantial impact on all flood risk factors, with maximum change observed in the coefficients for the LAND flood risk factor. In fact, the observed changes overall were greater than those observed when using the high-resolution elevation data in Section 3. The reason for these changes again stems from the fact that the 1-m dataset used to extract the LAND flood risk factor values and to estimate the resulting contributions of all flood risk factors to flood susceptibility is much more accurate than the previous 30-m dataset.

Figure 4.1 shows the resulting flood susceptibility map when using the 1-m land cover dataset to estimate the LAND flood risk factor. Since the current comparison again uses the sub-regional flood models (as opposed to the single regional model used above in Section 2), the artifact between sub-regions is still observed, especially between the rural and coastal sub-regions in the southern portion of the map. Even though the 1-m land cover dataset is much more accurate than the previously used 30-m NLCD, the resulting flood susceptibility map in Fig. 4.1 is similar to the original 2017 map (refer to Fig. 2.1a) except that, similar to what was observed in Section 3, the extent of areas of “very high” risk (bright red) are slightly reduced, especially within the vicinity of Middletown and along the coast, and that areas with “very low” risk (bright green) are more homogeneous.

Table 4.1: Differences between the average values of the sub-regional flood risk factor coefficients computed in the current study using the 1-m land cover dataset and the sub-regional coefficients computed in the 2017 study using land cover data from the 30-m NLCD.

Factor	All	Coastal	Rural	Urban
ELEV	37%	9%	81%	22%
CURV	464%	6649%	149%	61%
IMP	67%	698%	690%	114%
DIST	31%	69%	39%	22%
VEG	102%	72%	92%	164%
LAND	124%	2901%	186%	451%
GEO	32%	186%	129%	29%
SOIL	43%	265%	148%	92%
SLOPE	66%	199%	136%	379%

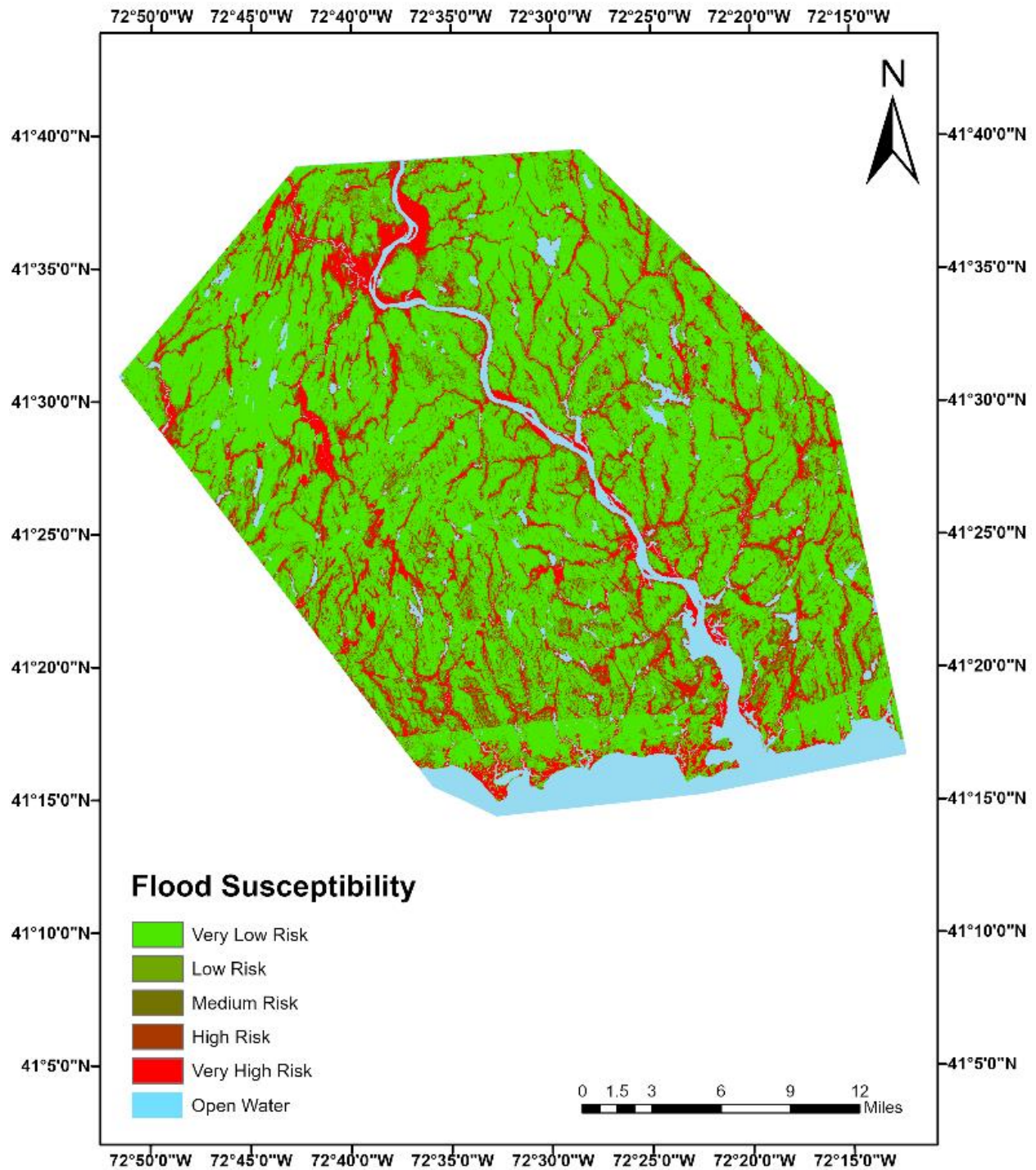


Figure 4.1: Flood susceptibility map using separate logistic models for the coastal, rural, and urban sub-regions and the higher-resolution 1-m NOAA land cover data. Flood susceptibility is classified as “very low risk” (0 – 20%), “low risk” (20 – 40%), “medium risk” (40 – 60%), “high risk” (60 – 80%), or “very high risk” (80 – 100%).

Final Analysis and Overall Conclusions

The final analysis that was performed incorporates all of the changes that were tested in the previous four sections: 1) omitting flood risk factors found to be insignificant, 2) developing one flood model for the entire region, and utilizing the high-resolution 3) elevation and 4) land use datasets. The resulting logistic coefficients for each flood risk factor class are provided in Table 5.1. It was interesting that after incorporating all the updates mentioned above, all flood risk factors were found to be significant and thus were retained in the final flood model. The resulting final flood susceptibility map is shown in Fig. 5.1. The major difference when compared to the original flood susceptibility map is that a much larger percentage of the region is either identified “very low” (bright green) or “very high” (bright red) flood risk with very limited areas in between. The overall extent of “very high” flood risk has also been reduced.

The reduction in the size of the area of “very high,” as well as “medium” and “high” flood susceptibility compared to the original 2017 study, can also be seen in Fig. 5.2. Figure 5.2a compares the FEMA flood zone (hatched area) with the results of the 2017 study by overlaying the layer of “medium” to “very high” susceptibility in order to identify “very high” risk areas located outside of the FEMA flood zone; the opposite is done in the second map of Fig. 5.2a in order to identify areas where the FEMA flood zone extends outside of the areas identified as “very high” risk in the 2017 study. Figure 5.2b shows the same comparison for the current study that incorporates the high-resolution data layers and the regional analysis. It can be seen that the areas of “very high” risk (bright red) lying outside of the FEMA flood zone (hatched area) are reduced with fewer critical infrastructure being located within these areas. Also, whereas there was a negligible portion of the FEMA flood zone lying outside of the areas of “very high” risk in the 2017 study, there are now such areas, although small, located northwest of Middletown and within Middletown near the river. These results demonstrate that the higher resolution data and the size of the study area (regional vs. sub-regional) that is analyzed do have an impact on the extent of the area identified as having a “very high” flood risk and the particular critical infrastructure located therein.

Based on this extended analysis the flood susceptibility map using the analysis of the entire region, combined with the higher resolution elevation and land cover data is recommended for future field verification and planning activities.

Table 5.1: Regression coefficients for each class of each flood risk factor for regional flood model using the higher resolution 1-m LIDAR data for the ELEV, CURV, and SLOPE flood risk factors and the higher resolution 1-m land use data for the LAND flood risk factor.

Factor	Class	Logistic Coefficient	Factor	Class	Logistic Coefficient
ao	--	7.66	DIST (m)	0.00 – 39.21	--
ELEV (m)	-2.65 – 2.88	--		39.22 – 117.64	-1.33
	2.89 – 20.58	-5.04		117.65 – 235.27	-2.13
	20.59 – 39.39	-5.36		235.28 – 352.91	-2.36
	39.40 – 55.98	-5.59		352.92 – 470.54	-2.63
	55.99 – 74.78	-5.51		470.55 – 588.18	-2.84
	74.79 – 92.48	-4.99		588.19 – 745.02	-2.94
	92.49 – 109.07	-5.63		745.03 – 980.29	-2.49
	109.08 – 127.88	-5.14		980.30 – 2352.71	-2.39
	127.89 – 152.21	-5.61		>= 2352.72	0.56
	>= 152.22	-6.03	SOIL	not rated	--
CURV	<= -0.66	--		excessively drained	-0.87
	-0.65 – 0.65	-0.51		somewhat excessively	-0.52
	>= 0.66	-0.11		well drained	-0.86
SLOPE	0.00 – 0.00	--		moderately well	-0.45
	0.01 – 0.35	-0.65		somewhat poorly	0.87
	0.36 – 0.69	-0.92		poorly drained	0.25
	0.70 – 1.04	-0.87		very poorly drained	0.20
	1.05 – 1.73	-1.18	IMP (%)	0.00 – 0.00	--
	1.74 – 2.43	-1.15		0.01 – 1.96	-0.64
	2.44 – 3.12	-1.02		1.97 – 4.71	-0.34
	3.13 – 4.16	-1.26		4.72 – 10.98	-0.20
	4.17 – 5.89	-1.42		10.99 – 18.82	-0.52
	>= 5.90	-1.17		18.83 – 28.62	-0.35
VEG (%)	0.00 – 0.00	--		28.63 – 38.82	-0.22
	0.01 – 31.73	-0.05		38.83 – 49.80	-0.37
	31.74 – 54.71	-0.18		49.81 – 63.92	-0.61
	54.72 – 69.66	-0.31		63.93 – 100.00	-0.56
	69.67 – 79.87	-0.25	GEO	thin till	--
	79.88 – 85.71	-0.26		sand/ gravel/talus	1.22
	85.72 – 87.89	-0.18		finer	2.68
	87.90 – 88.99	-0.58		floodplain alluvium	3.66
	89.00 – 89.72	-0.72		swamp deposits	1.62
	89.73 – 93.00	-0.73		thick till	-0.47
LAND	developed, open space	--		End Moraine deposits	-0.01
	impervious	-0.13		artificial fill	3.17
	unconsolidated shore	0.01		salt/tidal marsh deposits	1.99
	bare land	-0.17		beach deposits	3.97
	mixed forest	0.18			
	scrub/shrub	0.22			
	grassland	0.27			
	pasture/hay	-0.05			
	cultivated land	0.27			
	wetlands (woody/emer.)	1.00			

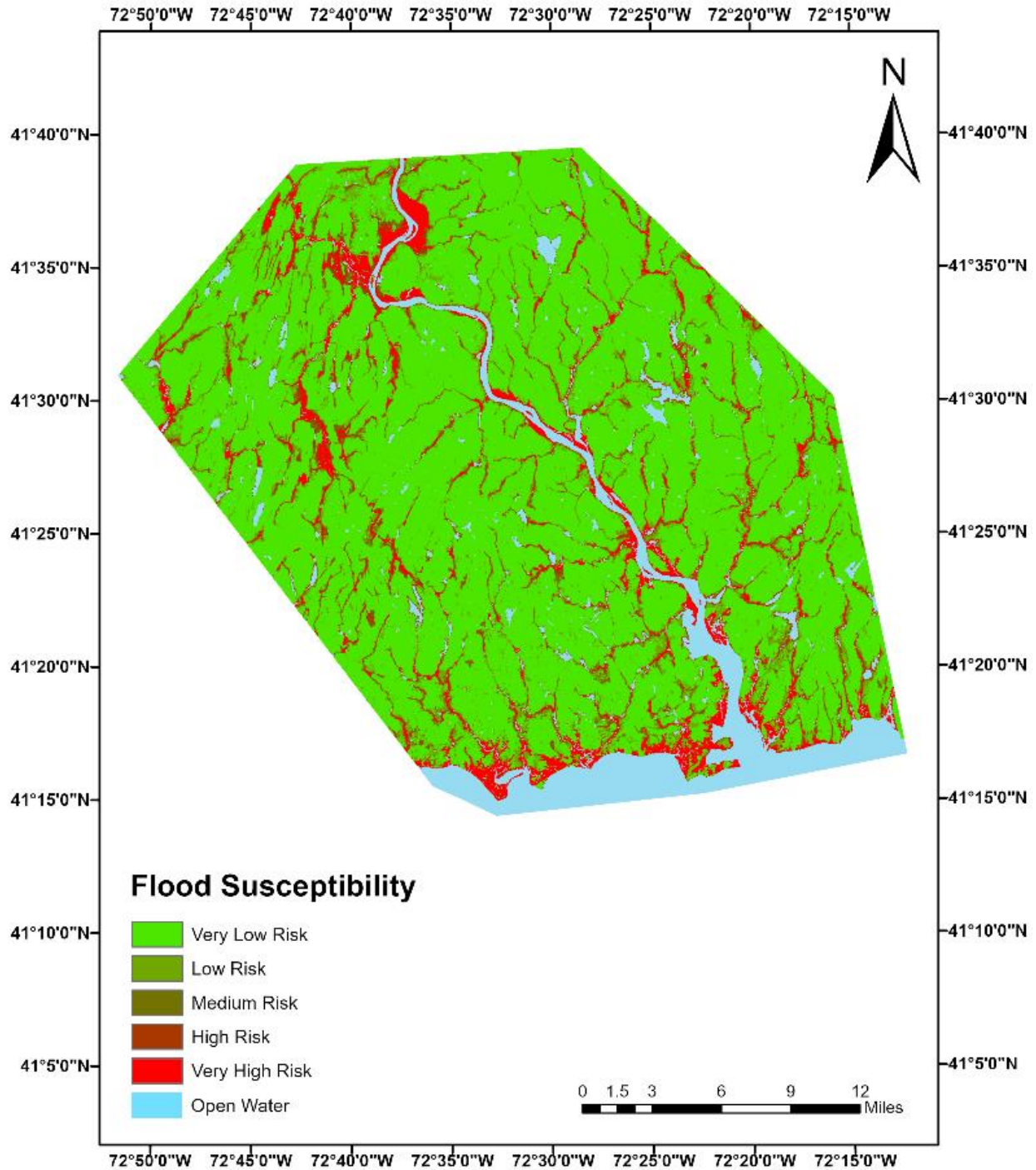
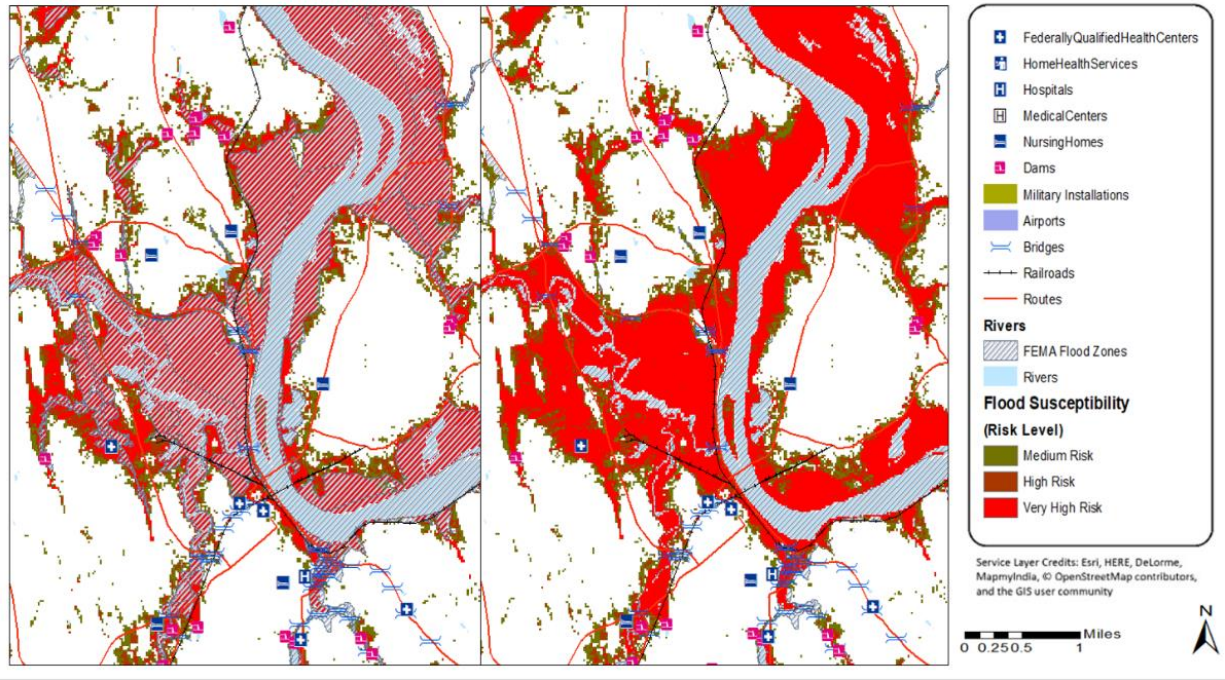
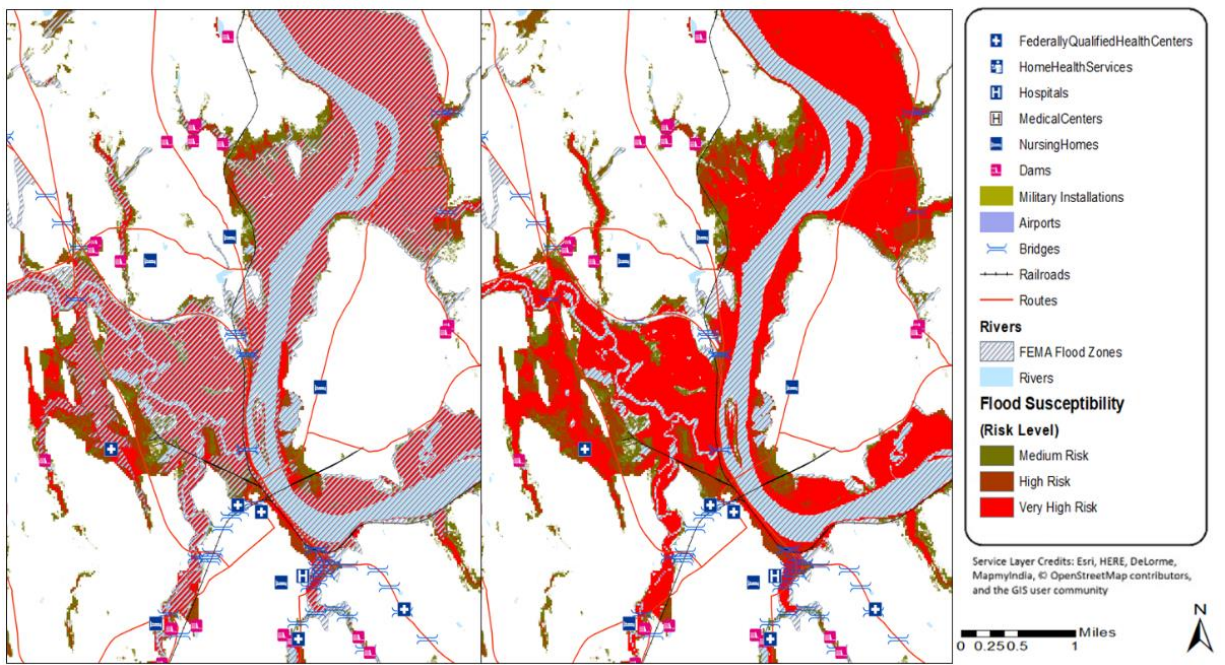


Figure 5.1: Flood susceptibility map that results when using one flood model for the entire LCRVR and that incorporates the higher-resolution 1-m elevation and land cover datasets. Flood susceptibility is classified as “very low risk” (0 – 20%), “low risk” (20 – 40%), “medium risk” (40 – 60%), “high risk” (60 – 80%), or “very high risk” (80 – 100%).



(a)



(b)

Figure 5.2: Comparison between areas identified as “medium” to “very high” flood susceptibility (dark green to red) and the FEMA Flood Zones (hatched) for (a) the original 2017 study and (b) the current study. Maps in each figure overlay either the flood susceptibility results on top of the FEMA flood zone or vice versa. Locations of various critical infrastructure are also shown. Flood susceptibility is classified as “medium risk” (40 – 60%), “high risk” (60 – 80%), or “very high risk” (80 – 100%).

Appendix

Table A.1: Logistic coefficients for each class of each flood risk factor for all sub-regions (C = coastal sub-region; R = rural sub-region; U = urban sub-region). NS indicates that the link between a particular flood risk factor and flood extent in a particular sub-region was found to be insignificant (refer to Table 1.1).

Factor	Class	Logistic Coefficient (A/C/R/U)	Factor	Class	Logistic Coefficient (A/C/R/U)
a₀	--	4.71/4.75/20.02	DIST (m)	0.00 – 39.21	--/--/--
ELEV (m)	-2.65 – 2.84	--/--/--		39.22 – 117.64	-1.22/-2.14/-1.58
	2.85 – 20.42	-4.08/-2.09/-15.08		117.65 – 196.06	-2.06/-3.29/-2.63
	20.43 – 40.19	-20.45/-1.65/-15.93		196.07 – 274.48	-2.96/-3.61/-2.59
	40.20 – 56.67	-18.83/-1.58/-16.45		274.49 – 392.12	-3.04/-3.96/-3.18
	56.68 – 75.35	--/-1.36/-16.56		392.13 – 509.75	-4.61/-4.72/-3.50
	75.36 – 92.93	--/-1.50/-16.77		509.76 – 627.39	-4.45/-4.99/-3.80
	92.94 – 109.40	--/-2.18/-17.39		627.40 – 784.24	-5.56/-4.85/-3.99
	109.41 – 128.08	--/-2.46/-18.42		784.25 – 1,019.51	-19.64/-4.55/-3.83
	128.09 – 152.25	--/-2.78/-17.88		1,019.52 – 2,352.71	-16.64/-3.91/-2.65
	152.26 – 277.50	--/-3.60/-18.15			
CURV	Convex (-6.05 – -0.66)	--/--/--	SOIL	not rated	--/--/--
	Flat (-0.65 – 0.65)	NS/0.08/-0.41		excessively drained	0.17/0.03/-1.96
	Concave (0.66 – 6.05)	NS/1.82/1.06		somewhat excessively	0.26/-0.63/-1.37
SLOPE	0.00 – 0.47	--/--/--		well drained	0.25/-0.04/-1.23
	0.48 – 1.89	-0.20/-0.04/0.03		moderately well	0.44/0.62/-1.11
	1.90 – 3.31	-0.01/0.09/-0.29		somewhat poorly	--/2.51/0.63
	3.32 – 4.73	-0.33/-0.53/-0.60		poorly drained	1.44/1.39/-0.33
	4.74 – 6.62	-0.86/-0.51/-0.90	IMP (%)	very poorly drained	1.07/0.95/1.02
	6.63 – 8.52	-1.15/-0.84/-1.12		0.00 – 0.00	--/--/--
	8.53 – 10.88	-0.79/-0.73/-1.11		0.01 – 1.96	NS/NS/NS
	10.89 – 14.20	-0.91/-1.31/-2.28		1.97 – 4.70	NS/NS/NS
	14.21 – 19.40	-1.36/-1.07/-1.83		4.71 – 10.98	NS/NS/NS
	19.41 – 120.72	-0.74/-1.92/-2.07		10.99 – 18.82	NS/NS/NS
VEG (%)	0.00 – 0.00	--/--/--		18.83 – 28.62	NS/NS/NS
	0.01 – 32.00	-0.25/0.14/NS		28.63 – 38.82	NS/NS/NS
	32.01 – 55.00	-0.37/-0.29/NS		38.83 – 49.80	NS/NS/NS
	55.01 – 70.00	0.02/0.27/NS		49.81 – 63.92	NS/NS/NS
	70.01 – 80.00	-1.08/0.44/NS	GEO	63.93 – 99.61	NS/NS/NS
	80.01 – 86.00	-0.36/0.49/NS		thin till	--/--/--
	86.01 – 88.00	-1.58/0.35/NS		sand/ gravel/talus	0.90/0.88/0.80
	88.01 – 89.00	-0.95/-0.37/NS		finer	--/1.79/1.03
	89.01 – 90.00	-1.37/-0.19/NS		floodplain alluvium	16.56/3.05/2.89
	90.01 – 93.00	-1.73/-0.33/NS		swamp deposits	-0.12/1.30/1.47
LAND	developed, open space	--/--/--		thick till	-0.68/-1.99/-0.73
	dev., low intensity	NS/-0.08/-0.48		End Moraine deposits	0.10/-1.79/--
	dev., med.-high intensity	NS/-0.07/-0.91		artificial fill	17.50/14.83/1.93
	barren (rock/sand/clay)	NS/-1.09/-16.60		salt/tidal marsh deposits	1.37/13.53/--
	forest	NS/-0.40/-0.46		beach deposits	2.56/--/--
	shrub/scrub	NS/-1.43/-0.84			
	grassland/herbaceous	NS/-0.57/-0.56			
	pasture/hay	NS/-0.98/-0.29			
	cultivated crops	NS/-0.20/-0.85			
	wetlands (woody/emerg.)	NS/0.61/0.41			

Table A.2: Regression coefficients for each flood risk factor class and each sub-region (C = coastal sub-region; R = rural sub-region; U = urban sub-region) using the higher resolution 1-m LIDAR data for the ELEV, CURV, and SLOPE flood risk factors.

Factor	Class	Logistic Coefficient (C/R/U)	Factor	Class	Logistic Coefficient (C/R/U)
ao	--	5.20/5.35/19.07	DIST (m)	0.00 – 39.21	--/--/--
ELEV (m)	-2.65 – 2.84	--/--/--		39.22 – 117.64	-1.06/-2.08/-1.72
	2.85 – 20.42	-5.20/-2.93/-14.80		117.65 – 196.06	-1.84/-3.23/-2.63
	20.43 – 40.19	-21.27/-2.53/-15.64		196.07 – 274.48	-2.55/-3.58/-2.66
	40.20 – 56.67	-20.19/-2.38/-16.13		274.49 – 392.12	-2.75/-3.82/-3.33
	56.68 – 75.35	--/-2.28/-16.34		392.13 – 509.75	-4.44/-4.54/-3.64
	75.36 – 92.93	--/-2.33/-16.52		509.76 – 627.39	-4.09/-4.80/-3.92
	92.94 – 109.40	--/-3.03/-17.29		627.40 – 784.24	-5.57/-4.62/-4.17
	109.41 – 128.08	--/-3.32/-17.85		784.25 – 1,019.51	-19.24/-4.38/-3.85
	128.09 – 152.25	--/-3.69/-17.42		1,019.52 – 2,352.71	-15.91/-3.76/-2.75
	152.26 – 277.50	--/-4.38/-18.29			
CURV	Convex (-6.05 – -0.66)	--/--/--	SOIL	not rated	--/--/--
	Flat (-0.65 – 0.65)	-0.06/0.20/-0.15		excessively drained	-0.23/-0.09/-2.11
	Concave (0.66 – 6.05)	0.14/-0.00/-0.10		somewhat excessively well drained	-0.06/-0.71/-1.31
SLOPE	0.00 – 0.47	--/--/--		moderately well	0.04/0.62/-1.26
	0.48 – 1.89	-0.06/-0.37/-0.10		somewhat poorly	--/2.54/0.60
	1.90 – 3.31	0.07/-0.27/-0.25		poorly drained	1.28/1.47/-0.40
	3.32 – 4.73	-0.47/-0.20/-0.49		very poorly drained	0.09/1.01/0.63
	4.74 – 6.62	0.33/-0.18/-0.13	IMP (%)	0.00 – 0.00	--/--/--
	6.63 – 8.52	0.46/-0.76/0.55		0.01 – 1.96	-0.51/-1.56/-0.25
	8.53 – 10.88	-2.98/0.08/-0.19		1.97 – 4.70	-0.01/-0.31/-0.25
	10.89 – 14.20	-17.93/0.05/-2.16		4.71 – 10.98	-0.05/-0.14/-0.24
	14.21 – 19.40	--/-13.95/17.56		10.99 – 18.82	-0.29/-0.90/-0.32
	19.41 – 120.72	--/--/-17.71		18.83 – 28.62	-0.51/-0.30/-0.05
VEG (%)	0.00 – 0.00	--/--/--		28.63 – 38.82	-0.31/-0.03/-0.44
	0.01 – 32.00	-0.16/0.26/0.04		38.83 – 49.80	-0.08/0.09/-0.54
	32.01 – 55.00	-0.22/-0.17/0.21		49.81 – 63.92	0.04/-1.17/-1.19
	55.01 – 70.00	-0.20/0.30/0.11		63.93 – 99.61	-0.58/-0.28/-0.62
	70.01 – 80.00	-1.45/0.55/0.48	GEO	thin till	--/--/--
	80.01 – 86.00	-0.68/0.62/0.47		sand/ gravel/talus	1.08/1.05/1.02
	86.01 – 88.00	-1.73/0.41/0.56		finer	--/1.94/1.35
	88.01 – 89.00	-1.07/-0.20/0.26		floodplain alluvium	16.08/3.27/3.27
	89.01 – 90.00	-1.66/-0.09/-1.17		swamp deposits	0.74/1.49/1.71
	90.01 – 93.00	-0.18/-0.18/-0.68		thick till	-0.22/-1.96/-0.72
LAND	developed, open space	--/--/--		End Moraine deposits	0.01/-2.28/--
	dev., low intensity	0.27/0.01/-0.19		artificial fill	17.28/15.02/1.83
	dev., med.-high intensity	0.12/0.07/-0.24		salt/tidal marsh deposits	1.33/13.03/--
	barren (rock/sand/clay)	1.28/-1.57/-17.40		beach deposits	2.61/--/--
	forest	0.13/-0.75/-1.00			
	shrub/scrub	-1.38/-1.66/-0.92			
	grassland/herbaceous	-0.34/-0.97/-0.87			
	pasture/hay	0.30/-1.15/-0.51			
	cultivated crops	1.58/-0.34/-1.28			
wetlands (woody/emer.)	0.37/0.46/0.07				

Table A.3: The land use categories used in each class of the land use flood risk factor are provided for the 1-m NOAA land use dataset (Columns 1 and 2) and the 30-m NLCD land use dataset (Columns 4 and 5). The classes used in the current analysis that are associated with each category are listed in Column 3.

NOAA Land Use Code	Category	Class	NLCD Land Use Code	Category
5	developed open space	1	21	developed open space
N/A	N/A	2	22	developed, low intensity
2	impervious	3	23/24	developed, medium/high intensity
19	unconsolidated shore	4	31	barren land
20	bare Land	4	31	barren land
11	mixed forest	5	41	forest
12	scrub/shrub	6	52	scrub/shrub
8	grassland	7	71	grassland
7	pasture/hay	8	81	pasture/hay
6	cultivated land	9	82	cultivated crops
13	palustrine forested wetland	10	90/95	wetland
14	palustrine scrub/shrub wetland	10	90/95	wetland
15	palustrine emergent wetland	10	90/95	wetland
17	estuarine scrub/shrub wetland	10	90/95	wetland
18	estuarine emergent wetland	10	90/95	wetland
21	open water	null	11	open water
22	palustrine aquatic bed	null	11	open water

Chester

Clinton

Cromwell

Deep River

Durham

East Haddam

East Hampton

Essex

Haddam

Killingworth

Lyme

Middlefield

Middletown

Old Lyme

Old Saybrook

Portland

Westbrook



**Long Term Recovery and Land Use Resiliency
Through Community Flood Resilience Study
*Flood Susceptibility Mapping for the
Lower Connecticut River Valley***

July 2018

Prepared by:
Dewberry Engineers Inc.



Photo: Chester Historical Society – Chester Center

This work was funded by the United States Department of Housing and Urban Development (HUD) Community Development Block Grant – Disaster Recovery (CDBG-DR) Program – Federal Grant Number B-13-DS- 09-0001 and administered by the Connecticut Department of Housing (DOH) – Grant Number 6202. Additional funding was obtained through a sub-award agreement with the University of Connecticut’s (UConn) Institute for Resilience and Climate Adaption (CIRCA) – Grant Number PO#43280 and the Connecticut Department of Energy and Environmental Protection (DEEP) – Grant Number PS#2014-14249.

Plan contents are solely the responsibility of the authors and do not necessarily represent the official views of UConn or CT Dept. of Energy and Environmental Protection.

Table of Contents

Executive Summary.....	3
1. Introduction and Literature Review.....	4
2. Data and Method.....	4
Flood Susceptibility.....	4
Analysis of Climatic Factors.....	4
<i>Climate Variability</i>	5
<i>Historical Precipitation Analysis</i>	6
<i>Future Projections</i>	7
3. Results.....	8
Flood Susceptibility.....	8
Climate Variability.....	9
Climate Change.....	12
<i>Historical Analysis</i>	12
<i>Future Projections</i>	16
4. Practical Applications of Study Findings.....	20
Workshops.....	21
Survey.....	21
Review of Planning Documents.....	22
Applications of Flood Susceptibility Mapping and Climate Data.....	23
5. Summary.....	25
6. Future Work.....	26
7. References.....	27
APPENDIX A: Input Data Metadata.....	29
APPENDIX B: NOAA Atlas 14 Heavy Precipitation Statistics for the Lower CT Region.....	30
APPENDIX C: Climate Modeling.....	31
APPENDIX D: Community and Stakeholder Survey Results.....	32
APPENDIX E: Flood Resilience Checklist.....	40

Executive Summary

A summary of the data, methodology, results, and conclusions related to the flood susceptibility analysis of the Lower Connecticut River Valley Region (LCRVR) can be found in Giovannettone et al. (2018).

Regarding climatic factors affecting the LCRVR, an analysis looking at the major climatic mechanisms linked to rainfall in the region was performed through a simple correlation analysis between long-term total precipitation and long-term averages of nearly 40 climate indices. It was found that by incorporating a time difference, or lag time, between the period over which rainfall is totaled and the corresponding period over which climate indices are averaged, 12 and 48 months maximized the predictive skill of the correlation. The reason for incorporating a lag time is based on the assumption that the effects of a particular climate mechanism on rainfall do not occur immediately; there is some delay before the corresponding impact on rainfall manifests itself. The 12-month lag time revealed a strong and significant correlation with El Niño, while the 48-month lag time revealed a strong and significant correlation with the Caribbean SST (sea-surface temperature) index. The correlations at the 48-month lag time were used to create a statistical model to predict future 48-month rainfall totals; predictions were shown to be relatively accurate when compared to historic observations. This model provides a long-term window into the future and can be used to predict the future onset and persistence of extended periods of high rainfall and drought.

Local- and regional-scale statistical analyses were performed for the city of Hartford and for a region encompassing several Mid-Atlantic and Northeastern states to detect changes in historical rainfall statistics over and near the LCRVR. Tests were performed on trends (i) in the Annual Maximum Series (AMS) of 24-hour rainfall and (ii) Peaks-Over-Threshold (POT). Slight linear trends were found at Hartford but were not significant at the 95% and 90% confidence levels. On a regional level, 20% of rain gauges, including gauges in northwestern Connecticut, experienced statistically significant increases in AMS over the period of record, while 32% showed statistically positive trends in POT, which indicates significant increase in heavy rainfall outside of the LCRVR. The change in the 70th and 98th percentiles of rainy day rainfall was also investigated to determine if the change in light/moderate rainfall is consistent with changes in heavier rainfall. Comparing two periods (1955 – 1985 and 1986 – 2016) revealed that even though there are significant increases in heavy rainfall on a regional basis, there are very few locations that experienced a significant change in light/moderate rainfall, suggesting a disproportionate effect of climate change on heavier events as opposed to an overall wetter climate. In contrast, as the local-scale analysis revealed no significant increase in heavy rainfall intensity and frequency, it is likely that the LCRVR has “beat the odds” by not experiencing an increase in heavy rainfall activity. It is also possible that there may be some other effect, perhaps from Long Island Sound, that has caused differences in rainfall trends in the region. This cannot be said for sure without additional analysis.

An analysis of future rainfall projections was then conducted to determine how heavy rainfall will change over the LCRVR in the mid- and long-term future using data from the Intergovernmental Panel on Climate Change’s (IPCC’s) CMIP5 modeling experiments. The high emission Representative Concentration Pathway (RCP) 8.5 (W/m²) scenario was used to provide an upper bound on expected changes. All raw model data used for future projections were bias-corrected by comparing model results from a historical period (1950 – 2005) to observations at the National Oceanographic and

Atmospheric Administration (NOAA) Global Historical Climatology Network (GHCN) rain gauge (ID# GHCND:USW00014740), at Hartford Bradley International Airport.

Projections in the future Precipitation-Frequency (P-F) curve at Hartford were then investigated. It was found that projected mid-term (2045) and long-term (2075) P-F curves show increases across the full range of frequencies, with higher percentage changes occurring for the more frequent events. Results indicate that today's 100-year 24-hour rainfall event will become a ~53-year event in 2045 and a ~45-year event in 2075, whereas more drastic changes are seen for more frequent events. These and prior results demonstrate the importance of determining which present-day recurrence intervals (e.g. 100-year) are important for land use and recovery planning, hazard mitigation, design standards and/or flood warning plans and then building socioeconomic models to show how a more frequent occurrence of such events will impact response and/or recovery costs. This analysis is also useful for informing the possible changes in the shorter-duration flash flood risk, which is more driven by precipitation compared to riverine flooding (especially on the Connecticut River). Although the latter is also driven by rain and snow, it is also driven strongly by additional factors such as upstream flow, land cover, impervious area and ice jams and dam releases.

A series of three outreach workshops for community officials, an online survey of stakeholders, and a review of planning and regulatory documents throughout the region were conducted. The workshops were used to review methodology and present results, and most importantly, to discuss the practical applications of the susceptibility mapping for community planning and operations, with a focus on resiliency. Practical applications range from quantitative analysis of at risk property and infrastructure, for planning, to modifications of design standards for new development and post disaster recovery.

1. Introduction and Literature Review

The Introduction and Literature Review pertaining to the flood susceptibility analysis can be found in Giovannettone et al. (2018).

2. Data and Method

Flood Susceptibility

A description of the data and methodology used to perform the flood susceptibility analysis can be found in Giovannettone et al. (2018).

Analysis of Climatic Factors

In addition to developing flood susceptibility maps, the impacts of climate variability and climate change on heavy precipitation in the LCRVR were studied. The impact of natural climate variability, which can have significant influence on year to year changes in heavy precipitation, was analyzed through a

correlation analysis using large-scale Hydro-Climate Indices (HCI's). HCI's characterize repeated relationships between various climate regimes on a global scale and a host of associated hydrologic responses. The effects of these climate regimes on regional hydrologic flow and reservoir operations have been heavily researched, and the HCI's were developed to provide a quantitative point of reference for these relationships. The relationship between the climate and water supply has quickly evolved into a matter of national interest and concern during the past decade as periods of deep drought gripped several portions of the country creating regional water supply crises. Meanwhile, the impact of climate change was assessed from two perspectives: a historical analysis using observed, long-record rain gauge data, and an analysis of future projections of daily precipitation from relatively high resolution downscaled atmospheric models forced with increasing greenhouse gas emissions. Below, we describe the data used in each analysis in more detail.

Climate Variability

In addition to trends in a changing climate, there also exist various mechanisms of low-frequency climate variability that can result in significant changes in weather over time. The current study attempts to identify the climate mechanisms that affect precipitation in the LCRVR and surrounding region using various hydro-climate indices (HCI's), including those given in Table 2-3. The method used to accomplish this is referred to as "long-window" correlation analysis and entails utilizing a long-duration (60-month) moving average of monthly index values and precipitation to smooth out much of the noise in both time series. It was found that by incorporating a time difference, or lag time, between the period over which rainfall is totaled and the corresponding period over which climate indices are averaged, the predictive skill of the correlation could be optimized. The reason for incorporating a lag time is based on the assumption that the effects of a particular climate mechanism on rainfall do not occur immediately; there is some delay before the corresponding impact on rainfall manifests itself. Various lag times between the two datasets were analyzed, and it was found that lag times near 12 and 48 months resulted in the best correlations; further analyses were therefore limited to these two lag times. Strong correlations provide a type of predictive mechanism by which future annual or multi-annual precipitation can be estimated. Longer lead times also allow a window into the future from which the onset and/or persistence of a long-term extreme event can be identified with substantial lead time.

Precipitation data were obtained from the Global Historical Climatology Network (GHCN; see Menne et al., 2012) for locations throughout the States of Connecticut, Massachusetts, and Rhode Island, while the National Oceanographic and Atmospheric Administration (NOAA) contains a compilation of the climate index data used here (NOAA 2016). Precipitation data were composited into 60-month rainfall totals, while climate index data were averaged over 60-month periods that lagged the rainfall periods by 12 and 48 months for the short- and long-term analyses, respectively.

The current analysis required the use of a frequency analysis software referred to as the HydroMetriks – Frequency Intensity Tool (Hydro-FIT), which was developed, tested, and validated, by HydroMetriks, Ltd. Hydro-FIT allows the identification of any of nearly 40 climate indices that correlate well with total precipitation over a user-specified period, which is defined by a beginning month, duration, and lag

Table 2-3: Abbreviations and names of global climate indices analyzed in the current study.

Index Abbreviation	Index Name
SOI	Southern Oscillation Index
ONI	Oceanic Niño Index
EPI	ENSO Precipitation Index
TNI	Trans-Niño Index
MEI	Multivariate ENSO Index
NAO	North Atlantic Oscillation
AMO	Atlantic Multidecadal Oscillation
AMM	Atlantic Meridional Mode
CAR	Caribbean SST Index
PDO	Pacific Decadal Oscillation
NOI	Northern Oscillation Index
WP	Western Pacific pattern
PNA	Pacific/North American pattern
AO	Arctic Oscillation
EAWR	Eastern Asia/Western Russia Index
CIP	Central Indian Precipitation index
MJO	Madden-Julian Oscillation

time. A previous version of Hydro-FIT had been used to perform such analyses for rainfall in South America and for hurricane genesis in the Atlantic Ocean (Giovannettone, 2017). The strength of each correlation was measured using Pearson’s correlation coefficient, while the significance or the likelihood that a given correlation coefficient will occur while assuming there is no relationship in the population ($r = 0.0$) is measured using the statistical t-value and critical values from the Student’s t Distribution for two-tailed distributions:

$$t = r \sqrt{\left(\frac{n-2}{1-r^2}\right)}, \quad (3)$$

where t represents the statistical t-value, r is the Pearson correlation coefficient, and n is the number of data values ($n - 2 =$ degrees of freedom). If the computed t-value is greater than a critical value, then the null hypothesis can be rejected and the correlation is significant at the selected confidence level.

Historical Precipitation Analysis

Daily rainfall records from the Global Historical Climatology Network (GHCN) (see Menne et al., 2012) were accessed. We focused on a region that has similar heavy precipitation statistics as the LCRVR, hereafter termed the LCRVR “climate region”. The LCRVR “climate region” was subjectively determined by analyzing precipitation-frequency data (e.g. Appendix A) and noting that the LCRVR behaves similarly to other rain gauges roughly within 250 km of the Atlantic Ocean. In all, gauges were selected based on the following criteria:

- Roughly 250 km (155 miles) from Atlantic Ocean coastline,
- Years with more than 9 days of missing data were excluded,
- The last qualifying year was 2007 or later (see Appendix B),
- At least 60 qualifying years.

Quantitative evidence of significant non-stationarity, which suggests that climate and flood risk are being altered through substantial anthropogenic changes, in heavy precipitation statistics was assessed using three methods, trends in Annual Maximum Series (AMS), trends in Peaks over Threshold (POT) and changes in the daily rainfall distribution, from 1955-1985 to 1986-2016 at various percentiles. The AMS consists of a times series of annual maximum 24-hour precipitation totals, while the POT consists of a time series of the total number of days annually experiencing total precipitation over a pre-determined threshold.

Future Projections

The projected impact of climate change on rainfall intensity for medium (2045) and longer term (2075) planning purposes was estimated. This analysis is especially useful for informing the possible changes in the shorter-duration flash flood risk, which is more driven by precipitation than riverine flooding typically is (especially on the Connecticut River). Although the latter is also driven by precipitation, it is also driven strongly by additional factors such as upstream flow as well as land cover and impervious area.

The most comprehensive and commonly used source of climate change projections is organized by the Intergovernmental Panel on Climate Change (IPCC). We used data originating from IPCC's 5th Assessment Report (AR5), which is the latest available report as of 2017. The findings in AR5 are based on the simulation of many Global Climate Models (GCMs) from institutions across the world. While GCMs are adequate for studying continental and global-scale changes in climate, computational limitations constrain their horizontal resolution to be inadequate for the local scale analysis such as the one here. Thus, some manner of "downscaling", or using larger-scale variables to inform smaller-scale conditions, is required. A comprehensive dataset of downscaled Coupled Model Inter-comparison Project Phase 5 (CMIP5) output was developed in 2014 by a joint effort of several federal, academic, and commercial partners (Brekke et al. 2013). Although we considered the use of this data, we ultimately decided against using it because it strongly underestimated daily heavy rainfall statistics over the LCRVR.

Instead, results from a recent high-resolution downscaling effort called the North American Coordinated Regional Climate Downscaling Experiment (NA-CORDEX) were used. The NA-CORDEX was designed by taking the output of the relatively coarse GCMs belonging to CMIP5 and using these as boundary conditions to force much higher resolution atmospheric models centered on North America. Although many NA-CORDEX simulations were available, the analysis was restricted to those with the highest horizontal resolution of 11 km (7 miles). All selected simulations were forced by the Intergovernmental Panel on Climate Change's (IPCC's) CMIP5 modeling experiments high emission Representative Concentration Pathway (RCP) 8.5 (W/m^2) scenario boundary conditions. The focus on just the high emission scenario was done for two reasons: (i) to provide for an estimate of an upper bound to the impact of climate change on heavy precipitation (because previous studies have shown a quasi-linear response of heavy precipitation to scenario in the LCRVR), and (ii) to allow for the investigation of multiple model simulations that would otherwise not be possible if multiple scenarios were chosen.

Table A-1 in Appendix A shows the four model simulations that were analyzed. A fifth simulation, in which the RegCM4 was forced with the MPI-ESM-LR GCM, was available but not used because it had incomplete data.

3. Results

Flood Susceptibility

The overall results of the logistic analysis for each sub-region within the AOI are given in Giovannettone et al. (2018). In summary, it was found that ‘elevation’ and ‘distance to water’ have the most influence on flood susceptibility in the urban and coastal sub-regions, whereas ‘elevation’ has substantially less influence within the rural sub-region with ‘distance to water’ and ‘surficial materials’ having the greater influence. It was also found that ‘surficial materials’ has a strong influence in the coastal and rural sub-regions, whereas it has little influence in the urban sub-region, while ‘land cover’ has the opposite trend. Finally, it was observed that the urbanization in the sub-region including and surrounding the City of Middletown has resulted in a significant increase (greater than 200 percent) in the contribution of ‘land cover’ to the flood susceptibility of the area.

There were several areas identified as ‘very high’ and ‘high’ risk outside of the FEMA map, which includes various types of critical infrastructure (Giovannettone et al., 2018). When comparing the susceptibility mapping to the FEMA 100-year flood maps, it is important to understand key distinctions between the two. The FEMA 100-year flood maps are limited to the sub-watersheds of greater than one square mile that FEMA chose to study with limited resources. Other limiting factors are the age of the underlying studies illustrated by the FEMA maps (often more than two decades old) and their focus on only areas where development existed or was imminently anticipated. FEMA’s flood mapping is developed using physical models to perform hydrologic and hydraulic analysis of a statistical rainfall event with a one percent chance of being equaled or exceeded in any given year (referred to as the 100-year flood). In general terms, hydrologic analysis is the study of transforming rainfall amount into quantity of runoff. Hydraulic analysis takes that quantity of water and uses a physical model to route it through existing terrain, while considering such factors as topography and vegetative density. This modeling is referred to as “detailed analysis.” Some areas are studied by “approximate methods.” In general, areas studied by approximate methods use a simplified hydrologic analysis methodology and route runoff quantity through best available topography alone.

The susceptibility maps from this study provide a less expensive method of covering all land area within the region. By using the statistical modeling methodology described in this report it was possible to identify the contribution of flood factors within the physically modeled FEMA 100-year floodplain and apply them to the entire study region to identify areas thought to be vulnerable to flooding. One important disclaimer about the flood susceptibility map is that it was created for present-day conditions and is only to be used for planning purposes. It is not intended to replace the FEMA mapping for regulatory or flood insurance decisions.

The scale of the flood susceptibility map and data are most appropriately used at the regional scale. However, use of the data at the municipal scale should allow local officials to examine areas of concern for planning purposes. A GIS tool, which accompanies this report, was developed to enable any location within the region to be looked at in more detail. As more accurate input datasets (e.g. higher resolution LiDAR data and imagery) become available, they can be easily incorporated into an updated flood susceptibility analysis as well as a revised GIS tool. Higher resolution input datasets also allow smaller areas to be analyzed in more detail if desired (e.g. the City of Middletown, which is dominated by an area of ‘very high’ flood susceptibility in the northern portion of the AOI in Fig. 3-3).

Climate Variability

An idea of the climatic mechanisms that may contribute to precipitation and flooding in the region surrounding and including the LCRVR can be obtained from the results of the climate variability analysis shown in Fig. 3-4.

It can be observed in Fig. 3-4 that there are a few dominant hydro-climate indices that correlate with precipitation throughout the State of Connecticut and the surrounding region for both the 12-month and 48-month lead times, which include indices related to the El Niño/Southern Oscillation (ENSO), the Madden-Julian Oscillation (MJO), and the Caribbean SST (sea-surface temperature) Index (CAR), which is a time series of SST anomalies averaged over the Caribbean Sea. Within the LCRVR itself, ENSO has the highest correlation with precipitation at the 12-month lead time (Fig. 3-4a) using the beginning months given in Table 3-1, which contrasts with other sites within the State of Connecticut that correlate best with the MJO. The strength of these correlations is between $R = 0.60$ to 0.79 ($r^2 = 0.36$ to 0.62), which is strong enough to make qualitative predictions concerning whether the following 12 months will experience higher- or lower-than-normal precipitation, but was found not to be sufficient to make

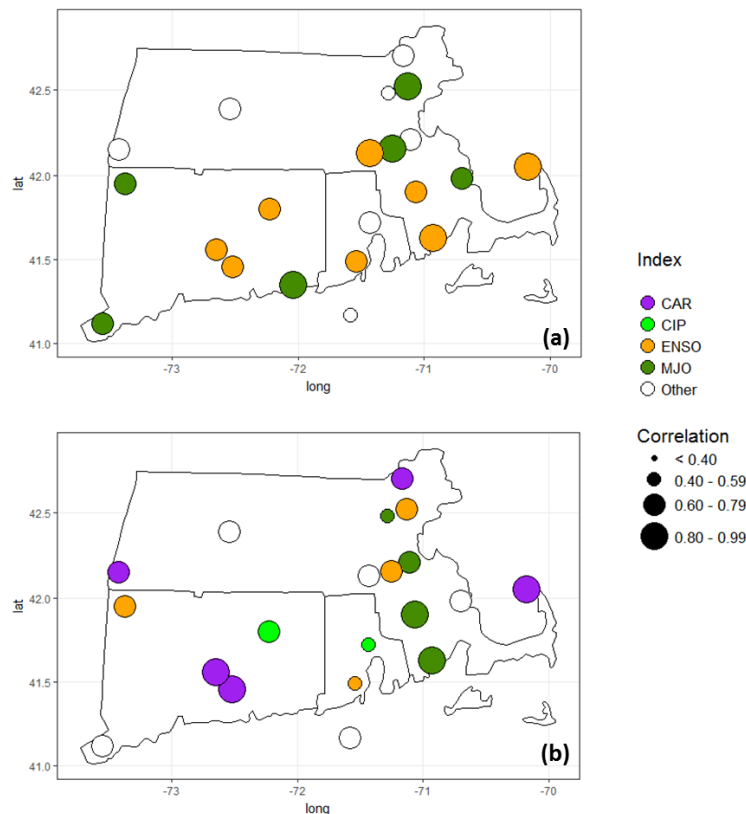


Figure 3-4: Results of hydro-climate index analyses at several locations throughout the states of Connecticut, Rhode Island, and Massachusetts using lag times of (a) 12 months and (b) 48 months. The color and size of the circles represent the index and correlation strength, respectively.

Table 3-1: Strong correlations between 60-month average climate index values and 60-month total precipitation were identified for Middletown and Cockaponset State Forest using the climate indices given in Column 3 and beginning months and lead times in Columns 2 and 4, respectively.

City	Precipitation Beginning Month	Index	Lead Time (months)
Middletown, CT	January	ENSO	12
Cockaponset, CT	July	ENSO	12
Middletown, CT	January	CAR	48
Cockaponset, CT	January	CAR	48

quantitative predictions of future rainfall. To perform a complete statistical analysis of each correlation, the significance was also estimated so that the null hypothesis that there is no relationship in the data can be rejected. The results for the Student's t test are given in the column labeled t/t_{crit} in Table 3-2. The first value represents the t-value computed for each site using the corresponding correlation coefficient (r) and number of data points (n). The second value represents the critical value from the Student's t distribution at the 0.01% confidence level. The fact that the t-value does not exceed the critical value at Middletown means that the null hypothesis cannot be rejected at the 0.01% confidence level, but it was found that the t-value exceeds the critical value at the 0.05% confidence level (not shown). The t-value for Cockaponset does exceed the critical value by a small amount, which means that the null hypothesis can be rejected at the 0.01% confidence level.

Precipitation within the LCRVR was found to correlate strongest with the CAR at a 48-month lead time (Fig. 3-4b) using the beginning months given in Table 3-1, which again contrasts with other locations in the state. In this case, the strength of the correlations at Middletown and Cockaponset are between $r = 0.80$ and 0.99 . The results for the Student's t test are given in Rows 3 and 4 of Table 3-2. The fact that the t-value exceeds the critical value at both locations by a substantial amount means that the null hypothesis can be rejected at the 0.01% confidence level in both cases.

Due to the high strength and significance of the correlations identified at a lag time of 48 months, predictions of 48-month rainfall using the respective linear relationships with CAR are made at Middletown and Cockaponset State Forest and compared to observations in Figs. 3-5a and b, respectively; model parameters are given in Table 3-2 for both the 12-month and 48 month correlations. Predictions closely match observations for almost all years where sufficient rainfall data were available except for a few short periods. These results demonstrate that, using only one variable, long-term total precipitation can be predicted with good accuracy, which can be extrapolated to being able to predict long-term changes in precipitation accurately with sufficient lead time. For example, the onset and end of a drought or an extended period of high rainfall are capable of being detected with a 48-month lead time, thus providing a method by which to estimate persistence long in advance.

Table 3-2: Linear regressions were developed for Middletown and Cockaponset State Forest using the climate indices, beginning months, and lead times given in Table 3-1. Columns 3 and 4 give the slope and intercept of the regressions, respectively, while Columns 5 – 7 give Pearson’s correlation coefficients (r), number of data points (n), and ratio of t-values to the critical value from the Student’s t distribution at the 0.01% confidence level for a two-tailed distribution.

City	Lead Time (months)	Slope (m)	Intercept	r	n	t/t _{crit}
Middletown, CT	12	-76.75	243.49	0.65	25	4.10/4.69
Cockaponset, CT	12	40.82	241.91	0.74	23	5.04/4.78
Middletown, CT	48	-276.54	241.81	0.81	22	6.18/4.84
Cockaponset, CT	48	-162.10	233.62	0.87	18	7.06/5.13

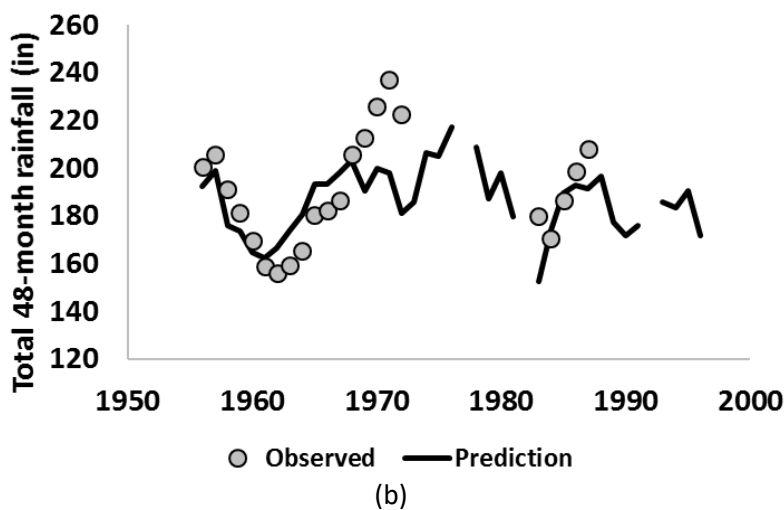
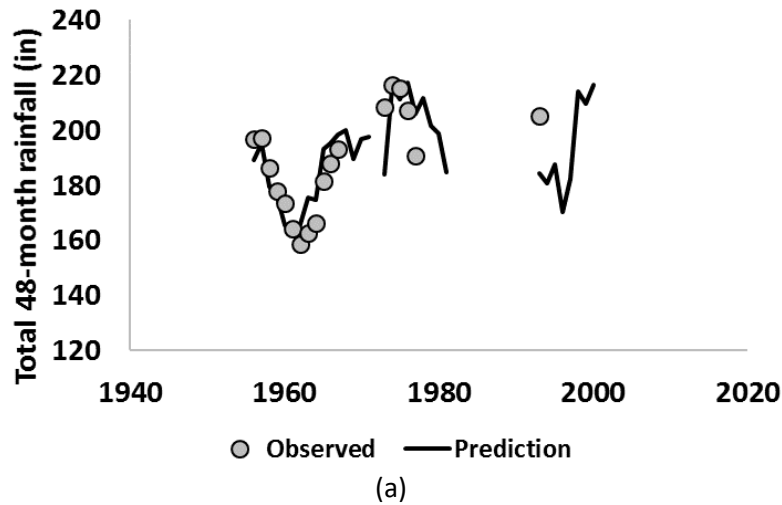


Figure 3-5: Time series of projected (line) vs. observed (circles) 48-month total precipitation at (a) Cockaponset State Forest and (b) Middletown.

Climate Change

Historical Analysis

A local- and regional-scale statistical analyses to detect changes in historical rainfall statistics over the LCRVR was performed. For the local-scale, the Hartford-Bradley International Airport rain gauge was selected, from the Global Historical Climatology Network (id: USW00014740). This gauge had a nearly-complete record of daily data from 1949 – present. Heavy precipitation statistics for the Hartford/Middletown area are shown in Appendix B. The magnitude of the 100-year 24-hour event is about 8.2 inches (Appendix B, Fig. B-1). Meanwhile, there is a distinct seasonality of heavy rainfall occurrence, with highest chances in the late summer and fall (Appendix B, Fig. B-2). For the regional-scale analysis, we selected all long-record rain gauges within about 250 km of the Atlantic Ocean over the Mid-Atlantic and Northeastern states. This region experiences similar heavy rainfall statistics and thus can be considered a more general proxy for trends in the LCRVR’s climate.

For the local and regional-scale analyses, we performed tests on trends (i) in the Annual Maximum Series (AMS) of 24-hour rainfall and (ii) Peaks-Over-Threshold (POT), where a threshold of 1.25 inches per day was used. For the regional analysis only, we also investigated the change in the 70th and 98th percentiles of rainy day rainfall. This allowed us to determine if the change in light to moderate rainfall amounts was consistent with changes in heavy rainfall days, respectively.

Local-scale

Figure 3-6 shows the Annual Maximum Series (AMS) of daily rainfall at the Hartford gauge, which ranges from about 1.5 inches to over 7.0 inches. A linear trend test was applied to this time series and revealed a weak positive trend, but the trend was not significant at the 95% and 90% significance levels. Due to the presence of isolated, very high amounts such as in 1955, 1982 and 1999, we also performed a Spearman correlation (less sensitive to outliers) between year and AMS and again found the correlation to be insignificant at the 90% and 95% confidence levels.

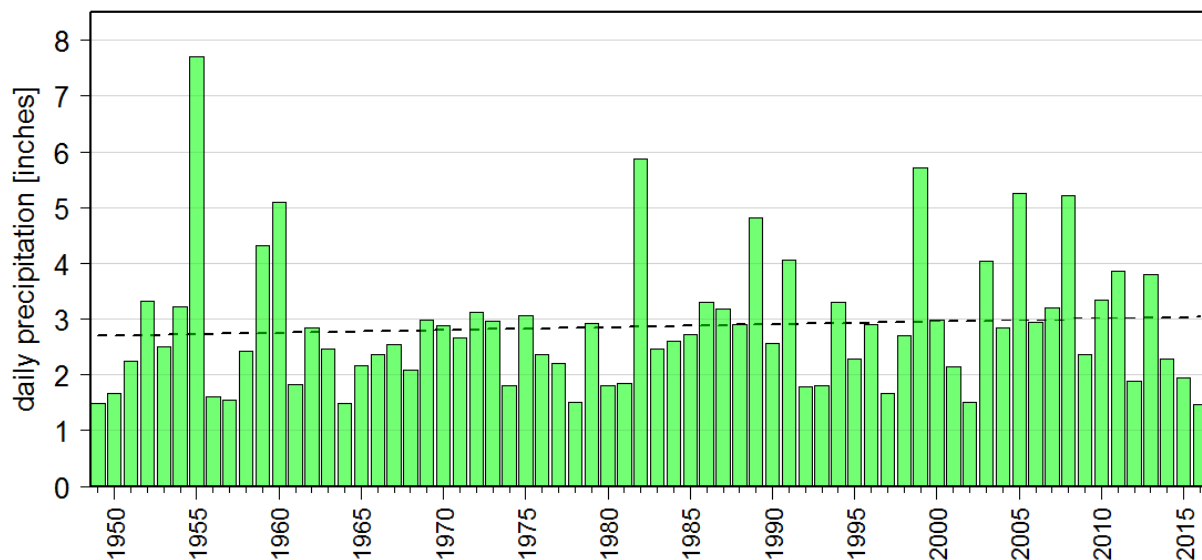


Figure 3-6: Annual Maximum Series of daily rainfall at Hartford Airport over the 1949-2016 period. A linear trend is shown for reference, but this trend was NOT significant at the 95% confidence level.

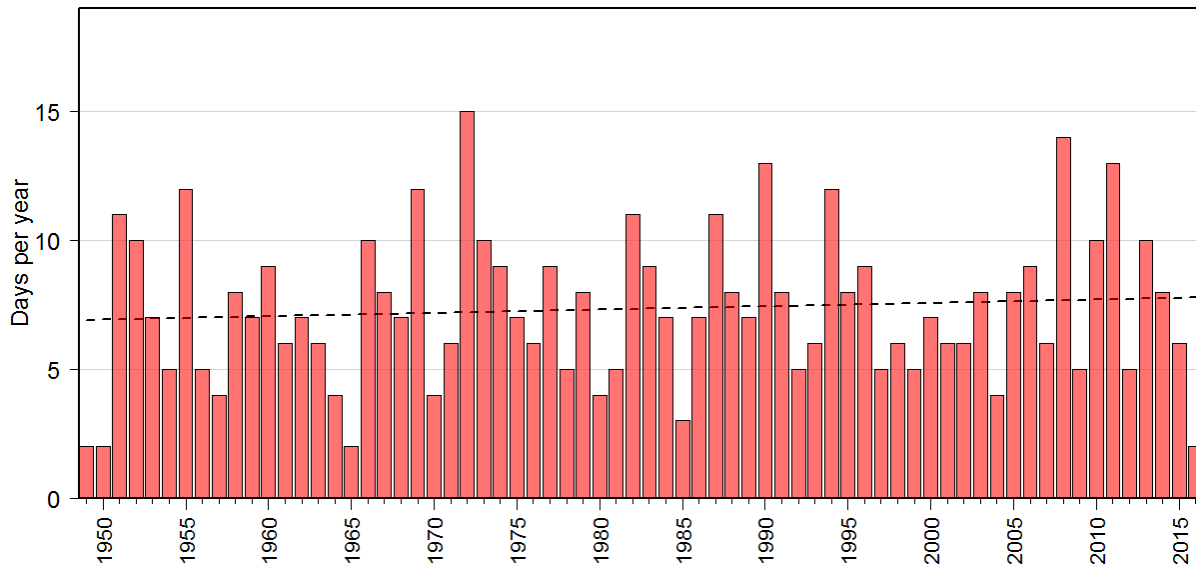


Figure 3-7: As in Fig. 3-6, except for annual Peaks-Over-Threshold using 1.25 inches per day as the threshold. The trend line was NOT found to be significant at the 95% confidence level and is shown for reference only.

Because AMS time series can have significant year-to-year variability that may mask longer-term trends, we also investigated the trend in POT with a threshold of 1.25 inches per day. The result, shown in Fig. 3-7, shows a range of values from 2 to 15 days per year, though a linear trend was once again found to not be significant at the 90% and 95% confidence levels.

Thus, our conclusion from the local-scale analysis was that there has not been a significant change in heavy rainfall statistics using the Hartford Bradley Airport gauge, which serves as a good proxy for the LCRVR. A regional-scale analysis was then performed to determine if the local-scale result can be corroborated when using other nearby rain gauges.

Regional-scale

The 3rd National Climate Assessment (NCA3; Melillo et al. 2014) has documented a substantial increase in heavy rainfall events across the Northeast United States. However, that analysis aggregated the Northeast US into a single region, which could have mixed together sub-regional differences (e.g. we did not find any increases in heavy rainfall at Hartford). Here, we perform a similar analysis as NCA3 but investigate trends in heavy rainfall frequency and intensity on a *gauge-specific level* for gauges in close proximity to the LCRVR. Because heavy precipitation is relatively rare and a single gauge could miss showing a trend due to chance, we include in the analysis gauges across the Northeast and Mid-Atlantic US, roughly within 250 km of the Atlantic Ocean. We chose this region because the heavy rainfall statistics are roughly the same within this region. This can be deduced by looking at the 100-year 24-hour rainfall estimate from NOAA Atlas 14 (Fig. 3-8) – note that the contours roughly parallel the coastline.

Gauges belonging to the Daily Global Historical Climatology Network (GHCN; Menne et al. 2012) were used in this analysis. A gauge must have at least 60 years of data to qualify, where a year is counted as

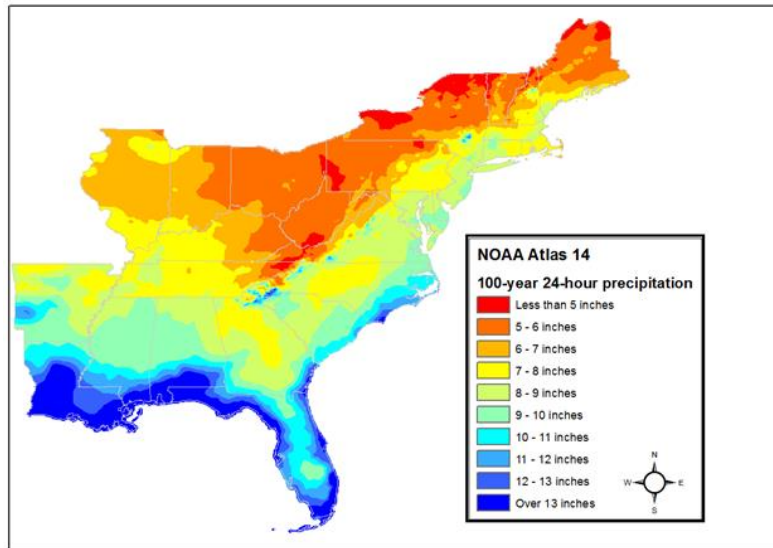


Figure 3-8: 100-year, 24-hour rainfall across the eastern United States (adapted from NOAA Atlas 14; see Perica et al, 2015 for details).

qualifying if it had less than 10 missing days of data. A total of 179 qualifying gauges were found (using data through 2016), and trends in the AMS and POT (exceeding 1.25 inches per day), as well as changes in the distribution, were determined in a gauge-by-gauge manner.

Figure 3-9 shows the trends in AMS of 24-hour rainfall for data through 2005 and 2016. The former is shown for comparison to highlight the drastic changes that have occurred over only the past 10 years. Looking at the right panel in Fig. 3-9, it is seen that out of 179 qualifying gauges, 36 (20%) show statistically significant increases in the AMS. By pure chance, we would only expect 10% (or 18 gauges) to show a trend (both positive and negative). Whereas, **it is seen that there are no gauges that show significant decreases in AMS, providing substantial evidence that large-scale AMS trends are positive in the region.** Note that the Hartford gauge does not show an increase, but gauges in northwest Connecticut do show increases.

Figure 3-10 investigates regional trends in a different manner by considering trends in the POT (threshold: 1.25 inches per day). Similar results are observed as in Fig. 3-9, but now 57 (32%) of the gauges show statistically significant positive trends, while only two gauges show significant decreases. Figure 3-10 also shows that most of the gauges with significant positive trends are located in the northeast United States, with less significant results farther south. To some degree, Fig. 3-10 provides more robust evidence of increases in heavy rainfall statistics because this data includes many storms each year, whereas Fig. 3-9 only identifies the wettest storm each year.

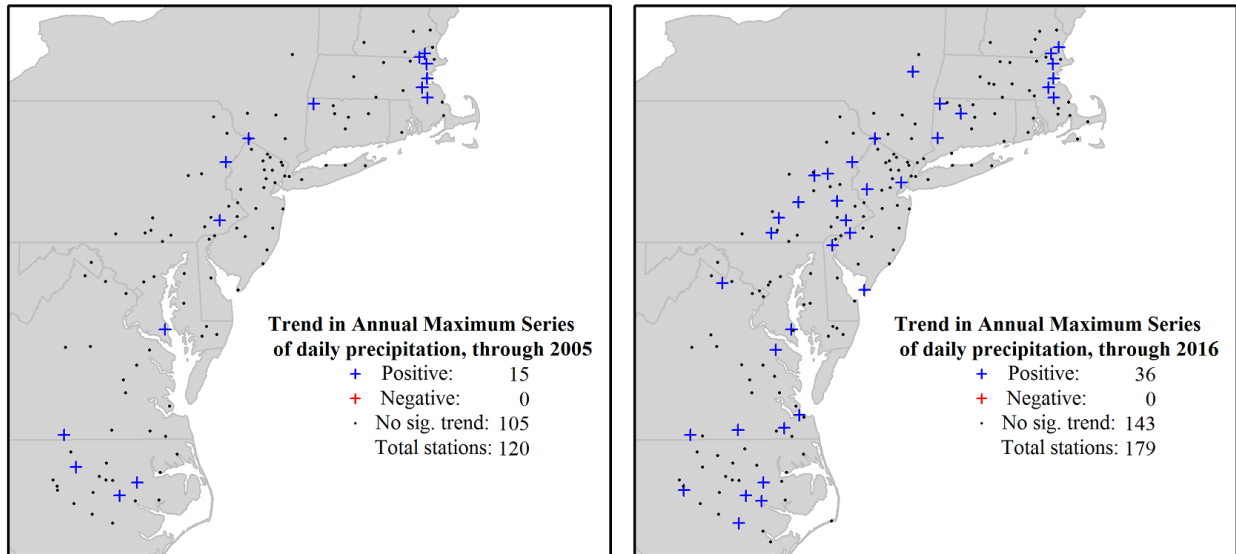


Figure 3-9: Trends in the Annual Maximum Series of qualifying long-record gauges using data through (left) 2005, and (right) 2016. A 95% confidence level is used to denote statistical significance.

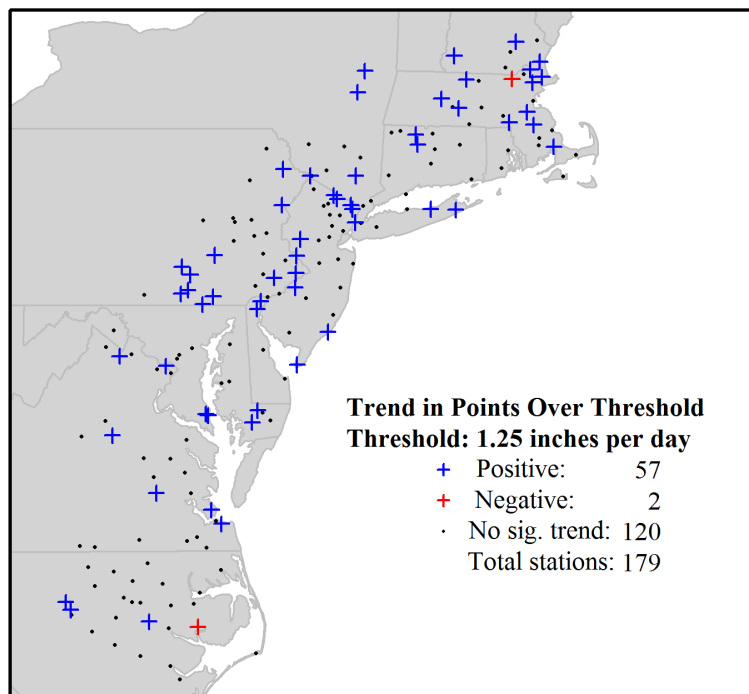


Figure 3-10: As in Fig. 3-9, except for annual Points-Over-Threshold. A 95% confidence level is used to denote statistical significance.

Figure 3-11 shows the changes in 70th and 98th percentiles of rainy day rainfall for each gauge. This was calculated by determining the 70th and 98th percentiles of daily rainfall separately during 1955-1985 and 1986-2016 periods and then dividing the latter value by the former. Statistical significance is more difficult to assign in such a scenario because the value depends on each gauge's distribution; however, a

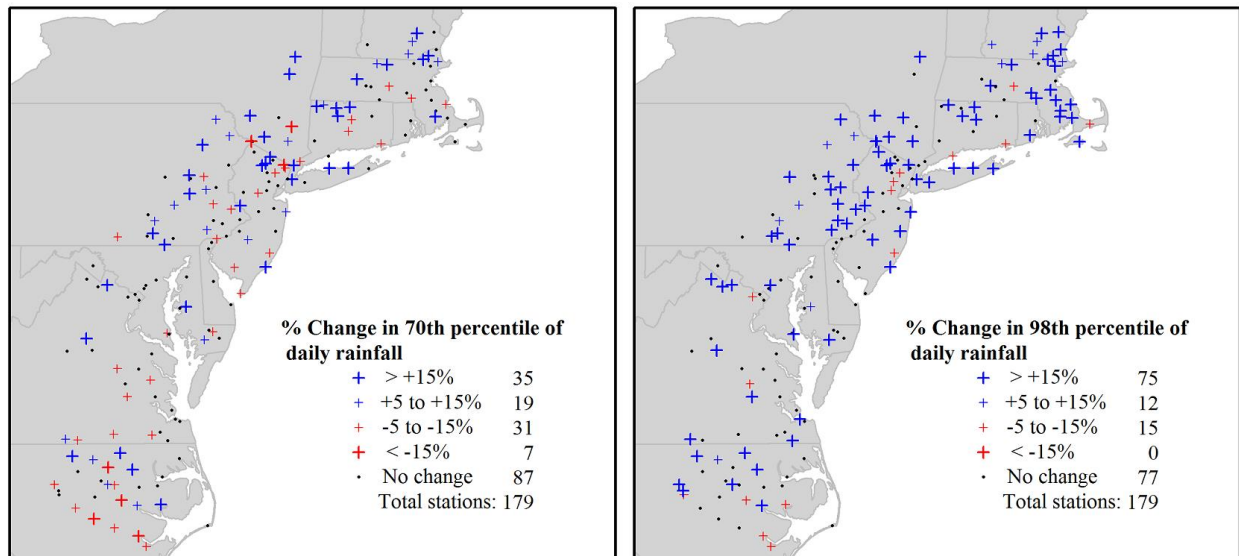


Figure 3-11: Percent changes in the (left) 70th and (right) 95th percentiles of rainy day rainfall, when comparing the 1955-1985 and 1986-2016 periods. For the Hartford, CT gauge, the 70th percentile is about 0.40 inches per day; the 98th percentile is about 1.95 inches per day.

change exceeding +/- 10% can roughly be used as a guideline for statistical significance. Focusing first on the 98th percentile changes, it is seen that the results of Figs. 3-9 and 3-10 are largely corroborated, though even more gauges now show significant increases in heavy rainfall. For example, 75 gauges (42%) now show significant increases, while zero gauges show significant decreases (exceeding 15%). A secondary interesting finding can be seen in the left panel of Fig. 3-11, which shows that there have been no significant changes in the 70th percentile (though regionally, increases are seen in the NY, CT, and MA area). This suggests that it is the heavy rainfall events that are being disproportionately influenced by climate change as opposed to an overall wetter climate.

Whereas the local-scale analysis of Figs. 3-6 and 3-7 show no significant increase in heavy rainfall intensity and frequency at the Hartford gauge, Figs. 3-9 and 3-10 show significant regional-scale increases. Thus, we can conclude that it is likely that the LCRVR has “beat the odds” by not experiencing an increase in heavy rainfall activity at this point. This is not entirely unexpected due to the hit-or-miss character of heavy rainfall events. Next, an analysis of future rainfall projections is conducted to determine how heavy rainfall will change over the LCRVR in the mid- and long-term future.

Future Projections

To investigate future projections of heavy rainfall events in the LCRVR, data from the IPCC’s CMIP5 modeling experiments were used. However, using raw Global Climate Model (GCM) data would be insufficient for informing regional and local-scale rainfall. Thus, we used output from the North American Coordinated Regional Modeling Experiment (NA-CORDEX; Castro et al. 2015). NA-CORDEX is a set of medium- to high-resolution regional models that uses boundary conditions from the CMIP5 GCMs (refer to Table A-3 in Appendix A). Although NA-CORDEX used both RCP4.5 (medium emission) and RCP8.5 (high emission) scenarios, we accessed only the latter. The rationale for this was that if a strong signal was found for RCP8.5, it may warrant consideration of other conditions. On the contrary, if no significant changes were found for RCP8.5, then it is unlikely that other scenarios would show significant changes.

Daily model output of precipitation was accessed over the 1950 – 2100 period. The 1950-2005 period was termed a “historical hindcast” where observed greenhouse gas forcing was used, whereas, the 2006-2100 period was forced by RCP8.5 emissions. Greenhouse gas forcing refers to the effects of changes in atmospheric greenhouse gas concentrations on radiative forcing (see the Atmospheric Concentrations of Greenhouse Gases indicator). Energy that radiates upward from the Earth’s surface is absorbed by these gases and then re-emitted to the lower atmosphere, which results in a warming of the Earth’s surface. After obtaining the required data, the first step in assessing future rainfall was to compare model climatology with the Hartford gauge over the historical period. Figure 3-12 shows that three of the four models were slightly wetter than observations, while one model was drier than observations. Figure 3-12 was used to perform a bias correction through quantile mapping (Themeßl et al. 2011). In this procedure, the model daily rainfall amount is first converted into a quantile (quantile increment was 0.005) and then mapped to its analogous quantile using the Hartford rain gauge data.

To determine future rainfall amounts, the raw model data for the 2006 – 2100 period was corrected using the same quantile mapping transfer function. Thus, **the key assumption is that the future quantile-quantile relationship is identical to the past** (Themeßl et al. 2011). However, in situations where future modeled rainfall exceeded the highest value over the historical modeled period, the quantile-quantile ratio of the highest historical modeled value was applied. In practice, this was only noted to happen on, at most, five different future days for any given model simulation.

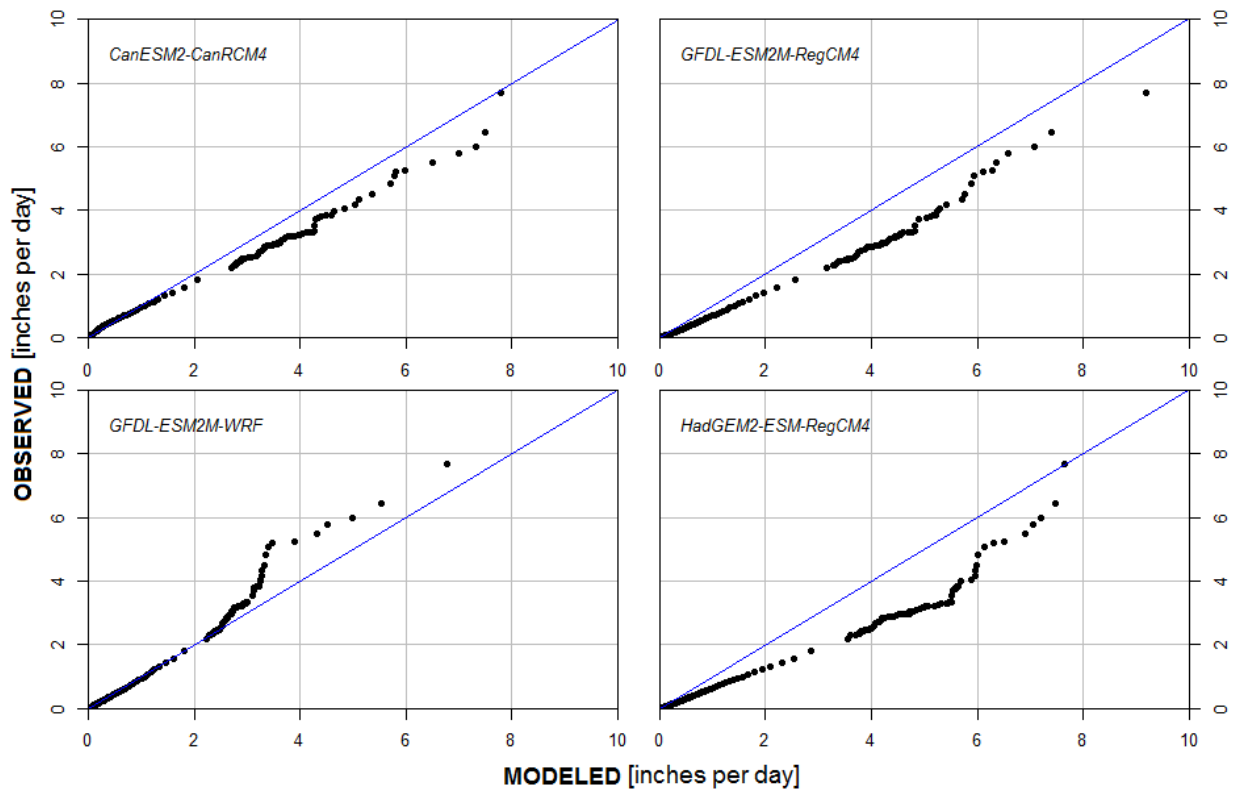


Figure 3-12: Quantile-quantile plots comparing modeled 24-hour precipitation with the Hartford gauge over the historical period. The blue line represents the result for a perfect model. Points to the right of the line imply the model is wetter than observations, while points to the left of the line show the model is drier.

After bias corrected future projections of daily rainfall were computed using quantile mapping, potential changes in the future Precipitation-Frequency (P-F) curve were investigated. The P-F curve is derived by fitting a distribution to Annual Maximum Series of daily rainfall. Analogous P-F curves can be developed for other durations, but our model output, and thus our focus, was restricted to daily rainfall.

Figure 3-13 shows that after bias-correction, a Generalized Extreme Value (GEV) distribution provides an excellent fit to the *observed* empirical Hartford P-F data within the 90% confidence level. The 90% uncertainty band was calculated by randomly sampling the historically modeled time series 1000 times and calculating a Generalized Extreme Value (GEV) for each randomization. Similar uncertainty estimates were prepared for future projections. The excellent fit in Fig. 3-13 confirmed that we could use the historical model simulations as a baseline to which future model simulations could be compared.

Figures 3-14 and 3-15 show the projected mid-term (2045) and long-term (2075) P-F curves compared to the historical period. The mid-term value was calculated using data from 2026-2065, while the long-term value was calculated using data from 2056-2095. Bias-corrected model projections were concatenated into a single 160-year time series to estimate future P-F curves. This was done after testing each individual model's projection and finding little difference between each model, which was somewhat expected because bias-correction was applied. Figures 3-14 and 3-15 show increases in the P-F curve across the full range of frequencies. However, the highest fractional changes occur for higher frequency (i.e. more frequent, lower intensity) events.

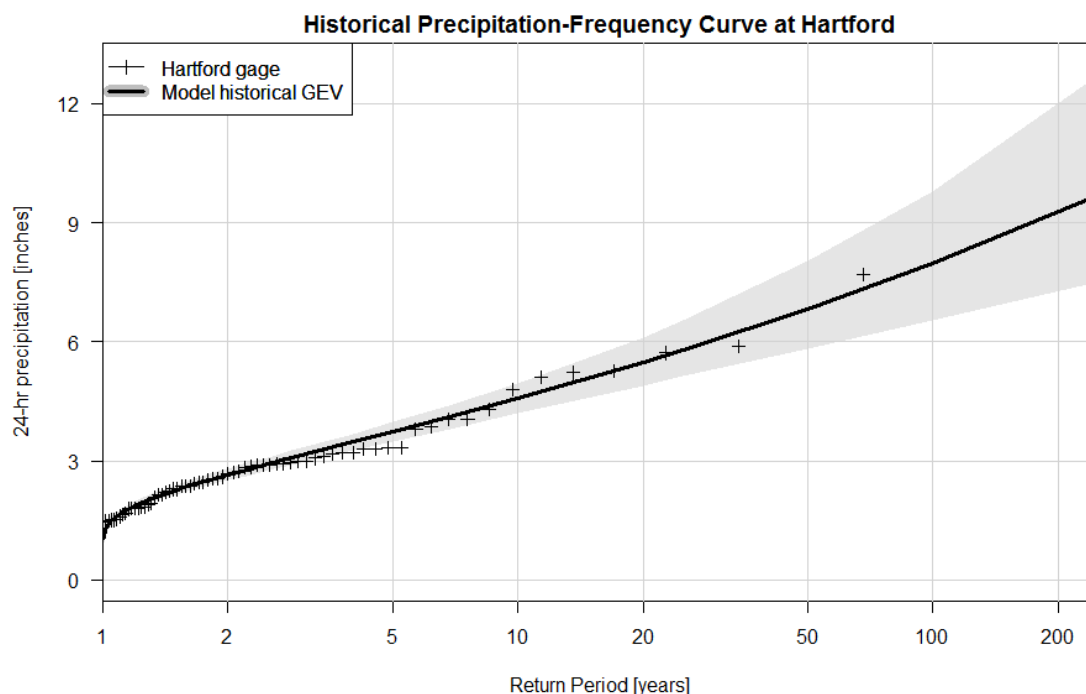


Figure 3-13: Hartford rain gauge empirical Precipitation-Frequency curve (+) compared to a Generalized Extreme Value distribution fit to bias-corrected historical model output. The GEV is assumed to be the best distribution for the Hartford gauge.

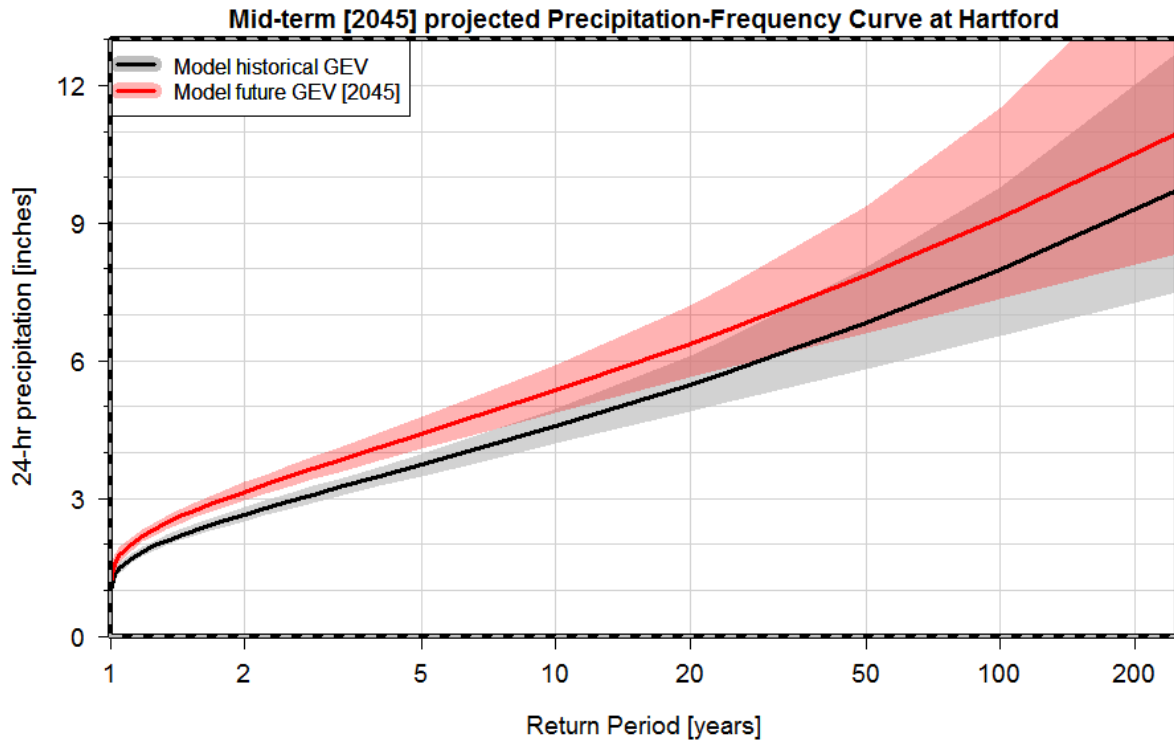


Figure 3-14: Modeled Precipitation-Frequency curves for the Hartford area. The black line and gray shading denote historical (1950-2005) conditions while the red line and light red shading denote the estimate for the 2045 period.

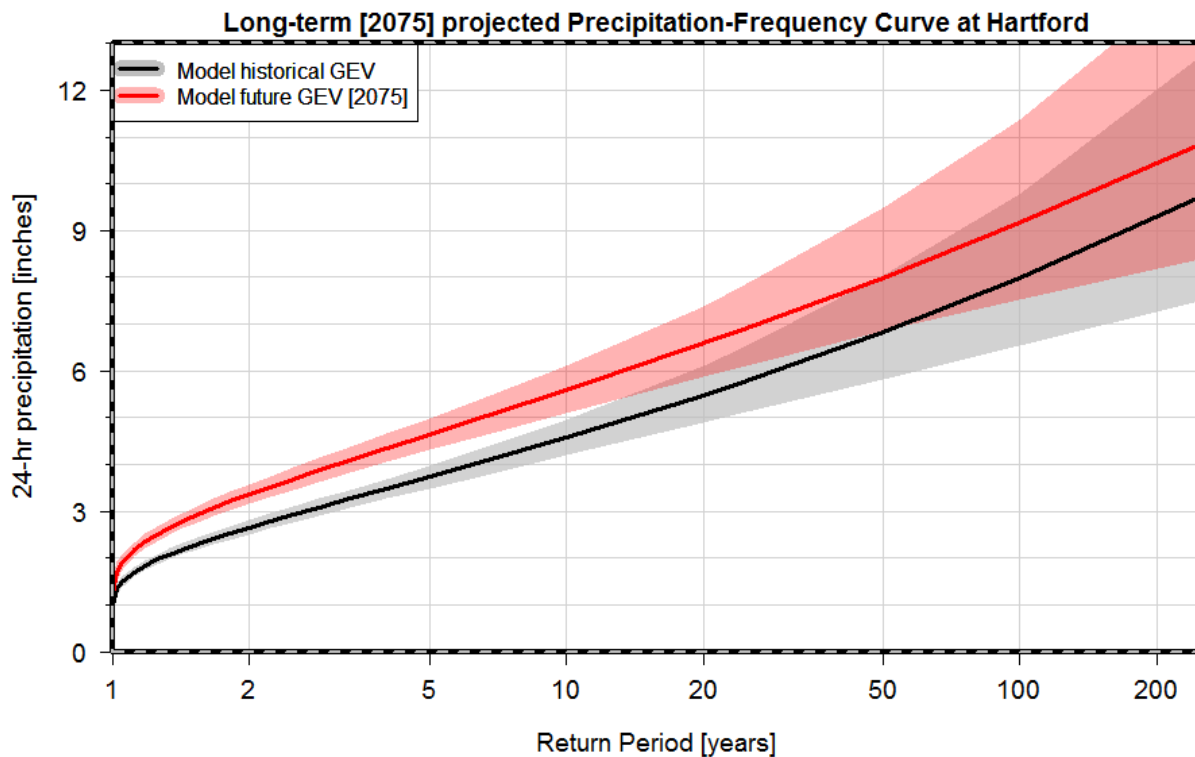


Figure 3-15: As in Fig. 3-14 except for the 2075 period.

Table 3-3: Percent changes in projected 24-hour rainfall at Hartford by 2045 and 2075. Bold font denotes projections are outside the band of historical uncertainty.

Return Period	Change in 2045	Change in 2075
1 year	+17%	+25%
2	+19%	+27%
5	+18%	+24%
10	+17%	+22%
20	+16%	+20%
50	+15%	+17%
100	+14%	+15%

Table 3-3 summarizes the percent changes in the most likely P-F curve value for the 2045 and 2075 periods. In general, increases up to 19% are found by 2045, while increases up to 27% are found by 2075. Comparing the uncertainty bands between the future and historical periods shows that the future band is completely outside of the historical band for up to the 5-year event by 2045 and up to the 10-year event by 2075. Increases found here appear to be slightly less than those described by Prein et al. (2016), who found increases of between 30 and 50% in the statistics of shorter duration hourly heavy rainfall across the LCRVR.

Another perspective on interpreting the results in Figs. 3-14 and 3-15 is to compare how current return periods are projected to change. For example, Fig. 3-14 shows that today's 100-year 24-hour rainfall event will become a ~53-year event in 2045, while Fig. 3-15 shows that it will become a ~45-year event in 2075. More drastic changes are seen for more frequent events. For example, a current 20-year event will become a ~12-year event by 2045 and a ~8-year event by 2075. Thus, one method of assessing the practical impacts from these changes is by determining which present-day recurrence intervals (e.g. 100-year) are important for design standards and/or flood warning plans and building socioeconomic models of how a more frequent occurrence of such events will impact response and/or recovery costs.

A notable disclaimer about the analysis presented herein is that there was little effort placed in investigating the *climate dynamics* causing the changes. For example, it is not entirely clear whether the changes are arising from stronger Nor'easters, tropical cyclones, and/or stationary frontal systems, all of which can cause heavy rainfall in the LCRVR. It is suggested that any further analyses on this topic more closely investigate these respective processes, which could increase the confidence that we can place in the final results.

4. Practical Applications of Study Findings

Another part of the study included outreach to community officials from the 17 municipalities and select additional stakeholders. An online survey and a series of three workshops were held throughout the LCRV region. A cursory review of representative planning and regulatory documents was also performed to determine how, in general, communities are addressing flooding conditions outside of FEMA mapped flood hazard areas. Table 4-1 lists the municipal departments and stakeholders that were invited to participate in the workshops and the survey.

Table 4-1: Survey and Workshop Participant Invitees.

Municipal Officials	Other Stakeholders
Town Planners	CT Maritime Trades
Town Engineers	U.S. Coast Guard
Public Works Directors	CT Institute of Resilience and Climate Adaptation (CIRCA)
Emergency Management Directors	U.S. Army Corp of Engineers
Economic Development Directors	Land Trusts
Public Health Officials	Nature Conservancy
Agricultural Commission	CT Department of Energy and Environmental Protection
	CT Department of Housing

Workshops

The workshops included the following content:

Workshop 1 – March 28th, 2017 - 1-3pm, Haddam Fire Department Rec, 439 Saybrook Rd, Higganum

Provided an overview of the project and an update on its status. A brief overview of planning in the region around this hazard was presented and input sought on factors that contribute to flooding. Input was also sought on the format of the subsequent workshops.

Workshop 2 – April 18th, 1-3pm, Old Lyme Town Hall Meeting Room, 52 Lyme St., Old Lyme

Provided an overview of the flood susceptibility model and near final mapping. There was a breakout session to review mapping in the GIS viewer and to provide feedback.

Workshop 3 – May 9th, 1-3pm, Middletown City Hall, Council Chambers, 245 DeKoven Dr., Middletown

Focused on using the results and products of the study to foster public awareness, resilience action and public policy for the region. It included recommendations or best practices for planning documents, capital budgeting, and regulatory tools.

Survey

The survey was completed by 27 respondents, nearly all of whom answered all questions asked. The distribution of respondents among the community officials listed in Table 4-1 was nearly even, with the exception of no responses from agricultural commissions and fewer from economic development officials. There were more responses from Town Planners. Approximately 30% of the overall responses came from those listed in the stakeholder column. Distribution of survey responses were also fairly even across the communities in the region, with noticeably higher responses from Old Saybrook, Essex and East Haddam and none from Lyme and Middlefield.

Notable findings of the survey included:

- 48% of respondents felt there have been moderate increases in flooding due to high intensity rainfall events in the last 10-years
- 65% of respondents believed that the stormwater system capacity in their community needed at least some improvements to handle future storm events

- 60% of respondents believed that community plans (e.g. Hazard Mitigation, Conservation and Development, Emergency Management) do not adequately address the impacts of climate change on future flooding conditions
- 55% of respondents indicated the residents are somewhat (50%) or very (5%) concerned about the impacts of climate change
- When asked which planning, regulatory or policy documents were best suited to address future flooding issues, the distribution was fairly even, with the most respondents indicating Hazard Mitigation Plans and Plans of Conservation and Development as the best places. Zoning Regulations were a close third.
- Roads and bridges, residences and businesses, and the environment were ranked as most at risk, respectively.

Full results of the survey are included in Appendix D.

Review of Planning Documents

As part of a previous project, Dewberry conducted a review of planning and regulatory documents from the 17 communities in the region. To supplement that review, representative plans from urban, rural and coastal communities were also performed as part of this project. Reviews included:

- Plans of Conservation and Development (POCD)
- Hazard Mitigation Plans (HMP)
- Coastal Resilience Plans (CR)
- Zoning / Subdivision Regulations

Findings from the review included:

- Thirteen of the 17 communities have a flood/hazard element or chapter in their POCD.
 - East Hampton, Lyme, Middletown and Old Lyme do not
 - Most do not get specific about flooding type and trends as they are broader-based, long term policy documents.
 - Older plans (not updated in the last 3-5 years) do not address climate change in a comprehensive way.
 - Most or all do not call out increased intensity rainfall events and associated drainage flooding issues.
- All of the communities have or participate in a regional hazard mitigation plan.
 - Most plans use FEMA inundation mapping, coastal storm surge, and sea level rise layers to evaluate risk
 - Some plans mention high intensity rainfall events as problematic, but most do not address it in terms of climate change.
 - Many plans address “hot spots” of localized flooding, mostly anecdotally.
 - Many plans have mitigation actions that address specific infrastructure or drainage improvements.
- Old Saybrook is the only community in the region that is developing a Coastal Resiliency Plan.
- Most Zoning and National Flood Insurance Program (NFIP) ordinances rely on FEMA mapping alone for regulating flood prone development.
- Subdivision and site plan review usually include peak flow and stormwater volume provisions.
 - Most look at existing sources of rainfall data to design – not future conditions.

Applications of Flood Susceptibility Mapping and Climate Data

This section builds upon the findings from the survey, review of plans, and discussions at the workshops (primarily Workshop 3) to outline some of the ways that the data from this study can be practically utilized at the local level to increase flood resilience. It is not intended to be an exhaustive analysis of practical applications. The U.S. Environmental Protection Agency (EPA) published a document entitled: *Planning for Flood Recovery and Long-Term Resilience in Vermont: Smart Growth Approaches for Disaster-Resilient Communities (EPA 231-R-14-003 – July 2014)*. In addition to the applications discussed below, that document provides an excellent overview of flood recovery and resilience actions that can be taken at the local level. In the appendices of the document is a Flood Resilience Checklist. That appendix is included for reference in this document as Appendix E.

Plans of Conservation and Development

Communities can use the study and associated mapping to incorporate discussion of flooding other than the Federal Emergency Management Agency (FEMA) mapped flood hazard area. Plans could reference the flood susceptibility mapping and the importance of increased scrutiny on development and infrastructure siting in areas outside of the FEMA mapping that share flood risk factors in common. The susceptibility mapping is more granular than the FEMA mapping and includes areas outside of the FEMA mapped floodplain. The FEMA mapping program typically only studied sub-watersheds greater than one square mile. The focus was on developed areas and those where development was anticipated at that time. Many areas were purposefully not mapped by FEMA to save limited resources or because development was not expected to occur there at the time of mapping, which in most cases was more than a decade ago. A complete listing, by water body, including dates studied and methods used can be found in Sections 1.0 and 2.0 of the February 6, 2013 FEMA Flood Insurance Study report for Middlesex County, Connecticut. The susceptibility mapping created by this project includes all land area in the region. For the towns of Lyme and Old Lyme, the same listings are available in the same sections of the August 5, 2013 FEMA Flood Insurance Study report for New London County, CT.

Discussion of the factors that contribute to flooding, as identified in the report, can be used to guide policy that will ensure that future activities are not making those factors contribute more (e.g. increases in impervious surfaces). Areas outside of the FEMA mapped floodplain could be noted for further evaluation and, if warranted, conservation.

In general, POCDs can use the data to encourage review of subdivision and development review policies to incorporate flood susceptibility outside of the FEMA floodplain. POCDs can reference Hazard Mitigation Plans for more specific strategies and actions. Use of climate change projections to compare how current return periods are projected to change. For example, Fig. 3-14 (above) shows that today's 100-year 24-hour rainfall event will become a ~53-year event in 2045, while Fig. 3-15 (above) shows that it will become a ~45-year event in 2075. More drastic changes are seen for more frequent events. For example, a current 20-year event will become a ~12-year event by 2045 and a ~8-year event by 2075. Thus, one method of assessing the practical impacts from these changes is by determining which present-day recurrence intervals (e.g. 100-year) are important for design standards and/or flood warning plans and building socioeconomic models of how a more frequent occurrence of such events will impact response and/or recovery costs.

Hazard Mitigation Plans

Many of the applications noted for POCDs can also be applied to Hazard Mitigation Plans (HMPs). Additionally, the following uses should be considered:

- Use flood susceptibility mapping to overlay and quantify what is at risk in areas outside of the FEMA Special Flood Hazard Area (SFHA).
- Evaluate contributing factors to determine what mitigation could be done to minimize their impacts.
- Compare and align mapped areas of susceptibility with community identified “hot-spots” of flooding.
- Use the model and mapping to prioritize mitigation actions.
- Build in a strategy to periodically update the model with new storm data or higher resolution datasets in general.
- Identify strategies to further study most impactful susceptible areas (e.g. physical models).

Zoning and Ordinances

The following are a few examples of considerations for updating zoning regulations or ordinances:

- Consider using flood susceptibility mapping to create or contribute to a flood hazard overlay zone.
- Create a future flood conditions overlay based on climate change analysis.
- Consider using flood susceptibility mapping done at a local scale to help inform some level of protection for new construction in susceptible areas not on FEMA mapping (e.g. graduated risk zones).
- Require developers to conduct further analysis of flood potential (e.g. physical models) in susceptible areas not mapped by FEMA.

Design Standards for Subdivisions and Site Plan Review

Many communities already use some or all of the techniques described below to reduce increase flood flows and volume resulting from new development. In general, development in areas identified on the susceptibility mapping should undergo additional scrutiny. If further “in-field” analysis confirms that areas outside the FEMA Special Flood Hazard Areas (SFHA) that are identified as susceptible, based on common flood risk factors, are indeed at risk, floodplain building design and development standards should be used in those areas.

- Consider using or developing a stormwater model ordinance for green infrastructure.
- Require developers to make decisions informed by future climate, and local governments to incorporate climate change into decision-making processes.
- Use Bioretention to collect stormwater runoff.
- Use permeable pavement to allow runoff to flow through and be temporarily stored prior to discharge.
- Use Underground storage systems to detain runoff in underground receptacles.
- Use retention ponds to manage stormwater.
- Use extended detention wetlands to reduce flood risk and provide water quality and ecological benefits.

Capital Improvement Planning

During the annual budgeting cycle, the results of this study could be used to:

- Assist with prioritization of stormwater improvement projects;
- Assist with decision making around siting infrastructure and public facilities; and,
- Make arguments for the funding of additional studies in identified susceptible areas.

Emergency and Evacuation Planning

Areas on the flood susceptibility mapping, particularly those that are not mapped by FEMA and which intersect with roads and bridges, should be considered when developing flood evacuation routes. Overlaying the mapping with more local transportation layers will identify areas to be further evaluated for low lying roadways.

Long Term Recovery Planning

In the event of a catastrophic flooding event, such as Hurricane Sandy, or a large dam breach, mapped areas of susceptibility could be considered in the rebuilding decision making process.

5. Summary

Flooding is one of the most severe and potentially devastating natural disasters that can occur. Awareness of areas that are currently prone and will be more prone to flooding in the future is essential to consider in short-term, as well as long-term, planning. Such awareness comes from an understanding of a combination of not only regional climatic factors, but also of non-climate factors that relate to regional and site characteristics.

A summary and conclusions from the flood susceptibility analysis can be found in Giovannettone et al. (2018). One important disclaimer about the flood susceptibility map that was developed herein is that it was created for present-day conditions and is only to be used for planning purposes. There are several prominent factors that could affect the *future* flood susceptibility map: changes in impervious area (through urbanization), a higher sea level (for coastal areas) and heavier precipitation. A *future* flood susceptibility map can be created by studying how these factors are expected to change. However, it is expected that the present-day flood susceptibility map provides an excellent relative foundation from which to consider future changes. In other words, it is logical to assume that higher-risk present-day regions will remain as higher-risk regions in the future. As part of this study an Environmental Systems Research Institute, Inc. (ESRI) geographic information system ArcGIS software map document file is available for the region's municipalities for future planning analysis containing the flood susceptibility, land use, and critical infrastructure datasets created as part of this project. Please contact the Lower Connecticut River Valley Council of Governments to obtain this data.

Regarding climatic factors affecting the LCRVR, it was found that El Niño correlates with total rainfall at Middletown and Cockaponset State Forest (significance at the 0.05% and 0.01% levels, respectively) when using a lead time of 12 months, whereas the Caribbean SST index showed stronger correlation strength at a 48-month lead time (significance at the 0.01% level for both). The strength and significance of these correlations and the fact that future 48-month precipitation could be predicted

with substantial skill using statistical models based on these correlations demonstrates the potential for using such an analysis as a tool to estimate the onset and persistence of long-term extreme events. Insight into the onset and persistence of a present or future drought with a 48-month or even a 12-month lead time represents valuable information within the water resources management and agricultural sectors, for example.

Local- and regional-scale statistical analyses were also performed for the city of Hartford and for a region encompassing several Mid-Atlantic and Northeastern states, respectively, to detect changes in historical rainfall statistics over the LCRVR. Slight linear trends in the Annual Maximum Series and Peaks-Over-Threshold were identified at Hartford but were not found to be significant. In contrast, several gauges, including some within Connecticut, revealed statistically positive trends. It was also found that there were significant increases in heavy rainfall at several locations on a regional basis, but less so when looking at more frequency rainfall events. Also, even though local-scale analyses of rainfall within the LCRVR revealed no significant increase in heavy rainfall intensity and frequency at Hartford, the fact that significant regional-scale increases were identified suggests that it is likely against the odds that the LCRVR has not seen an increase in heavy rainfall activity. The contrast between the local and regional analyses is likely due to the hit-or-miss character of heavy rainfall events. An analysis of future rainfall projections was then conducted to determine how heavy rainfall will change over the LCRVR in the mid- and long-term future.

An analysis of future rainfall projections was then conducted to determine how heavy rainfall will change over the LCRVR in the mid- and long-term future using bias-corrected data from the IPCC's CMIP5 modeling experiments and the high emission scenario. Final conclusions related to future projections, in addition to the historical analysis, can be summarized as follows:

- Results from the local-scale historical analysis reveal that a significant change in heavy rainfall statistics at Hartford, which serves as a good proxy for the LCRVR, has not been detected.
- A regional-scale historical analysis did reveal that heavy rainfall events are being disproportionately influenced by climate change, as opposed to a transition to an overall wetter climate, at additional locations in close proximity to the LCRVR.
- Local future analyses revealed increases in projected mid-term (2045) and long-term (2075) Precipitation-Frequency curves at the city of Hartford for all event frequencies.
- Future analyses at Hartford also revealed that today's 100-year 24-hour rainfall event is estimated to become a ~53-year event in 2045 and a ~45-year event in 2075
- Even though the historical analysis revealed a heavier influence of climate change on less frequency events, future projections are suggesting that more drastic changes will occur for more frequent events.

These conclusions demonstrate the importance of determining which present-day recurrence intervals (e.g. 100-year) are important for land use and recovery planning, hazard mitigation, zoning, design standards and/or flood warning plans and then building socioeconomic models to show how a more frequent occurrence of such events will impact response and/or recovery costs.

6. Future Work

Projects and studies that utilize novel methods in accomplishing their final objectives typically identify several additional new directions in which to extend the work as well as additional questions that come

up as a result of the analysis and final conclusions. The current project is no exception with the following list providing potential avenues for future work:

- Utilize local experts' and residents' experiences related to flooding in the region to ground-truth the 100-year flood susceptibility map that was developed in the current study.
- Maintain awareness of data collection for future events. Given the increase in forecast skill of severe floods, it may be possible for River COG to work with its neighbors/partners to make sure that any future flood inundation events are well sampled by specialized satellite and/or synthetic aperture radar missions. These would provide the horizontal resolution to significantly enhance the current model past the 30-m grid size.
- Create additional flood susceptibility maps for more frequent flood exceedance frequencies using the method used for the 100-year flood events. This is limited by the availability of satellite data during maximum inundation caused by the flood, but images for very frequent events (e.g. 5-year) should be available and would provide inundation information for floods that are considered a frequent annoyance rather than a potentially rare disaster.
- Re-run the analysis for future flood events. If and when a flood event occurs in the future over the LCRVR and resources and satellite imagery permitting, recreate a flood susceptibility map for the exceedance frequency associated with the event. The final goal would be to analyze a sufficient number of events of varying frequencies to enable interpolation of the risk factor regression coefficients for any flood event exceedance frequency.
- Test the effect of the flood risk factor 'impervious area' by performing the logistic regression while excluding the flood risk factor 'land cover'. 'Impervious area' did not show a strong correlation with flooding as indicated by the low regression coefficients in Table 2-2, while 'land cover' did show an increasing trend between the rural and urban sub-regions. One hypothesis for this result concerns the fact that 'land cover' and 'impervious area' overlap in terms of the type of information that they convey; this may affect the results in that one of these risk factors (e.g. 'land cover') drowns out the effects of the other (e.g. 'impervious area'). This hypothesis can be tested by rerunning the analysis without considering 'land cover' to determine if the contribution of 'impervious area' becomes more significant.
- Encourage the development of improved datasets related to flood risk factors that were identified as having substantial impacts on flooding in each sub-region; this would include the flood-risk factors 'elevation', 'distance to water', and 'land cover'. Improved resolutions (e.g. 30 meters to 1 meter) of each input dataset would contribute substantially to improved flood susceptibility maps at any desired exceedance frequency.
- As resources permit, flood susceptibility map(s) should be revised, which includes rerunning the analysis described in this report, as improved datasets of flood risk factors become available.

7. References

- Brekke, L., B. L. Thrasher, E.P. Maurer, and T. Pruitt. (2013) "Downscaled CMIP3 and CMIP5 climate projections: release of downscaled CMIP5 climate projections, comparison with preceding information, and summary of user needs." *US Department of the Interior, Bureau of Reclamation, Technical Service Center, Denver, Colorado, USA.*
- Castro, C.L., H.I. Chang, L.O. Mearns, and M.S. Bukovsky. (2015) "Trend of climate extremes in North America: A comparison between dynamically downscaled CMIP3 and CMIP5 simulations." In *American Geophysical Union Fall Meeting Abstracts.*

- Giovannettone, J., T. Coperhaven, M. Burns, and S. Choquette. (2018) "A statistical approach to mapping flood susceptibility in the Lower Connecticut River Valley Region". *Water Resources Research*, accepted.
- Giovannettone, J. (2017) "Correlating MJO activity with Argentina rainfall and Atlantic hurricanes using ICI-RAFT". *Journal of Hydrologic Engineering*, 22. DOI: 10.1061/(ASCE)HE.1943-5584.0001249
- Flato, G., J. and co-authors. (2013) Evaluation of Climate Models. In: *Climate Change 2013: The Physical Science Basis. Contribution of Working Group I to the Fifth Assessment Report of the Intergovernmental Panel on Climate Change* [Stocker, T.F., D. Qin, G.-K. Plattner, M. Tignor, S.K. Allen, J. Boschung, A. Nauels, Y. Xia, V. Bex and P.M. Midgley (eds.)]. Cambridge University Press, Cambridge, United Kingdom and New York, NY, USA.
- Kam, J., and Co-authors. (2016) Multimodel Assessment of Anthropogenic Influence on Record Global and Regional Warmth During 2015 [in "Explaining Extremes of 2015 from a Climate Perspective"]. *Bulletin of the American Meteorological Society*, **97** (12), S4 –S8, doi:10.1175/BAMS-D-16-0149.
- Melillo, J.M., T. Richmond, and G.W. Yohe (eds.). (2014) "Climate Change Impacts in the United States: The Third National Climate Assessment." *U.S. Global Change Research Program*.
- Menne, M.J., et al. (2012) "An overview of the global historical climatology network-daily database." *Journal of Atmospheric and Oceanic Technology*, **29**, 897-910.
- National Oceanographic and Atmospheric Administration (NOAA). (2016) "Climate indices: Monthly atmospheric and ocean time series." Accessed 16 February 2016. [Available online at <https://www.esrl.noaa.gov/psd/data/climateindices/list/>]
- Perica, S., et al. (2015) "NOAA Atlas 14 Volume 10 Version 2, Precipitation-Frequency Atlas of the United States, Northeastern States." NOAA, National Weather Service, Silver Spring, MD.
- Prein, A.F., et al. (2017) "The future intensification of hourly precipitation extremes." *Nature Climate Change*, **7**, 48-52.
- Themeßl, M.J., Gobiet, A., and A. Leuprecht. (2011) "Empirical-statistical downscaling and error correction of daily precipitation from regional climate models." *International Journal of Climatology*, **31**, 1530-1544.

APPENDIX A: Input Data Metadata

Table A-1: NA-CORDEX experiments used for this analysis. All simulations were conducted using 11-km resolution modeling and RCP8.5 scenario boundary conditions.

Modeling Agency Responsible for Global Climate Model	Global Climate Model (Boundary)	Regional Climate Model
Canadian Centre for Climate Modeling and Analysis (Canada)	CanESM2	CanRCM4
Geophysical Fluid Dynamics Lab (United States)	GFDL-ESM2M	RegCM4
Geophysical Fluid Dynamics Lab (United States)	GFDL-ESM2M	WRF
Met Office Hadley Centre (United Kingdom)	HadGEM2-ESM	RegCM4

APPENDIX B: NOAA Atlas 14 Heavy Precipitation Statistics for the Lower CT Region

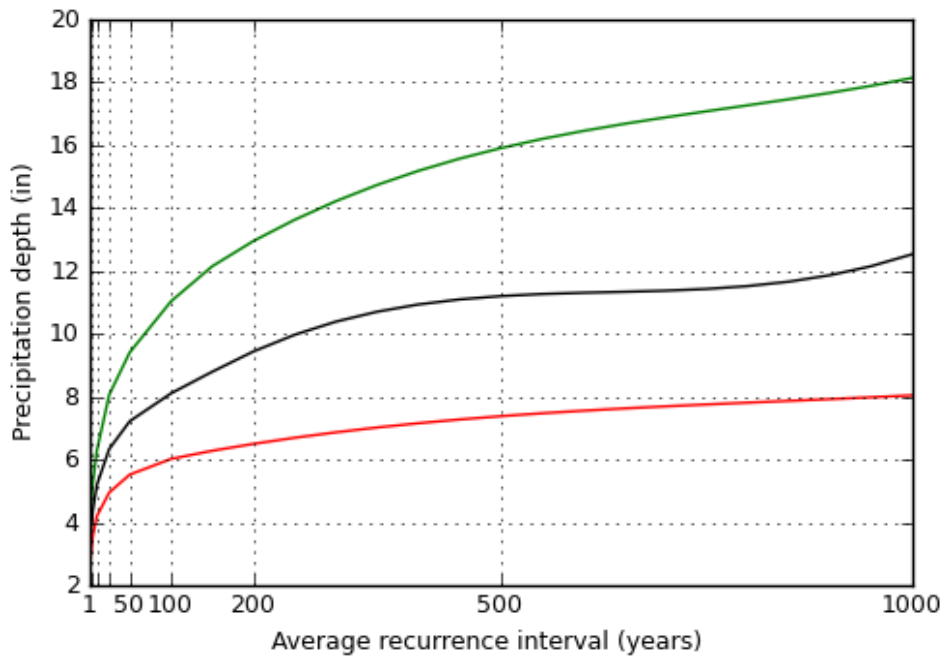


Figure B-1: Precipitation-frequency curves for 24-hour rainfall for a location near Middletown, CT. The black curve is the most likely estimate, while the green and red curves denote the high and low bounds using the 90% confidence level.

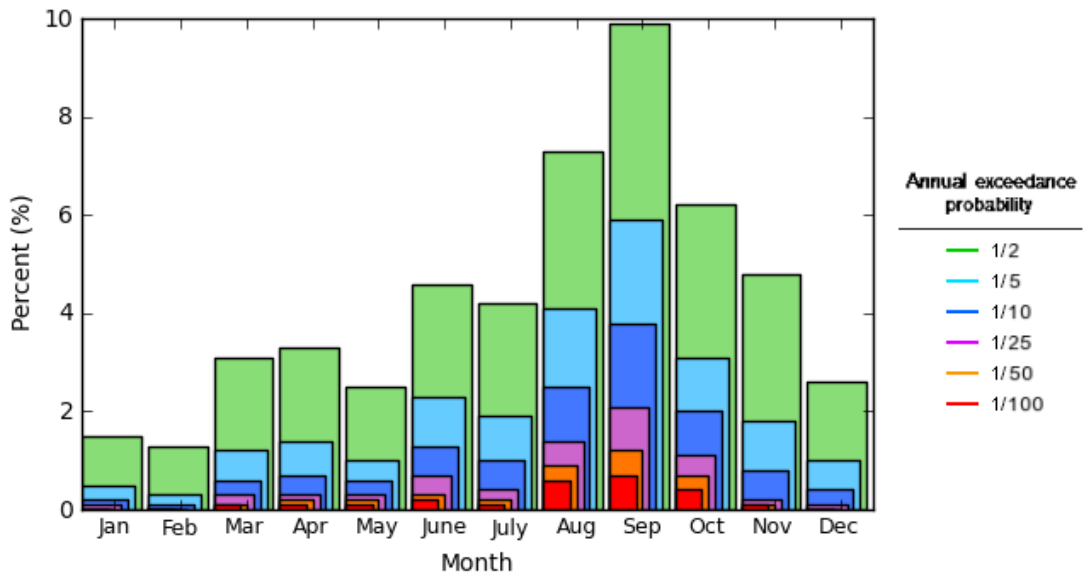


Figure B-2: Seasonality analysis for 24-hour precipitation for a location near Middletown, CT (same location as Fig. B-1). The percent chance of observing an event exceeding the indicated threshold is shown for the 2-, 5-, 10-, 25-, 50- and 100-year recurrence interval. Note that the late summer and fall months show the highest probabilities of occurrence.

APPENDIX C: Climate Modeling

A substantial amount of evidence (Flato et al. 2013) exists showing that climate change has already begun to affect the distributions of atmospheric variables. Figure C-1 shows the simulation of global temperature from a complementary set of Global Climate Model experiments with (red line) and without (blue line) anthropogenic emissions of greenhouse gases (Kam et al. 2016). Note the simulations with anthropogenic emissions are in excellent agreement with historically observed temperature (black line). The modeling suggests that, at least for temperature, the separation point after which the anthropogenic-forced climate differs from its natural state occurred in the late 1970s. This provides a complication for the stationarity analysis herein, since choosing stations (even those with long records) that have limited observations after the 1970s will be less affected by climate change than those with a more recent record. To address this issue, we removed stations that did not have a qualifying record after 2007, providing about 30 years of “climate-change affected” data.

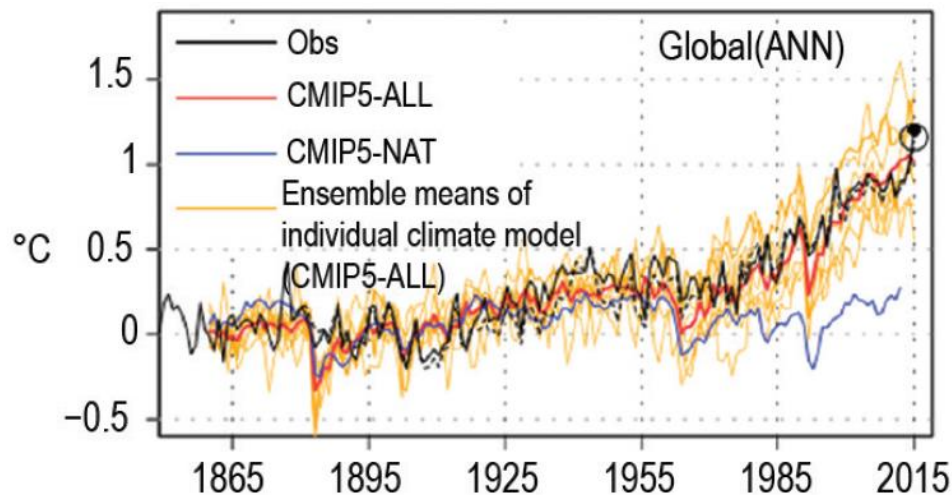
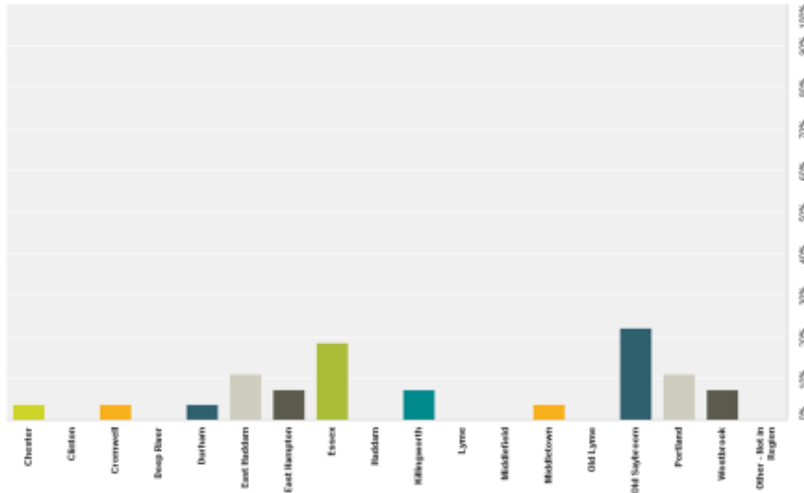


Figure C-1: Annual mean surface temperature anomalies (°C) for the globe. Red (CMIP5-ALL) and blue (CMIP5-NAT) curves indicate ensemble mean simulated anomalies through 2015 and 2012, respectively, with each available model weighted equally; orange curves indicate individual CMIP5-ALL ensemble members. Black curves indicate observed estimates from HadCRUT4v4 (solid) and NOAA NCEI (dotted). All time series are adjusted to have zero mean over the period 1881–19. [Reproduced from Kam et al. 2016; their Fig. 2.1(e)].

APPENDIX D: Community and Stakeholder Survey Results

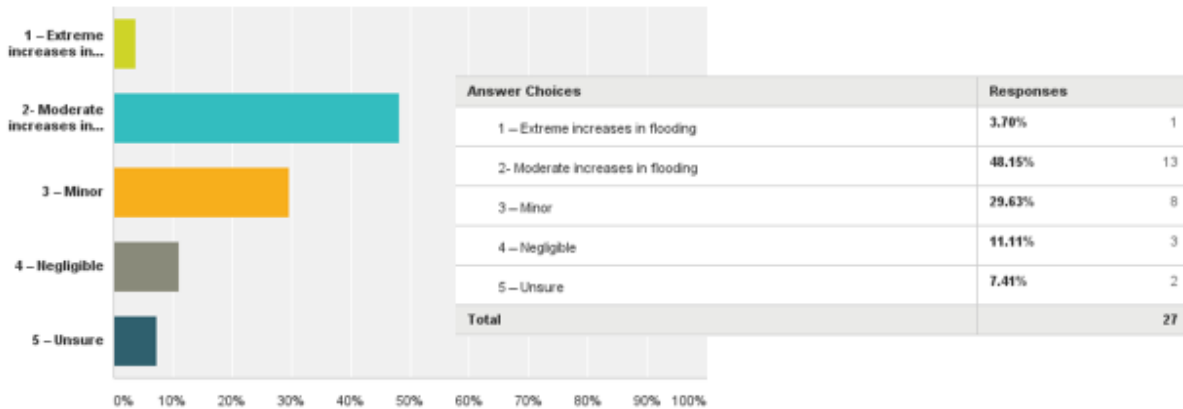
Q2: Community you are from or represent?



30 | Resilient Lower CT River Valley



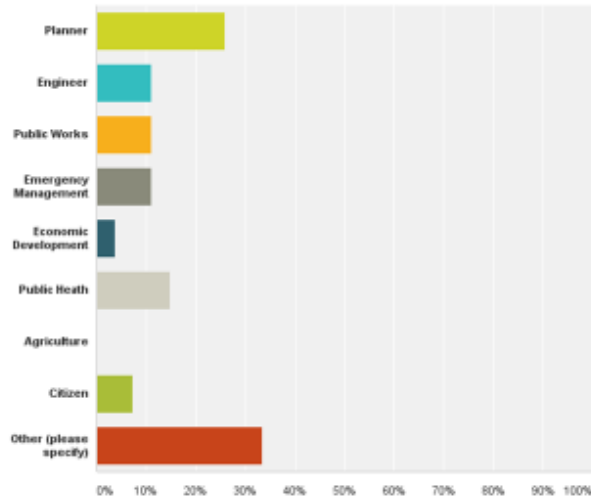
Q3: On a Scale of 1-5, in the last ten years, how would you rate changes in flood conditions due to high intensity rainfall events in your community?



31 | Resilient Lower CT River Valley



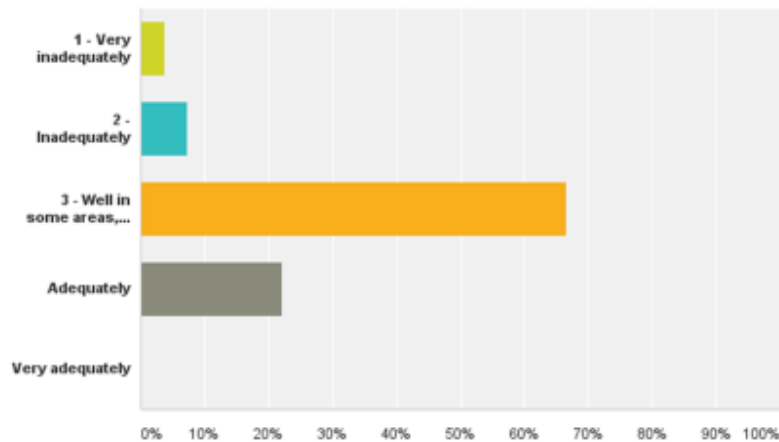
Q1: What is your position in your Community?



29 | Resilient Lower CT River Valley



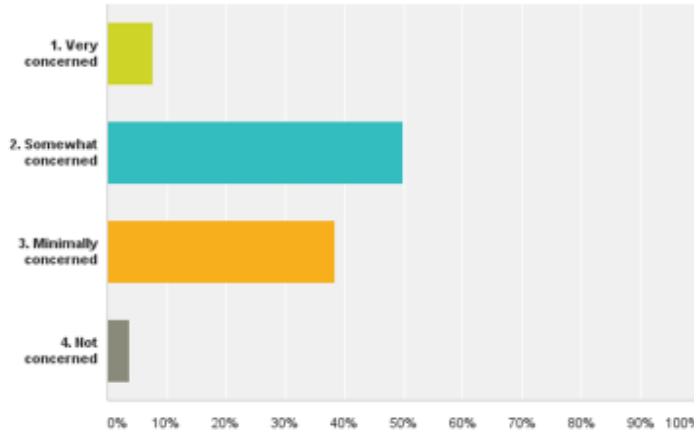
Q4: Overall, how would you rank your municipal storm water systems' ability to handle future storm events?



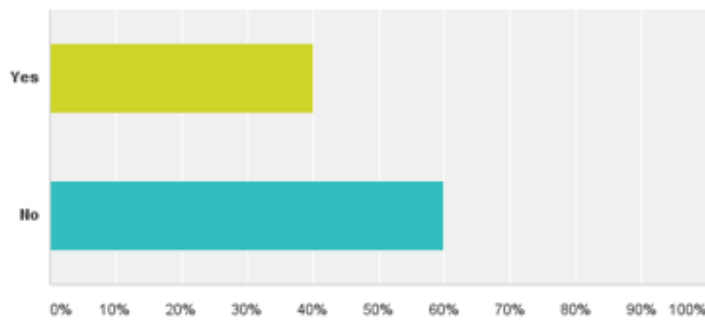
32 | Resilient Lower CT River Valley



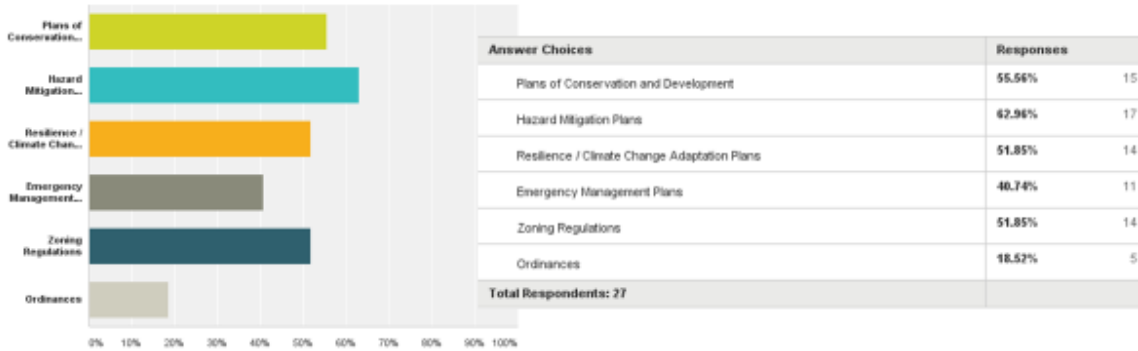
Q6: On a scale of 1-4, how concerned are residents in your community/region with the impacts of climate change?



Q5: Do you believe that your community's Region's plans (e.g. hazard mitigation, conservation and development, emergency management, etc.) adequately address the impacts of climate change on future flooding conditions?



Q7: Please choose the top three planning or regulatory instruments that you believe are best suited to address future policy and implementation strategies for reducing future damage due to increased flooding as a result of climate change.



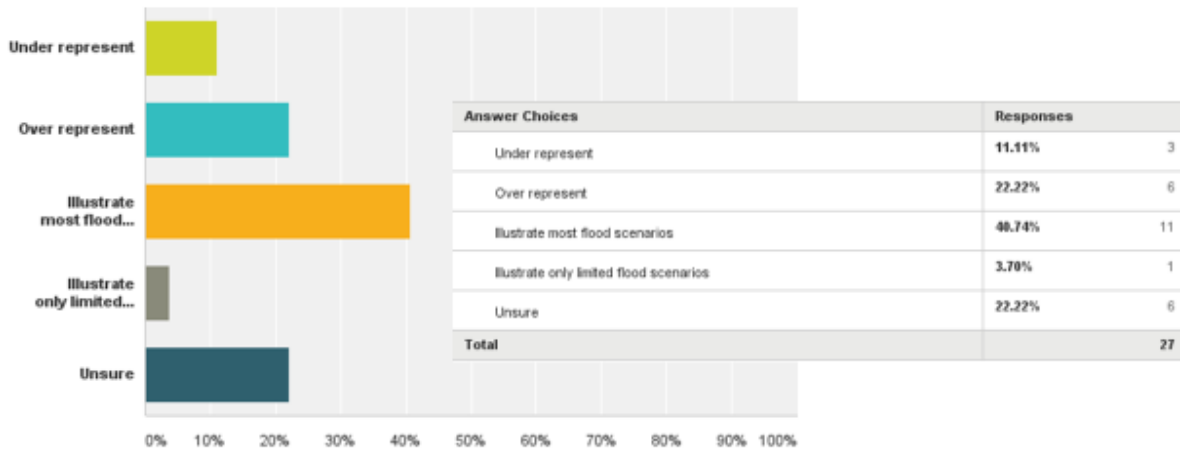
Q8. Please list what you believe to be the most effective way to educate the public on changing hazard conditions.

#	Responses	Date
1	Articles in local papers and posting on Town websites	3/24/2017 9:17 AM
2	A community education program focusing on increasing disaster risks that includes print and social media as well as public presentations. Inclusion in the IPOCD of flood sensitive areas as designated by the local Inland Wetlands Commission/Agent or state designated areas..	3/23/2017 3:47 PM
3	Regulation change, public hearings, articles in publications, social media, email newsletter(constant contact)	3/22/2017 11:19 AM
4	Give power point presentations of a certain area both before and after severe weather conditions adversely affected structure and surrounding area.	3/21/2017 7:21 PM
5	Saybrook Events quarterly magazine.	3/21/2017 4:21 PM
6	Town website information; mailed brochures; emergency text broadcasts	3/21/2017 8:07 AM
7	modelling and providing overlays on GIS mapping made available on Town's website.	3/21/2017 7:27 AM
8	Reverse 911	3/20/2017 7:36 PM
9	Routine education and outreach required by the MS4 Permits (which would have been among 3 choices in answering Q #7).	3/20/2017 1:02 PM
10	mailings, internet	3/20/2017 12:43 PM
11	Small public information meetings in the high hazard areas	3/20/2017 12:41 PM

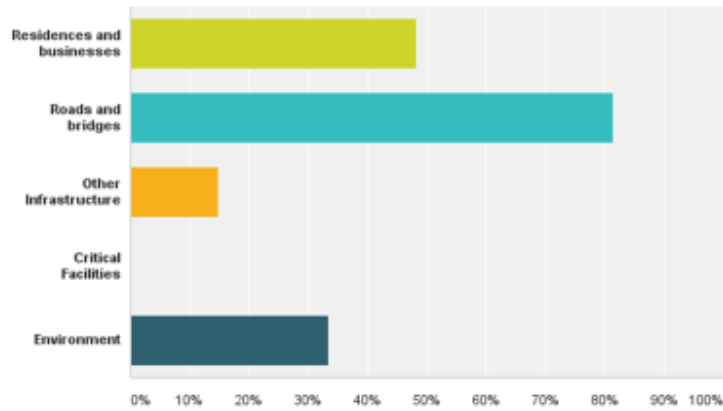
Q8: Please list what you believe to be the most effective way to educate the public on changing hazard conditions.

12	Public awareness campaigns	3/20/2017 12:36 PM
13	Too much money is being wasted on projects such as this. Phone should be used to actually make a difference and not just talk about it.	3/20/2017 12:31 PM
14	Offering local workshops	3/20/2017 12:27 PM
15	A major event can go a long way, as sarcastic as that comment may be.	3/20/2017 12:10 PM
16	Not sure. Those who believe in climate/flood change seem to be attentive. The challenge is educating those who believe this is a myth and reason for higher insurance rates.	3/16/2017 2:06 PM
17	Historical photos of previous events have the most effect. 1936, 1938, 1955, 1982, 1984. Some are so young that they have never been exposed to hazardous events.	3/16/2017 11:55 AM
18	Town Website Town Meetings Outreach Info Tents at events	3/15/2017 2:38 PM
19	direct mail in simple to understand terminology	3/15/2017 10:22 AM
20	Short, easily read articles for our Events magazines and local papers. These cannot be one-off, but sustained over time b/c of the publics' short memory and attention span. Outreach to civic groups who are always looking for speakers.	3/13/2017 4:33 PM
21	Mailing/emailing followed by public information meetings	3/13/2017 3:40 PM

Q9: How do you feel the current FEMA Flood Insurance Rate Maps represent flood risk?



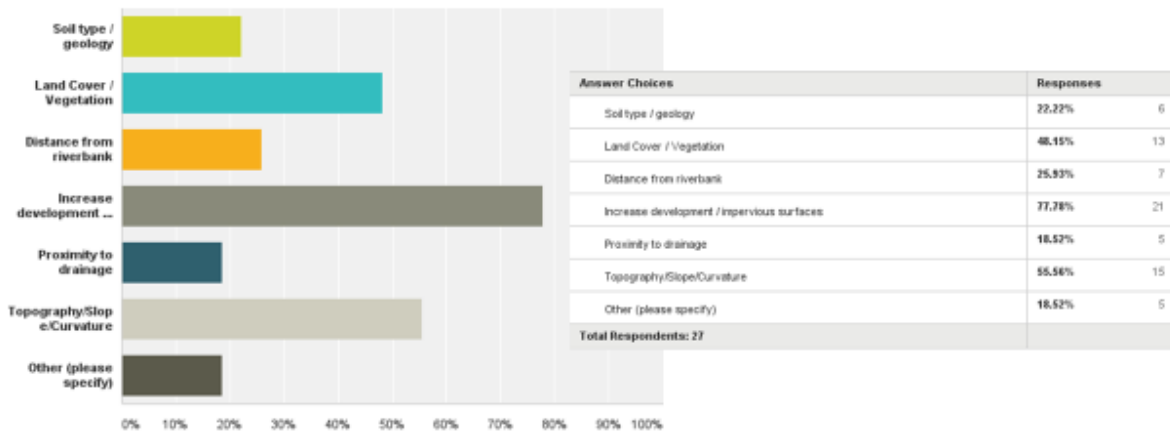
Q10: What assets do you believe are at most risk to flooding from increased rainfall intensity (e.g. flash, riverine, drainage flooding)?



39 | Resilient Lower CT River Valley



Q11: What factors do you think contribute the most to increase flooding from high intensity rain events?



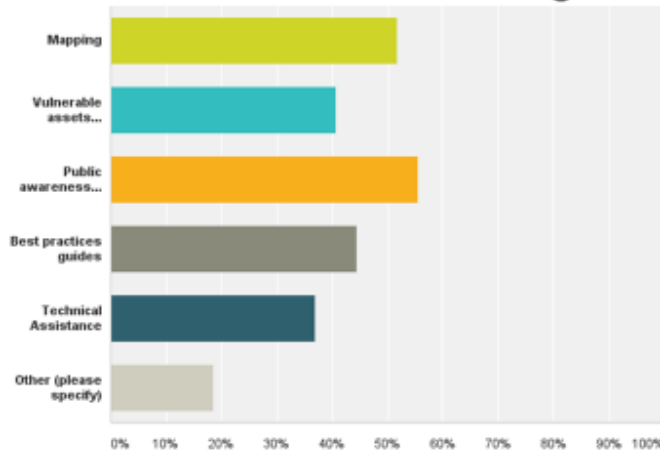
40 | Resilient Lower CT River Valley



Q11: What factors do you think contribute the most to increase flooding from high intensity rain events?

#	Other (please specify)
1	Why are you asking this?
2	Dams. We have several dams in succession which if either were to fail could cause a major flooding event downstream.
3	Inadequately designed drainage systems in some areas
4	Higher rate of intense storms
5	Cromwell has a lot of assets in low lying flood plain areas of the Ct River

Q12: What tools would best assist your community/organization to engage in planning, policy or other actions to reduce future damages from flooding?



Q12: What tools would best assist your community/organization to engage in planning, policy or other actions to reduce future damages from flooding?

#	Other (please specify)
1	Relocation assistance.
2	funding
3	funding for mitigation
4	Again stop the foolish waste of money on projects that just discuss change rather than actually implementing it
5	money

Q13: Opportunity to Provide Comments

#	Responses
1	Portland has experienced multiple flash flood events in our Village District/Main Street business zone as a result of high intensity rainfall events since 2011. These floods have resulted in damage to municipal, school, and commercial buildings.
2	Killingworth has damaging flooding events every few years; I'm not sure the frequency has increased. Would like to see some data on this.
3	How will you orient the staff at the local level to the results of your Study and how it can be used throughout the Region? (Please don't say: by handing it to the First Selectman at a COG meeting.)
4	We know what is needed to be able to address flooding from high intensity/short duration rainstorms, but we don't have the funds to address the needs
5	This issue could be the biggest challenge facing our shoreline towns, without much progress seen to date to deal with rise in sea level.
6	Please fix the spelling of Old Saybrook
7	it is our understanding that FEMA will be updating maps in 2018?

APPENDIX E: Flood Resilience Checklist

Planning for Flood Recovery and Long-Term Resilience in Vermont

Appendix C: Flood Resilience Checklist

Is your community prepared for a possible flood? Completing this flood resilience checklist can help you begin to answer that question.

What is the Flood Resilience Checklist?

This checklist includes overall strategies to improve flood resilience as well as specific strategies to conserve land and discourage development in river corridors; to protect people, businesses, and facilities in vulnerable settlements; to direct development to safer areas; and to implement and coordinate stormwater management practices throughout the whole watershed.

Who should use it?

This checklist can help communities identify opportunities to improve their resilience to future floods through policy and regulatory tools, including comprehensive plans, Hazard Mitigation Plans, local land use codes and regulations, and non-regulatory programs implemented at the local level. Local government departments such as community planning, public works, and emergency services; elected and appointed local officials; and other community organizations and nonprofits can use the checklist to assess their community's readiness to prepare for, deal with, and recover from floods.

Why is it important?

Completing this checklist is the first step in assessing how well a community is positioned to avoid and/or reduce flood damage and to recover from floods. If a community is not yet using some of the strategies listed in the checklist and would like to, the policy options and resources listed in this report can provide ideas for how to begin implementing these approaches.

FLOOD RESILIENCE CHECKLIST		
Overall Strategies to Enhance Flood Resilience (Learn more in Section 2, pp. 9-11)		
1. Does the community's comprehensive plan have a hazard element or flood planning section?	<input type="checkbox"/> Yes	<input type="checkbox"/> No
a. Does the comprehensive plan cross-reference the local Hazard Mitigation Plan and any disaster recovery plans?	<input type="checkbox"/> Yes	<input type="checkbox"/> No
b. Does the comprehensive plan identify flood- and erosion-prone areas, including river corridor and fluvial erosion hazard areas, if applicable?	<input type="checkbox"/> Yes	<input type="checkbox"/> No
c. Did the local government emergency response personnel, flood plain manager, and department of public works participate in developing/updating the comprehensive plan?	<input type="checkbox"/> Yes	<input type="checkbox"/> No
2. Does the community have a local Hazard Mitigation Plan approved by the Federal Emergency Management Agency (FEMA) and the state emergency management agency?	<input type="checkbox"/> Yes	<input type="checkbox"/> No
a. Does the Hazard Mitigation Plan cross-reference the local comprehensive plan?	<input type="checkbox"/> Yes	<input type="checkbox"/> No

Planning for Flood Recovery and Long-Term Resilience in Vermont

FLOOD RESILIENCE CHECKLIST		
b. Was the local government planner or zoning administrator involved in developing/updating the Hazard Mitigation Plan?	<input type="checkbox"/> Yes	<input type="checkbox"/> No
c. Were groups such as local businesses, schools, hospitals/medical facilities, agricultural landowners, and others who could be affected by floods involved in the Hazard Mitigation Plan drafting process?	<input type="checkbox"/> Yes	<input type="checkbox"/> No
d. Were other local governments in the watershed involved to coordinate responses and strategies?	<input type="checkbox"/> Yes	<input type="checkbox"/> No
e. Does the Hazard Mitigation Plan emphasize non-structural pre-disaster mitigation measures such as acquiring flood-prone lands and adopting No Adverse Impact flood plain regulations?	<input type="checkbox"/> Yes	<input type="checkbox"/> No
f. Does the Hazard Mitigation Plan encourage using green infrastructure techniques to help prevent flooding?	<input type="checkbox"/> Yes	<input type="checkbox"/> No
g. Does the Hazard Mitigation Plan identify projects that could be included in pre-disaster grant applications and does it expedite the application process for post-disaster Hazard Mitigation Grant Program acquisitions?	<input type="checkbox"/> Yes	<input type="checkbox"/> No
3. Do other community plans (e.g., open space or parks plans) require or encourage green infrastructure techniques?	<input type="checkbox"/> Yes	<input type="checkbox"/> No
4. Do all community plans consider possible impacts of climate change on areas that are likely to be flooded?	<input type="checkbox"/> Yes	<input type="checkbox"/> No
5. Are structural flood mitigation approaches (such as repairing bridges, culverts, and levees) and non-structural approaches (such as green infrastructure) that require significant investment of resources coordinated with local capital improvement plans and prioritized in the budget?	<input type="checkbox"/> Yes	<input type="checkbox"/> No
6. Does the community participate in the National Flood Insurance Program Community Rating System?	<input type="checkbox"/> Yes	<input type="checkbox"/> No
<u>Conserve Land and Discourage Development in River Corridors</u> (Learn more in Section 3.A, pp. 14-19)		
1. Has the community implemented non-regulatory strategies to conserve land in river corridors, such as:		
a. Acquisition of land (or conservation easements on land) to allow for stormwater absorption, river channel adjustment, or other flood resilience benefits?	<input type="checkbox"/> Yes	<input type="checkbox"/> No
b. Buyouts of properties that are frequently flooded?	<input type="checkbox"/> Yes	<input type="checkbox"/> No
c. Transfer of development rights program that targets flood-prone areas as sending areas and safer areas as receiving areas?	<input type="checkbox"/> Yes	<input type="checkbox"/> No
d. Tax incentives for conserving vulnerable land?	<input type="checkbox"/> Yes	<input type="checkbox"/> No

Planning for Flood Recovery and Long-Term Resilience in Vermont

FLOOD RESILIENCE CHECKLIST		
e. Incentives for restoring riparian and wetland vegetation in areas subject to erosion and flooding?	<input type="checkbox"/> Yes	<input type="checkbox"/> No
2. Has the community encouraged agricultural and other landowners to implement pre-disaster mitigation measures, such as:		
a. Storing hay bales and equipment in areas less likely to be flooded?	<input type="checkbox"/> Yes	<input type="checkbox"/> No
b. Installing ponds or swales to capture stormwater?	<input type="checkbox"/> Yes	<input type="checkbox"/> No
c. Planting vegetation that can tolerate inundation?	<input type="checkbox"/> Yes	<input type="checkbox"/> No
d. Using land management practices to improve the capability of the soil on their lands to retain water?	<input type="checkbox"/> Yes	<input type="checkbox"/> No
3. Has the community adopted flood plain development limits that go beyond FEMA's minimum standards for Special Flood Hazard Areas and also prohibit or reduce any new encroachment and fill in river corridors and Fluvial Erosion Hazard areas?	<input type="checkbox"/> Yes	<input type="checkbox"/> No
4. Has the community implemented development regulations that incorporate approaches and standards to protect land in vulnerable areas, including:		
a. Fluvial erosion hazard zoning?	<input type="checkbox"/> Yes	<input type="checkbox"/> No
b. Agricultural or open space zoning?	<input type="checkbox"/> Yes	<input type="checkbox"/> No
c. Conservation or cluster subdivision ordinances, where appropriate?	<input type="checkbox"/> Yes	<input type="checkbox"/> No
d. Other zoning or regulatory tools that limit development in areas subject to flooding, including river corridors and Special Flood Hazard Areas?	<input type="checkbox"/> Yes	<input type="checkbox"/> No
Protect People, Buildings, and Facilities in Vulnerable Settlements (Learn more in Section 3.B, pp. 19-26)		
1. Do the local comprehensive plan and Hazard Mitigation Plan identify developed areas that have been or are likely to be flooded?	<input type="checkbox"/> Yes	<input type="checkbox"/> No
a. If so, does the comprehensive plan discourage development in those areas or require strategies to reduce damage to buildings during floods (such as elevating heating, ventilation, and air conditioning (HVAC) systems and flood-proofing basements)?	<input type="checkbox"/> Yes	<input type="checkbox"/> No
b. Does the Hazard Mitigation Plan identify critical facilities and infrastructure that are located in vulnerable areas and should be protected, repaired, or relocated (e.g., town facilities, bridges, roads, and wastewater facilities)?	<input type="checkbox"/> Yes	<input type="checkbox"/> No
2. Do land development regulations and building codes promote safer building and rebuilding in flood-prone areas? Specifically:		

Planning for Flood Recovery and Long-Term Resilience in Vermont

FLOOD RESILIENCE CHECKLIST		
a. Do zoning or flood plain regulations require elevation of two or more feet above base flood elevation?	<input type="checkbox"/> Yes	<input type="checkbox"/> No
b. Does the community have the ability to establish a temporary post-disaster building moratorium on all new development?	<input type="checkbox"/> Yes	<input type="checkbox"/> No
c. Have non-conforming use and structure standards been revised to encourage safer rebuilding in flood-prone areas?	<input type="checkbox"/> Yes	<input type="checkbox"/> No
d. Has the community adopted the International Building Code or American Society of Civil Engineers (ASCE) standards that promote flood-resistant building?	<input type="checkbox"/> Yes	<input type="checkbox"/> No
e. Does the community plan for costs associated with follow-up inspection and enforcement of land development regulations and building codes?	<input type="checkbox"/> Yes	<input type="checkbox"/> No
3. Does the community require developers who are rebuilding in flood-prone locations to add additional flood storage capacity in any new redevelopment projects such as adding new parks and open space and allowing space along the river's edge for the river to move during high-water events?	<input type="checkbox"/> Yes	<input type="checkbox"/> No
4. Is the community planning for development (e.g., parks, river-based recreation) along the river's edge that will help connect people to the river AND accommodate water during floods?	<input type="checkbox"/> Yes	<input type="checkbox"/> No
5. Does the comprehensive plan or Hazard Mitigation Plan discuss strategies to determine whether to relocate structures that have been repeatedly flooded, including identifying an equitable approach for community involvement in relocation decisions and potential funding sources (e.g., funds from FEMA, stormwater utility, or special assessment district)?	<input type="checkbox"/> Yes	<input type="checkbox"/> No
Plan for and Encourage New Development in Safer Areas (Learn more in Section 3.C, pp. 26-27)		
1. Does the local comprehensive plan or Hazard Mitigation Plan clearly identify safer growth areas in the community?	<input type="checkbox"/> Yes	<input type="checkbox"/> No
2. Has the community adopted policies to encourage development in these areas?	<input type="checkbox"/> Yes	<input type="checkbox"/> No
3. Has the community planned for new development in safer areas to ensure that it is compact, walkable, and has a variety of uses?	<input type="checkbox"/> Yes	<input type="checkbox"/> No
4. Has the community changed their land use codes and regulations to allow for this type of development?	<input type="checkbox"/> Yes	<input type="checkbox"/> No
5. Have land development regulations been audited to ensure that development in safer areas meets the community's needs for off-street parking requirements, building height and density, front-	<input type="checkbox"/> Yes	<input type="checkbox"/> No

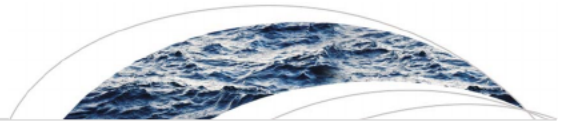
Planning for Flood Recovery and Long-Term Resilience in Vermont

FLOOD RESILIENCE CHECKLIST		
yard setbacks and that these regulations do not unintentionally inhibit development in these areas?		
6. Do capital improvement plans and budgets support development in preferred safer growth areas (e.g., through investment in wastewater treatment facilities and roads)?	<input type="checkbox"/> Yes	<input type="checkbox"/> No
7. Have building codes been upgraded to promote more flood-resistant building in safer locations?	<input type="checkbox"/> Yes	<input type="checkbox"/> No
<u>Implement Stormwater Management Techniques throughout the Whole Watershed</u> (Learn more in Section 3.D, pp. 27-31)		
1. Has the community coordinated with neighboring jurisdictions to explore a watershed-wide approach to stormwater management?	<input type="checkbox"/> Yes	<input type="checkbox"/> No
2. Has the community developed a stormwater utility to serve as a funding source for stormwater management activities?	<input type="checkbox"/> Yes	<input type="checkbox"/> No
3. Has the community implemented strategies to reduce stormwater runoff from roads, driveways, and parking lots?	<input type="checkbox"/> Yes	<input type="checkbox"/> No
4. Do stormwater management regulations apply to areas beyond those that are regulated by federal or state stormwater regulations?	<input type="checkbox"/> Yes	<input type="checkbox"/> No
5. Do stormwater management regulations encourage the use of green infrastructure techniques?	<input type="checkbox"/> Yes	<input type="checkbox"/> No
6. Has the community adopted tree protection measures?	<input type="checkbox"/> Yes	<input type="checkbox"/> No
7. Has the community adopted steep slope development regulations?	<input type="checkbox"/> Yes	<input type="checkbox"/> No
8. Has the community adopted riparian and wetland buffer requirements?	<input type="checkbox"/> Yes	<input type="checkbox"/> No

Water Resources Research

A publication entitled *A Statistical Approach to Mapping Flood Susceptibility in the Lower Connecticut River Valley Region* published in 2018 in *Water Resources Research*, a journal by the American Geophysical Union in 2018, provides more details on the initial research. It is included here, and can be found online at:

<https://agupubs.onlinelibrary.wiley.com/doi/epdf/10.1029/2018WR023018>



Water Resources Research

RESEARCH ARTICLE

10.1029/2018WR023018

Key Points:

- Elevation, distance to water, and surficial materials had the highest contributions to flood susceptibility throughout the study area
- The contribution of elevation and land use to flood susceptibility increased substantially when comparing the urban to the rural subregion
- Very high and high susceptible areas add over 6% of nonwater and wetland area to the SFHA, including 8% more developed area

Correspondence to:

J. Giovannettone,
jgiovannettone@dewberry.com

Citation:

Giovannettone, J., Copenhaver, T., Burns, M., & Choquette, S. (2018). A statistical approach to mapping flood susceptibility in the Lower Connecticut River Valley Region. *Water Resources Research*, 54, 7603–7618. <https://doi.org/10.1029/2018WR023018>

Received 26 MAR 2018

Accepted 17 AUG 2018

Accepted article online 24 SEP 2018

Published online 12 OCT 2018

A Statistical Approach to Mapping Flood Susceptibility in the Lower Connecticut River Valley Region

Jason Giovannettone¹ , Tom Copenhaver², Margot Burns³, and Scott Choquette⁴

¹Dewberry, Fairfax, VA, USA, ²Dewberry, Denver, CO, USA, ³RiverCOG, Essex, CT, USA, ⁴Dewberry, New Haven, CT, USA

Abstract Flood susceptibility in the Lower Connecticut River Valley Region attributable to nonclimatic flood risk factors is mapped using a quantitative method using logistic regression. Flood risk factors considered include elevation, slope, curvature (concave, convex, or flat), distance to water, land cover, vegetative density, surficial materials, soil drainage, and impervious surface. Values of factors at point locations were correlated to whether a location was located within or outside of the U.S. Federal Emergency Management Agency 100-year Special Flood Hazard Area (SFHA). The Lower Connecticut River Valley Region was divided into urban, rural, and coastal subregions to assess the differences in factor contributions to flood susceptibility between different region types; for each region flood risk factors were extracted from 4,000 points, of which an equal number were within or outside of the 100-year SFHA. Logistic regression coefficients were obtained. It was found that *elevation* and *distance to water* have the greatest contribution to flood susceptibility in the urban and coastal subregions, whereas distance to water and *surficial materials* dominate in the rural subregion. The contribution of *land use* to flood susceptibility increased by over 200% between the rural and urban regions. Probabilities of flooding were computed using each regional logistic regression equation. Several areas classified as *very high risk* (80–100%) and *high risk* (60–80%) were located outside of the SFHA and included several types of infrastructure critical for human health, safety, and education. This study demonstrates the utility of logistic regression as an efficient methodology to map regional flood susceptibility.

Plain Language Summary Flooding is one of the most severe and potentially devastating natural disasters that can occur. Floods can come in many forms, including river, coastal, and flash flooding. Whenever and wherever any of these types of flooding occur, long-term planning and adaptation, preparedness, and response time are all critical factors in reducing the overall impacts. Awareness of areas that are currently prone and will remain prone to flooding in the future is essential to consider in both short-term and long-term planning. Such awareness comes from an understanding of a combination not only of regional climatic factors but also of nonclimate factors that relate to natural, physical, and development characteristics. The current study estimates the risk of flooding throughout the Lower Connecticut River Valley Region (LCRVR) based on site and regional characteristics not related to climate. Several methods were considered to estimate flood risk; the method that was finally selected for this study involves a statistical approach in which a data set having one or more independent variables that produce a binary value of no or yes (0 or 1, respectively) for the dependent variable is analyzed. The independent variables in this case include several nonclimate factors related to flood risk that could potentially affect the region and for which sufficient data were available and are referred to as flood risk factors. Flood risk factors considered include elevation, land slope, land curvature (concave, convex, or flat), distance to water body, land cover, density of vegetation, surface geology, ability of the soil to drain water, and the percent of impervious surface (e.g., pavement). The objective is to link each of the flood risk factors to the dependent variables, which in this case is the occurrence of flooding for a flood event that is estimated to occur on average once in every 100 years. It was found that the overall quality of recent satellite images of the LCRVR during large flood events was not sufficient for the current analysis; therefore, it was decided to use the U.S. Federal Emergency Management Agency 100-year Special Flood Hazard Area (SFHA) to indicate areas where flood inundation would occur. The advantage of using the SFHA and the selected statistical modeling methodology is that they allow the contribution of each flood risk factor within the SFHA to be estimated and then applied to the entire study region to identify additional areas outside of the SFHA that have high flood risk. The LCRVR was divided into three subregions (urban, rural, and coastal) to accentuate the differences in the contributions of each flood risk factor to flood risk between an urban and a rural area and between inland and coastal

areas; for each subregion 4,000 point locations were randomly chosen from which to extract data for each flood risk factor. An equal number of these points were selected in locations that were within and outside of the SFHA for each subregion. Site data for each flood risk factor were extracted and associated with a 1 if the location was within the SFHA and a 0 otherwise. The resulting relations between each flood risk factor and flood occurrence were analyzed so that regression coefficients could be estimated for each factor, the magnitude of which indicates the relative strength of each flood risk factor's influence on flooding in a subregion. It was found that *elevation* and *distance to water* have the most influence on flood risk in the urban and coastal subregions, whereas *distance to water* and *surface geology* dominate in the rural subregion. The contribution of *elevation* and *land use* were also found to increase the most between the rural and urban subregions. The coefficients for each subregion are then used to assign probabilities of flooding to all locations over a grid covering that subregion. The results for each subregion were combined to create an overall flood probability map of the LCRVR. Probabilities were classified *very low risk* (0–20%), *low risk* (20–40%), *medium risk* (40–60%), *high risk* (60–80%), and *very high risk* (80–100%). It was observed that several areas classified as *very high risk* and *high risk* were located outside of the SFHA. Several types of infrastructure critical for human health, safety, and education were finally overlaid on the flood risk map to identify those assets that are most vulnerable to the 100-year flood and may therefore require additional flood risk mitigation.

1. Introduction

Flooding is one of the most severe and potentially devastating natural disasters. Flooding occurs in many forms, including river, coastal, and flash flooding, and arises from a variety of processes such as snow melt, severe precipitation events, storm surge, and on a more long-term scale, sea level rise. Whenever any of these types of flooding occur, long-term planning and adaptation, preparedness, and response time are all critical factors in reducing the overall impacts. The severity of flooding has increased over the last several decades in the northeast and throughout the Mississippi and Ohio River valleys (Peterson et al., 2013) because of a combination of factors related to the development of urban areas along rivers and coasts and potentially climate change, which have contributed to the total cost of flood damage escalating as well (Doocy et al., 2013). Awareness of areas that will be more prone to flooding because of these changes is essential to consider in long-term planning, whereas it can also inform short-term strategies, such as the development of early warning mechanisms (Li et al., 2018; Lopez et al., 2017; Rahman et al., 2013). Such awareness comes from an understanding of a combination not only of climatic factors impacting the region but also of nonclimate factors (e.g., urbanization) that relate to regional and site characteristics as well (Mahmoud & Gan, 2018; Miller & Hutchins, 2017; Zhu et al., 2007).

Various types of hydrological models can be used to model flood susceptibility (Devi et al., 2015) and can be categorized as physically based (Abbott et al., 1986; Gassman et al., 2007), conceptual (Crawford & Linsley, 1966), or data-driven (Gogoi & Chetia, 2011; Kia et al., 2012; Lee et al., 2012; Matori et al., 2014; Siddayao et al., 2014; Ullah & Choudhury, 2013) models. Physically based models rely on an understanding of complex physical processes and represent a mathematically idealized form of the real thing. These models use variables that are functions of both space and time and are measurable. Finite difference equations are used to model the hydrological processes associated with the movement of water. Even though physically based models do not require a large amount of hydrological and meteorological data for calibration, a large number of parameters are required to describe the physical characteristics of the catchment being modeled, including soil moisture, water depth, topography, and river network dimensions. Physically based models are versatile and have the advantage of using parameters that have a physical interpretation, but much time and resources are required to develop such models. There are a myriad of examples of physically based models, two of which include the Soil and Water Assessment Tool (Gassman et al., 2007) and the MIKE Systeme Hydrologique European model (Abbott et al., 1986).

Conceptual models are similar to physically based models in that they attempt to describe all of the component hydrological processes, albeit in a more simplified and less physical process manner. They are composed of interconnected reservoirs that are recharged by sources such as infiltration, percolation, and rainfall and emptied by runoff, evaporation, and drainage, and other types of sinks. The parameters that make up a conceptual model are assessed by analysis of field data and calibration. Unlike physically based model,

conceptual models require an extensive amount of meteorological and hydrological data for calibration, in addition to sophisticated analysis tools, which is not within the scope of the current project. One of the first conceptual models developed was the Stanford Watershed Model IV by Crawford and Linsley (1966).

In contrast to physically based and conceptual models, data-driven or empirical models rely completely on observations and an understanding of the hydrological and meteorological variables and regional characteristics that influence flood susceptibility with no consideration given to the physics of meteorological or hydrological processes. Many types of data-driven models use linguistic variables whose values include words or phrases, rather than the conventional numerical variables used in the models described above. Examples of linguistic data-driven models used for hydrological modeling purposes include (1) fuzzy logic (FL; Gogoi & Chetia, 2011; Hundecha et al., 2001; Sen & Altunkaynak, 2004), (2) artificial neural networks (ANN; Dawson & Wilby, 2001; Kia et al., 2012; Kovacevic et al., 2018), (3) Adaptive Neuro-Fuzzy Interface System (ANFIS; Ullah & Choudhury, 2013; Yaseen et al., 2018; Zounemat-Kermani & Teshnehlab, 2008), and (4) analytical hierarchy process (AHP; Matori et al., 2014; Richardson & Amankwatia, 2018; Siddayao et al., 2014).

The objective in most data-driven models is to produce a list of relative weights for whatever variables and local characteristics have been identified as affecting flood susceptibility; these weights can then be used to produce a flood susceptibility map. The method used to derive these weights represents the major difference between the various forms of data-driven models.

The first type of linguistic data-driven model is FL and is set up using membership functions and rules for factors related to flood susceptibility, hereafter referred to as flood risk factors. A membership function for each factor incorporates various classifications (e.g., high, medium, and low) of that factor. After the variables are partitioned into their different *fuzzy* classes, an IF ... THEN type of rule is set up to establish the response of any combination of these fuzzy classes. For example, Gogoi and Chetia (2011) used a fuzzy rule-based model to forecast runoff in the Jiadhil Basin in Northeast India. The authors used three flood risk factors (total monthly rainfall, mean monthly temperature, and previous month's discharge) and three categories (e.g., high, medium, and low) to describe projected runoff, resulting in a total number of $3^3 = 27$ rules. Sets of values for each variable were then tested against these rules to identify rules that are fulfilled to a point that exceeds a certain threshold value. The identified rules are then used to project runoff based on values of the identified flood risk factors.

The second type of data-driven model is the ANN. ANNs consist of layers of nodes or neurons, which include an input layer (number of neurons equals the number of flood causative factors), an output layer (number of neurons equals the number of types of desired outputs), and one or more hidden layers where algorithms are used to model the complex relations that are expected to exist between each flood risk factor and the influence that they have on the output. In the context of flooding, outputs would be water levels and/or flow. Kia et al. (2012) used ANN to predict water levels and flood inundation using seven potential flood risk factors: rainfall, slope, elevation, flow accumulation, soil, land use/cover, and geology.

Alternatively, the third linguistic model type is the ANFIS, which uses a combination of the numeric power of neural networks and the verbal power of FL. Such a model contains features of both types of models such as learning and optimization abilities and IF ... THEN rule thinking to map an input space to an output space. An example of this method was developed for the Barak River basin in Northeast India by Ullah and Choudhury (2013). Issues with using an ANN, ANFIS, or any other method that incorporates neural networks relate to their complexity and the substantial computing power that is required to run the networks. The quality of the resulting predictions in many cases has also been found to be inferior to other model types (Shorridge et al., 2016) and especially so when the data that are used to validate the model contain values outside of the range of data used to train the model.

The final type of linguistic data-driven model is the AHP. An AHP identifies potential flood risk factors, and their associated weights using expert opinions combined with geographical, statistical, and historical data. For example, Matori et al. (2014) and Siddayao et al. (2014) used an AHP in performing spatial assessments of flood susceptibility in northern Malaysia and the northern Philippines, respectively. Flood risk factors included rainfall, geology, soil type, land use, population density, distance from river bank, and site elevation and slope. The authors in both studies consulted with experts in their study areas and used the survey results to develop weights for each factor. They then combined the resulting weights with a Geographical

Information System to produce a color-coded map representing various levels of risk for each respective study region. The advantage of this method is that the final product is a flood susceptibility map based on the combined experience of several years of flooding events from various type of experts who are familiar with the region. The disadvantage is that the results can be based on subjective and conflicting opinions, especially when there are many flood risk factors being considered. This can be mitigated, however, when using the overall factor weighting mechanisms that are typically used in an AHP.

In contrast to the linguistic models, statistically based data-driven models use mathematical equations that are derived from concurrent input and output data (e.g., unit hydrograph). Regression and correlation models are two examples that attempt to find the functional relationship between the input and output time series. Other more quantitative types of data-driven models include multivariate statistical analysis (Allaire et al., 2015; Sharma et al., 2015; Singh et al., 2009; Wallis, 1965) and multivariate logistic regression (MLR; Park et al., 2017; Pradhan & Lee, 2010; Tehrany et al., 2014), or some combination of these. These methods rely on numerical expressions that characterize the relationships between the independent flood risk factors and flood inundation (Lee et al., 2012). The use of multivariate statistical analysis typically requires several strict assumptions to be made prior to the analysis and requires the relation between flooding and each flood risk factor to be considered independently from any potential relations between factors to develop weights for each factor. MLR can be used to solve this issue by examining the relations between a dependent variable (e.g., whether a location is flooded or not flooded) and any number of independent variables (e.g., flood risk factors; Pradhan & Lee, 2010). An advantage of MLR is that a separate analysis is not required to estimate the weight of each flood risk factor as this functionality is already built into such coding environments as R (R Development Core Team, 2018). Another advantage of MLR is that the variables can be continuous and/or categorical and is straightforward to implement.

Though somewhat ad hoc, after considering all of the advantages and disadvantages of the three major types of models described above (physically based, conceptual, and data driven) and due to the fact that one of the major objectives of the current study was to develop an accurate flood susceptibility mapping methodology that requires little resources in terms of time and money and can be applied not only to the study region used in the current study but also on a larger scale, it was decided to use a data-driven model of the Lower Connecticut River for the current project. In addition, it was decided to use MLR over the other types of data-driven models because of the fact that sufficient data were already available for a number of potential flood risk factors throughout the Lower Connecticut River; therefore, a quantitative relationship between these risk factors and flood inundation, which would provide more accuracy than the linguistic models, would be possible without expending significant additional resources in obtaining the required data. For these reasons, MLR was selected to model flood susceptibility for the current study.

2. Data and Methods

The Lower Connecticut River Valley Region (LCRVR) is located in the southeastern central part of the state of Connecticut and is focused around the confluence of the Connecticut River and Long Island Sound (Figure 1). Whereas the Connecticut River is tidally influenced throughout the study region, there are many smaller rivers and tributaries where the flood threat is primarily driven by local fluvial flooding. This region is also extremely heterogeneous in terms of the various land characteristics that can influence flood susceptibility. For these reasons, and the fact that the state of Connecticut hosts a large and relatively complete database of land and water characteristics throughout the state, the LCRVR was selected as the study region for the current study.

Even though the methodology used to develop the flood susceptibility map of the LCRVR is based on the method used in Tehrany et al. (2014), there are features of this work that differentiate it from previous studies. These studies, for example, all took place outside of the United States and involved land areas substantially smaller than the LCRVR. Because of the small size of each study region, these studies assumed that the study regions were homogeneous in terms of the influence of various regional characteristics on flood susceptibility. In contrast, the LCRVR is the first region within the United States for which the methodology described here has been used and is sufficiently large spatially that the assumption of homogeneity across the study area is less valid than it was in the international studies. The current study, therefore, includes different types of *subregions* (e.g., coastal, rural, and urban) for which separate flood

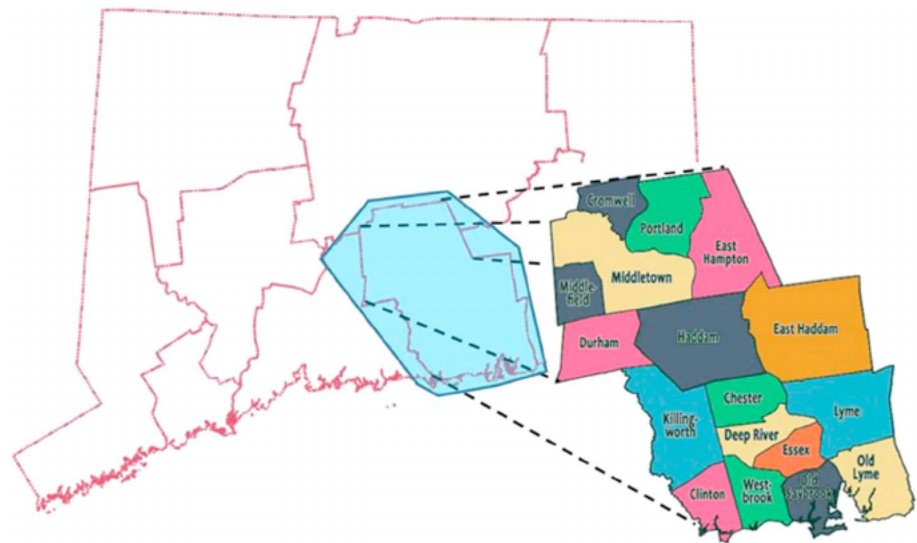


Figure 1. Map showing the location of the Lower Connecticut River Valley Region and the *area of influence* (shaded blue) within the state of Connecticut.

susceptibility analyses are performed and between which comparisons can be made on the influence of subregional characteristics (e.g., land use).

2.1. Flood Risk Factors

There are several types of nonclimatic data that are required as independent variables when using MLR to estimate flood susceptibility; these independent data represent parameters that may contribute to flooding in a region and are referred to as flood risk factors. Flood risk factors that are used for flood susceptibility mapping should be measurable and collected throughout the entire study region but should not represent information that is spatially uniform. Several risk factors may be prominent in one region but not in another; for example, the influence of flood factors will vary when comparing inland versus coastal regions or rural versus urban regions. In general, there is no agreement on which flood risk factors are the standard for any flood susceptibility analysis; however, there are factors that are more prominently used than others. Some of the most common factors are listed in Table 1 along with the citations for a few of the studies in which they were identified as influential. A subset of these flood risk factors was chosen for the present study after considering the availability, period of record, and completeness of each data set as applied to the study region: elevation, slope, land curvature, land cover, distance to water body, vegetation density, percent impervious surface, soil drainage class, and surficial materials. Several of these flood risk factors are related to each other so that some correlation is to be expected. Such correlation is common when a study is performed using MLR because the final objective is to develop a logistic regression that includes all factors that are expected to contribute to flooding and for which sufficient data are available. A potential issue occurs if detailed comparisons are made between the contributions of each flood risk factor; any correlation needs to be teased out if such comparisons are going to be made. Because the main objective of the current study is to provide a logistic regression equation that can be applied to the entire region, in addition to making some simple comparisons or observations related to each flood risk factor's contribution, no attempt was made to estimate these potential correlations.

Sources of flood risk factors for the LCRVR include the U.S. Geological Survey (USGS), the Connecticut Department of Energy and Environmental Protection (DEEP), the U.S. Department of Agriculture-National Resources Conservation Service, and the Federal Emergency Management Agency (FEMA). Abbreviations, sources, and the resolution/scale of each data set are given in Table 2.

All flood risk factor data were collected over the entire study region and compiled into spatial databases using the ArcGIS 10.2 software (Environmental Systems Research Institute, 2014). Flood risk factors *slope* and *curvature* were derived from the elevation data set, whereas the *distance to water* risk factor was computed as the minimum distance as the crow flies between each cell and the nearest water body as

Table 1
Flood Risk Factors and Examples of Studies in Which Each Has Been Considered

Flood risk factors	Literature
Temperature	Gogoi and Chetia (2011)
Previous month's discharge	Gogoi and Chetia (2011)
Population density	Siddayao et al. (2014), Sinha et al. (2008), and Zhang et al. (2005)
Distance from riverbank	Siddayao et al. (2014)
Landform: slope/elevation/curvature	Matori et al. (2014), Siddayao et al. (2014), Tehrany et al. (2014), Lawal et al. (2012), Saini and Kaushik (2012), Sinha et al. (2008), and Zhang et al. (2005)
Distance from access road	Qureshi and Harrison (2003)
Land-use zoning	Lawal et al. (2012) and Qureshi and Harrison (2003)
Drainage density	Lawal et al. (2012) and Saini and Kaushik (2012)
Proximity to drainage	Sinha et al. (2008)
Soil type/drainage	Matori et al. (2014), Tehrany et al. (2014), Lawal et al. (2012), Saini and Kaushik (2012), and Yahaya et al. (2010)
Distance from urban areas	Qureshi and Harrison (2003)
Precipitation/rainfall	Matori et al. (2014), Tehrany et al. (2014), Lawal et al. (2012), Gogoi and Chetia (2011), Yahaya et al. (2010), Zhang et al. (2005), and Qureshi and Harrison (2003)
Land cover/use and vegetation	Matori et al. (2014), Tehrany et al. (2014), Saini and Kaushik (2012), and Yahaya et al. (2010)
Geology	Matori et al. (2014) and Tehrany et al. (2014)
Timber type/size/density	Tehrany et al. (2014)

depicted on the USGS 7.5-min topographic quadrangle maps for the state of Connecticut (DEEP, 2005). All data sets were resampled using linear interpolation to a 30-m × 30-m grid comprised of 2,142 columns (north and south) and 1,957 rows (east and west) for a total of roughly 4.2 million points.

Prior to using each data set in the flood susceptibility analysis, each numerical flood risk factor was divided into classes. This is accomplished using the quantile method (Papadopoulou-Vrynioti et al., 2013; Tehrany et al., 2014; Umar et al., 2014), which partitions each numerical data set (e.g., elevation [0.0–277.5 m], slope [0.0–120.7°], vegetation density [0.0–93.0%], distance to water body [0.0–2,352.7 m], and percent impervious service [0.0–96.1%]) into classes containing the same number of features or pixels per class; partitioning the data in this manner ensures that data are included and that a regression coefficient can be determined for each flood risk factor class. For the purposes of this study, each of the numerical flood risk factor data sets

Table 2
Flood Risk Factors and Flood Event Data With Data Source and Resolution/Scale

Flood risk factors	Source (year)	Resolution/ scale	URL for data access
Land cover (LAND)	USGS (2011)	30 m	https://www.mrlc.gov/
Elevation (ELEV); slope (SLOPE); curvature (CURV)	USGS (2014)	30 m	https://earthexplorer.usgs.gov/
Distance from water (DIST)	DEEP (2005)	1:24,000	https://www.ct.gov/deep/cwp/view.asp?a=2698&q=322898&deepNav_GID=1707
Soil drainage (SOIL)	USDA-NRCS (2017)	varies	https://sdmdataaccess.nrcs.usda.gov/
Vegetation density (VEG)	USGS (2011)	30 m	https://www.mrlc.gov/
Impervious surface (IMP)	USGS (2011)	30 m	https://www.mrlc.gov/
Surficial materials (GEO)	DEEP (2005)	1:24,000	https://www.ct.gov/deep/cwp/view.asp?a=2698&q=322898&deepNav_GID=1707
FEMA 100-year NFHL	FEMA (2016)	1:12,000	https://fema.maps.arcgis.com/home/index.html

Note. USGS = U.S. Geological Survey; DEEP = Connecticut Department of Energy and Environmental Protection; USDA-NRCS = U.S. Department of Agriculture-National Resources Conservation Service; FEMA = Federal Emergency Management Agency; NFHL = National Flood Hazard Layer.

Table 3
Regression Coefficients for Each Risk Factor Class

Factor	Class	Logistic coefficient (C/R/U)	Factor	Class	Logistic coefficient (C/R/U)
a_0	—	5.18/5.06/20.24	DIST (m)	0.00–39.21	—/—/—
ELEV (m)	–2.65–2.84	—/—/—		39.22–117.64	–1.19/–2.16/–1.60
	2.85–20.42	–4.11/–2.17/–14.87		117.65–196.06	–2.01/–3.32/–2.64
	20.43–40.19	–20.48/–1.71/–15.70		196.07–274.48	–2.89/–3.63/–2.59
	40.20–56.67	–18.79/–1.59/–16.27		274.49–392.12	–3.00/–3.99/–3.20
	56.68–75.35	—/–1.40/–16.41		392.13–509.75	–4.63/–4.75/–3.57
	75.36–92.93	—/–1.54/–16.60		509.76–627.39	–4.45/–5.03/–3.87
	92.94–109.40	—/–2.22/–17.26		627.40–784.24	–5.61/–4.89/–4.07
	109.41–128.08	—/–2.53/–18.24		784.25–1,019.51	–19.61/–4.60/–3.91
	128.09–152.25	—/–2.84/–17.52		1,019.52–2,352.71	–17.33/–3.92/–2.68
	152.26–277.50	—/–3.72/–18.00		not rated	—/—/—
CURV	Convex (–6.05 – –0.66)	—/—/—	SOIL	excessively drained	–0.28/0.16/–2.24
	Flat (–0.65–0.65)	0.22/0.07/–0.46		somewhat excessively well drained	–0.19/–0.53/–1.57
	Concave (0.66–6.05)	–0.89/1.79/0.99		moderately well	–0.18/0.05/–1.43
SLOPE	0.00–0.47	—/—/—		somewhat poorly drained	0.03/0.70/–1.33
	0.48–1.89	–0.29/–0.08/–0.10		poorly drained	—/2.52/0.30
	1.90–3.31	–0.11/–0.01/–0.41		very poorly drained	1.02/1.48/–0.65
	3.32–4.73	–0.40/–0.62/–0.85	IMP (%)	0.00–0.00	0.60/1.02/0.68
	4.74–6.62	–0.97/–0.57/–1.06		0.01–1.96	—/—/—
	6.63–8.52	–1.25/–0.92/–1.42		1.97–4.70	–0.89/–1.51/–0.27
	8.53–10.88	–0.79/–0.82/–1.37		4.71–10.98	0.02/–0.21/–0.20
	10.89–14.20	–0.88/–1.39/–2.65		10.99–18.82	–0.19/–0.27/–0.32
	14.21–19.40	–1.29/–1.14/–2.17		18.83–28.62	–0.28/–1.14/–0.34
	19.41–120.72	–0.70/–2.02/–2.40		28.63–38.82	–0.34/–0.44/–0.03
VEG (%)	0.00–0.00	—/—/—		38.83–49.80	–0.21/–0.23/–0.39
	0.01–32.00	–0.20/0.20/0.12		49.81–63.92	0.06/–0.07/–0.57
	32.01–55.00	–0.11/0.29/0.37		63.93–99.61	0.16/–1.32/–1.22
	55.01–70.00	–0.42/–0.34/0.41	GEO	–0.42/–0.31/–0.71	
	70.01–80.00	0.00/0.35/0.32	thin till	—/—/—	
	80.01–86.00	–0.57/0.15/0.77	sand/gravel/talus	0.90/0.89/0.82	
	86.01–88.00	–1.07/0.67/0.86	finer	—/1.77/1.05	
	88.01–89.00	–1.04/0.42/0.83	floodplain alluvium	16.31/3.11/2.91	
	89.01–90.00	–1.26/–0.27/0.33	swamp deposits	0.08/1.37/1.41	
	90.01–93.00	–1.93/–0.31/–0.18	thick till	–0.58/–2.03/–0.73	
LAND	developed, open space	—/—/—	End Moraine deposits	0.08/–1.81/—	
	dev., low intensity	–0.08/–0.04/–0.23	artificial fill	17.30/14.71/2.07	
	dev., med.-high intensity	–0.34/0.04/–0.34	salt/tidal marsh deposits	1.18/13.38/—	
	barren (rock/sand/clay)	0.94/–1.16/–16.55	beach deposits	2.39/—/—	
	forest	0.00/–0.65/–0.95			
	shrub/scrub	–1.89/–1.77/–1.03			
	grassland/herbaceous	–0.20/–0.86/–0.69			
	pasture/hay	–0.10/–1.24/–0.38			
	cultivated crops	1.22/–0.47/–0.93			
	wetlands (woody/emerg.)	0.05/0.35/–0.03			

Note. C = coastal; R = rural; U = urban.

was divided into 10 categories using the classifications given in Table 3; examples of the spatial distribution of two numerical flood risk factors are shown in Figures 2a and 2b for *elevation* and distance to water, respectively. Regarding the other flood risk factor data sets, land curvature was divided into three classes of concavity (not shown); *land cover* was divided into 10 classes (Figure 2c); *soil drainage* was divided into eight classes (not shown); and *surficial materials* was divided into 10 classes (Figure 2d).

2.2. Flood Inundation

The overall objective is to develop relations between flooding and all dependent flood risk factors. Therefore, a method is required to compare the values of each factor at a point with whether flooding would be expected or not expected to occur at that point for a specific flood (annual) return period. Because of the

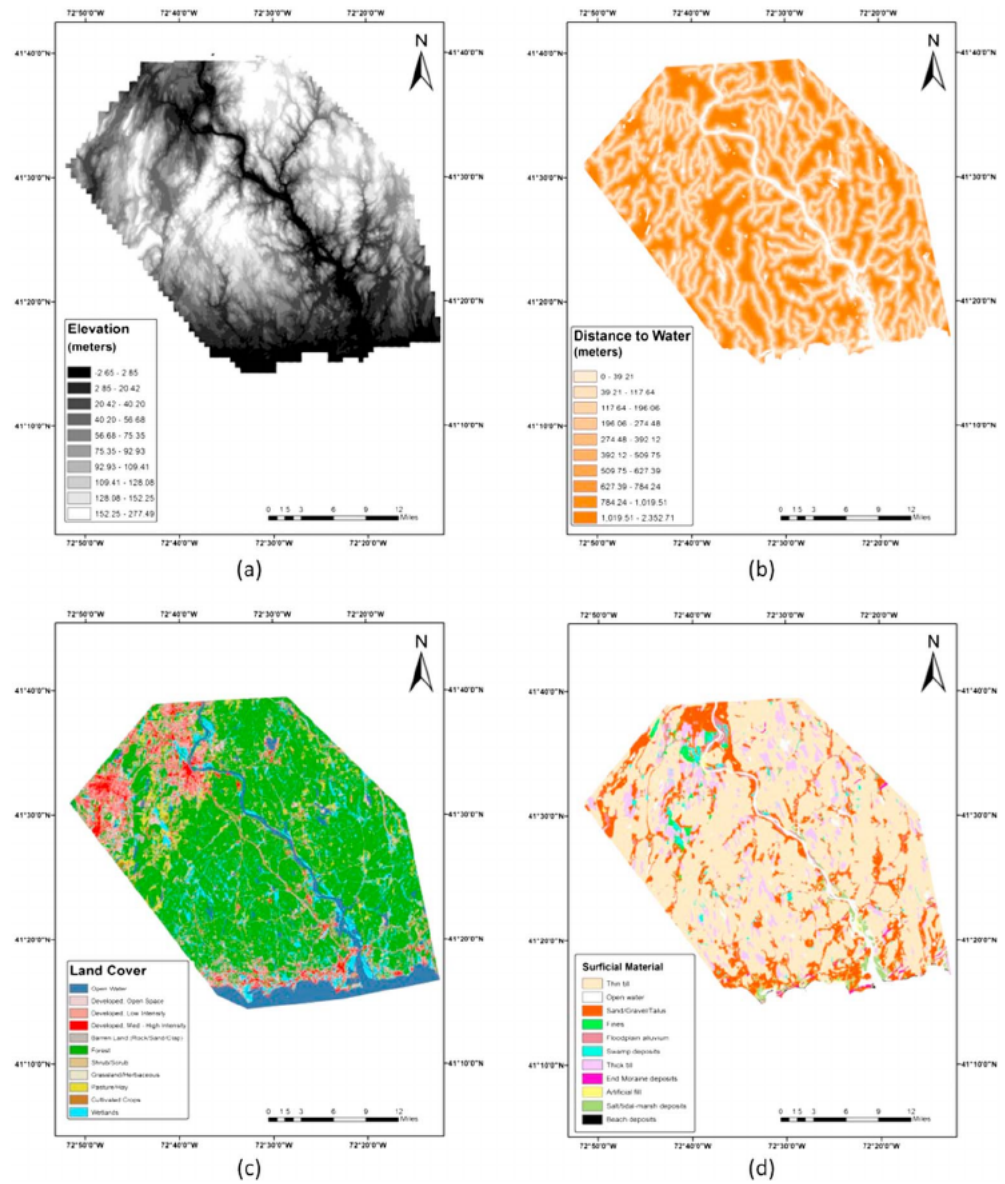


Figure 2. Spatial distribution of flood risk factors: (a) elevation (ELEV), (b) distance to water (DIST), (c) land cover (LAND), and (d) surficial materials (GEO).

fact that there has not been a flood event in the region greater in magnitude than a 1 in 25-year discharge for which USGS/National Aeronautics and Space Administration Landsat satellite images of sufficient quality are available, in addition to noting that the flood inundation delineation for all recent, but minor, flood events falls almost entirely within the boundary of the FEMA 100-year Special Flood Hazard Area (SFHA), it was decided to compare flood risk factors to flood inundation as defined by the FEMA 100-year SFHA (Federal Emergency Management Agency, 2016) for the region (Figure 3) to initially train the statistical model. Flood inundation data from the SFHA were compiled into a spatial database and resampled to a 30-m \times 30-m grid identical to those used for the flood risk factors.

It should be noted that the SFHA has received much scrutiny because of its past dependence on one-dimensional hydraulic models and low-resolution elevation data. For example, Blessing et al. (2017) found that the SFHA missed near 75% of flood claims made by those affected within several municipalities of the southeastern suburbs of Houston, Texas, during five major flood events between the years 1999 and 2009, although the version of the SFHA used in Blessing et al. (2017) would have been updated

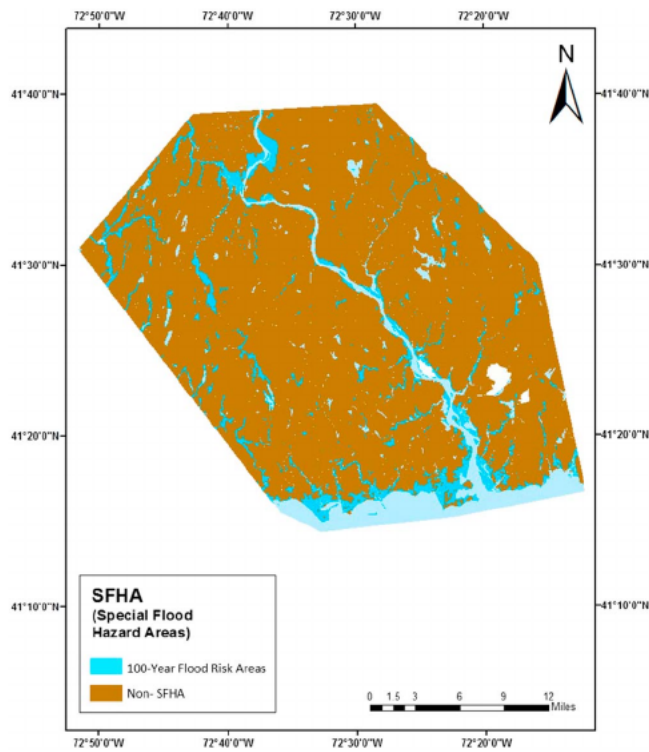


Figure 3. The 100-year Federal Emergency Management Agency SFHA within the Lower Connecticut River Valley Region. Light blue represents open water, whereas dark blue represents land areas within the SFHA.

prior to 1999 and would have employed lower-quality hydrologic and hydraulic models and lower-resolution elevation data than is currently used. In addition, the SFHA only takes into account riverine and coastal flooding, while many coastal events such as Hurricane Harvey are dominated by pluvial flooding. It should be noted that one limitation of the SFHA is that where there are combined effects of riverine and coastal flooding, the modeling that is used to develop the SFHA treats them as independent drivers, which may result in an inappropriate characterization of flood risk in some areas (Moftakhari et al., 2017). In another study where a high-resolution hydrodynamic model was developed for the entire conterminous United States using the well-accepted Height Above Nearest Drainage methodologies (Wing et al., 2017), it was found that the model matched up to 86% of the extent of the most current version of the SFHA, which employs higher-quality one-dimensional and two-dimensional hydraulic modeling tools and higher-resolution elevation data (down to 1 m) from the USGS National Elevation Dataset. Because of the improved performance of the SFHA in capturing areas that would be potentially impacted by a 100-year flood event and the fact that the SFHA is the only resource currently available within the LCRVR that provides an estimate of spatial flood inundation from an extreme flood event, the SFHA was assumed to provide a sufficiently accurate depiction of 100-year spatial flood inundation due to riverine and coastal events within the study region.

2.3. Logistic Regression

Logistic regression was implemented to develop a specific formula that measures the probability of flood inundation throughout the LCRVR during the 100-year flood event as defined in Figure 3. This is accomplished by designating several points throughout the LCRVR as testing points from which the logistic regression will be derived. Because of the large size of the LCRVR and in order to reduce the bias caused by one portion of the region on another part of the region, this was accomplished by first dividing the LCRVR into three separate subregions that represent urban, rural, and coastal environments (Figure 4). These subregions were selected based on land cover characteristics, particularly level of development, as depicted in Figure 2c; the relatively urban area of Middletown, CT, is observed in the northwest portion

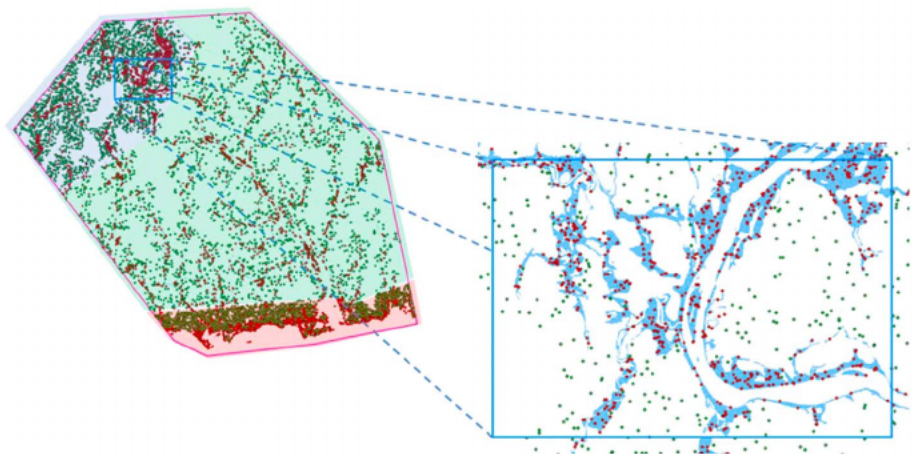


Figure 4. Map of the Lower Connecticut River Valley Region along with a zoomed-in area showing the distribution of sampling points used to train the logistic model. Green points represent locations where flooding did not occur, while red points represent locations where flooding did occur. Areas shaded in blue, green, and red, represent urban (U; blue), rural (R; green), and coastal (C; red) subregions, respectively.

of the region, while development can also be seen along the coast in the southern portion of the region; the remainder of the region is predominantly rural. A total of 4,000 points was randomly chosen from each subregion with the stipulation that an equal number of those points (2,000 per subregion) were within (green dots in Figure 4) or outside (red dots in Figure 4) of the FEMA 100-year SFHA. A total of 12,000 points, therefore, was chosen from which to extract flood inundation and flood risk factor data.

Flood data for all points consisted of either a 0 or a 1 to represent whether a location was not flooded or flooded, respectively; these values represented the dependent variable (L) in the logistic regression:

$$\ln\left(\frac{p}{1-p}\right) = L = a_0 + a_1x_1 + a_2x_2 + \dots + a_nx_n, \quad (1)$$

where p is the probability of flooding. All flood risk factor data at each location were categorized into classes according to the class ranges designated in Table 3 and represented the independent variables (x_1 to x_n ; $n = 9$) in equation (1). In some cases, the land cover, soil class, and/or surficial materials risk factors were classified as *open water* and/or the distance to water was equal to 0 even though the location was located outside of any particular body of water. This apparent artifact is attributable due to differences in the resolution of each data set, which can cause a slight shift in the boundaries of water bodies when the data sets are processed (*snapped* and *clipped*) within ArcGIS. The result is that extracted values from some layers will occur over open water, while extracted values from other layers will occur over the land that is adjacent to the same body of water. These points were justifiably eliminated from the analysis, which resulted in the total number of points being utilized in the urban, rural, and coastal subregional data sets, respectively, to be 3,815; 3,708; and 3,776. The independent and dependent variables were then analyzed using the function `glm(..., family = binomial)` in R to determine the regression intercept (a_0) and the coefficients (a_1 to a_n ; $n = 9$) for each flood risk factor in equation (1).

The final step in the development of the logistic model for flood susceptibility is to estimate the model's goodness of fit. One common method that works well for binary data is the Hosmer-Lemeshow (H-L) goodness of fit test (Hosmer et al., 2013). The H-L test computes a test statistic that compares the predicted values of the model with observations and that approximately follows a chi-square distribution. The resulting p value is then computed as the right-hand tail probability of the distribution. A low p value (<0.05) suggests that the model fit is poor, while a high p value suggests that the null hypothesis that there is no relation between flooding and the flood risk factors can be rejected. Refer to Hosmer et al. (2013) for more details on the H-L test. The H-L test was implemented in R using the `hoslem.test` function.

After the coefficients of the logistic regressions are determined for each flood risk factor class, the probability of flooding at each grid cell is calculated from the first two members of equation (1) using the following equation:

$$p = \frac{e^L}{(1+e^L)}, \quad (2)$$

which is used to create the final flood risk map. It should be noted that all flood risk factors are used but that for each flood risk factor only one coefficient is used that corresponds to the appropriate factor class (see Table 3) at each map grid cell.

2.4. Critical Infrastructure

The final step in the development of the flood susceptibility map involves identifying locations with vulnerable critical infrastructure, which included the following:

- dams;
- military compounds;
- airports;
- hospitals and other health-related facilities;
- fire and police stations;
- emergency operations centers;

Table 4
Critical Infrastructure Data Sets Used in the Current Study With Data Source and URL

Infrastructure	Source (year)	URL for data access
Airports	DEEP (2005)	https://www.ct.gov/deep
Bridges	National Bridge Inventory (Federal Highway Administration, 2016)	https://www.arcgis.com/home/item.html?id=775f08232eb1424189a4e8091edf893e
Dams	DEEP (1996)	https://www.ct.gov/deep
EOCs	RiverCOG (2017)	https://www.rivercog.org
Fire and police stations	RiverCOG (2017)	https://www.rivercog.org
Health	USDHHS (2012)	https://maps3.arcgisonline.com/ArcGIS/rest/services/A-6/HHS_IOM_Health_Resources/MapServer/
Land use and zoning	RiverCOG (2017)	https://www.rivercog.org
Military	MAGIC (2010)	https://magic.lib.uconn.edu/connecticut_data.html
Railroads	DEEP (2005)	https://www.ct.gov/deep
Routes	DEEP (2006)	https://www.ct.gov/deep
Schools	RiverCOG (2017)	https://www.rivercog.org
Town halls	RiverCOG (2017)	https://www.rivercog.org

Note. DEEP = Connecticut Department of Energy and Environmental Protection; NBI = National Bridge Inventory; FHWA = Federal Highway Administration; EOC = Emergency Operations Center; RiverCOG = The Lower Connecticut River Valley Council of Governments; USDHHS = U.S. Department of Health and Human Services; MAGIC = University of Connecticut Libraries' Map and Geographic Information Center.

- private and public K–12 schools;
- town halls;
- major routes;
- bridges; and
- railroads.

Data sets and sources related to critical infrastructure throughout the LCRVR and that were used in the current study are given in Table 4. All critical infrastructure data sets were clipped to the boundaries of the LCRVR and overlaid onto the final flood susceptibility map.

3. Results

3.1. Flood Risk

The coefficients from the logistic regression are listed in Table 3 for each class of each flood risk factor over the three subregions; the greater the magnitude of the coefficient, the stronger the impact of that risk factor class on flood inundation in the LCRVR. The p values computed for the logistic models in the coastal, rural, and urban subregions using the H-L test were approximately 0.76, < 0.01, and 0.60. Because of their high p values, there is no evidence of poor fit within the coastal and urban subregions, which are the two areas of highest concern in the LCRVR due to their relatively high population densities. The fit is much less reliable for the more sparsely populated rural subregion. The low p value indicates that the rural subregion is sufficiently large so that there is substantial variation in the relationship of each flood risk factor to flood inundation throughout its area.

In order to make a simple comparison of the results between subregions, especially due to the high variation in the relationships of the flood risk factors to flood inundation in the rural subregion, the regression coefficients for all flood risk factors were averaged for each subregion, the results of which are shown in Figure 5a. There are initially three flood risk factors that stand out as having a dominant correlation with flood susceptibility throughout the LCRVR: elevation (ELEV), distance to water (DIST), and surficial materials (GEO). Elevation has the most influence on flood susceptibility in the urban and coastal subregions because of the fact that both subregions are dominated by lower elevations, whereas elevation has less influence within the rural subregion where substantially higher elevations dominate. Distance to water has a large influence on flood susceptibility in all subregions because of the number of water bodies located throughout the LCRVR, which include a myriad of small lakes, ponds, and tributaries, in addition to the Connecticut River and Long Island Sound. Surficial materials has greater influence on flood susceptibility in the rural subregion and coastal subregions where much

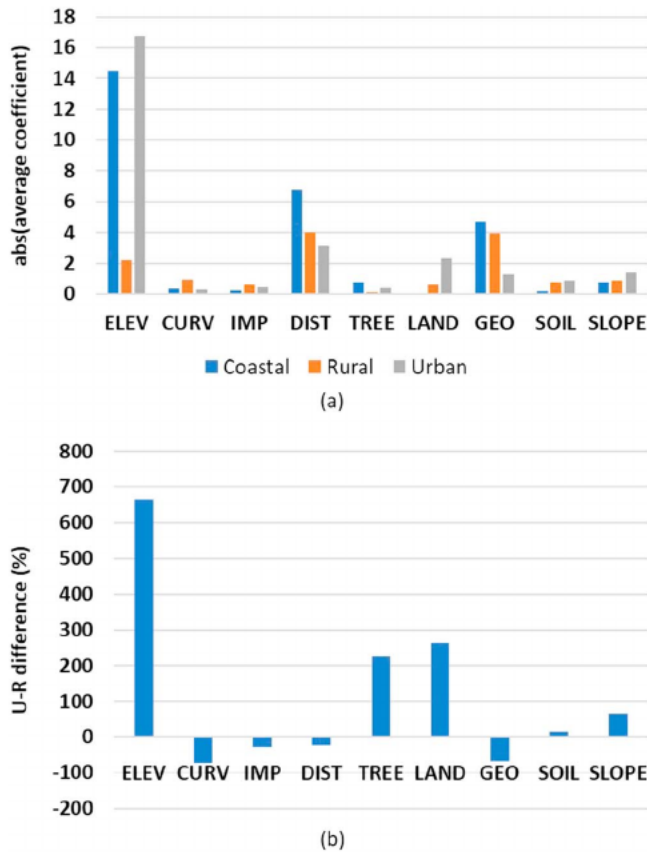


Figure 5. (a) Average absolute value of the logistic regression coefficients computed for each flood risk factor for the coastal (blue), rural (orange), and urban (gray) subregions, and (b) the percent difference between the urban (U) and rural (R) coefficients for each flood risk factor.

of the materials deposited from previous flood events are still present, whereas these same materials have likely been removed within the more urban Middletown area as development has occurred. To get an idea of additional impacts or sensitivity of urbanization on the contribution of each flood risk factor, Figure 5b shows a plot of the percent change in the contribution of each flood risk factor between the urban and rural subregions. Two flood risk factors stand out as having the largest impact: elevation (already discussed) and land cover. Assuming that elevation within the urban subregion has not changed substantially due to urbanization and that any differences in the contribution of elevation between the subregions can be attributed to natural differences in topographic features, Figure 5b shows that recent changes in land cover have had the most impact on changes in flooding behavior between the rural and urban subregions.

The results of the logistic regression for the initial set of data points were then applied to all map grid cells in the LCRVR to produce a flood susceptibility map for the entire region applicable to the 100-year flood event (Figure 6a). Flood susceptibility values are plotted as the percent chance that each 30-m × 30-m grid cell will be inundated and then classified into five categories according to the color scale shown in the figure: *very low risk* (0–20%), *low risk* (20–40%), *medium risk* (40–60%), *high risk* (60–80%), and *very high risk* (80–100%). The largest areas of *very high* and *high* risk are located along the Connecticut River and its major tributaries as well as along the coast. There are also several isolated areas of high susceptibility associated with smaller streams and creeks.

Finally, it is observed that when looking at the transitions between the different subregions, particularly between the coastal and rural subregions, the values are not continuous and there is a slight difference

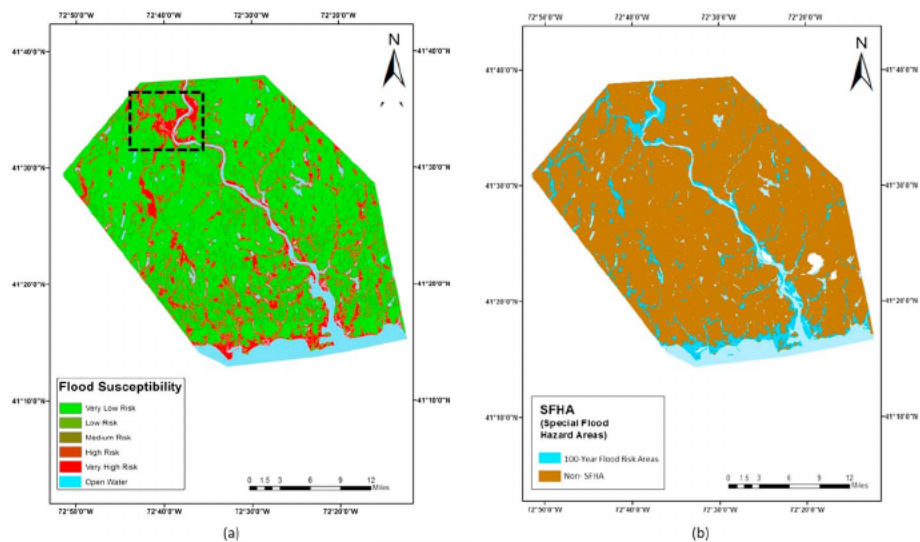


Figure 6. Flood susceptibility map for the Lower Connecticut River Valley Region for the Federal Emergency Management Agency 100-year flood event. Levels represent probabilities of flooding: *very low*: 0–20%; *low*: 20–40%; *medium*: 40–60%; *high*: 60–80%; *very high*: 80–100%. Dashed box (inset) shown in Figure 7. (b) The map showing the spatial extent of the SFHA is repeated for comparison purposes.

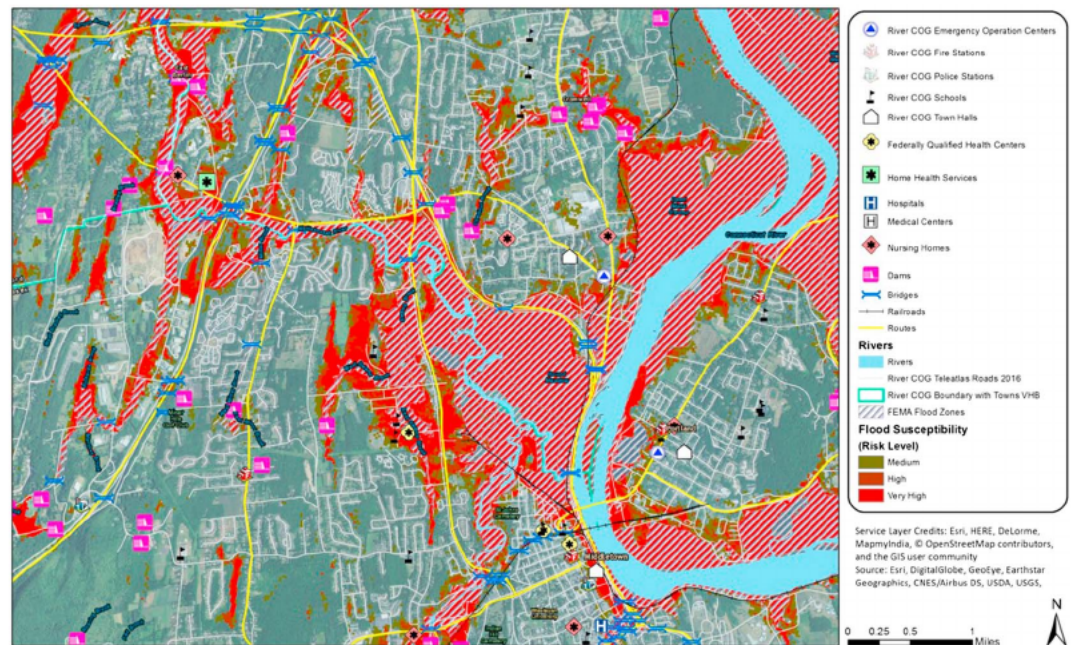


Figure 7. Locations of various vulnerable critical infrastructure relative to areas of *medium* (dark green), *high* (dark red), and *very high* (red) flood susceptibility; map is zoomed in on the city of Middletown, CT, and surrounding area (dashed box in Figure 6). The 100-year FEMA Special Flood Hazard Area (hatched) is also included for reference and comparison. USDA = U.S. Department of Agriculture; USGS = U.S. Geological Survey; COG = Council of Governments; FEMA = Federal Emergency Management Agency; CNES = Centre National d'Etudes Spatiales.

across the subregion boundary. This difference is a statistical artifact of splitting the region into three subregions and computing different values for the coefficients of each flood risk factor class; for example, the rural and urban sets of factor coefficients listed in Table 3 were used to separately compute the flood susceptibility maps for the rural and coastal zones, respectively. The result is a small discontinuity between the subregions, albeit this discontinuity seems to manifest itself more in the lower susceptibility categories as opposed to the areas of very high susceptibility risk. If the entire LCRVR was analyzed as one subregion, these discontinuities would disappear, but the results would include a substantial bias from the urban subregion in determining flood susceptibility in the coastal subregion, which would likely produce inaccuracies that are much more substantial than the current discontinuities. The only other way to eliminate these discontinuities would be to use a sufficient number of subregions so that the discontinuities between each are minimal, which is unrealistic, and the choice of how subregions were chosen would be difficult to defend.

When comparing the susceptibility map to the map of the FEMA 100-year SFHA (repeated in Figure 6b for comparisons purposes), it is important to understand key distinctions between the two. The FEMA 100-year SFHA is limited to the subwatersheds of $>2.59\text{ km}^2$. Other limiting issues with the FEMA 100-year SFHA are (1) the age of the underlying studies (often more than two decades old) and (2) their focus on only areas where development either already existed or was imminently to be and so was then anticipated. By using the statistical modeling described herein it was possible to identify the contribution of flood risk factors within the existing FEMA 100-year SFHA and apply such factors to the entire study region to identify additional areas outside of the FEMA flood hazard area that are susceptible to inundation by a flood event having a 1% chance of occurring in any given year. It should be noted that there also were areas (not shown) within the SFHA that were not identified as very high or high susceptibility in the present analysis because of the fact that values of the dominant flood risk factors in these locations are different than those identified throughout the remainder of the SFHA.

Geographical Information System spatial analyses were made to compare the susceptibility mapping to FEMA's SFHA map using the University of Connecticut's Center for Land, Education, and Research 2010 Land Cover 30-m data set (Center for Land Use Education and Research Land Cover, College of Agriculture and Natural Resources, University of Connecticut, 2010). Twenty-five percent of the region's FEMA mapped

flood zones are developed, which represents approximately 8% of the overall developed area in the region. When subtracting waterbodies and wetlands at the areas designated as very high, high, or *medium*, an additional 115 km² are added to areas identified as susceptible. In the very high and high classified areas only, this previously unidentified susceptible acreage adds greater than 6% of the region's nonwater and wetland area to a flood susceptibility zone, including an additional 8% of the region's developed area.

One important disclaimer about the flood susceptibility map is that it was created for present-day conditions and is only to be used for increasing engineering and stakeholder awareness; it is not intended to replace the FEMA mapping for regulatory or flood insurance decisions. It should also be noted that the scale of the flood susceptibility map and data are most appropriately used at the regional scale. However, use of the data at the municipal scale should allow local stakeholders to examine areas of special concern for planning purposes.

3.2. Critical Infrastructure

Data sets for several types of critical infrastructure (listed in Table 4) were obtained and overlaid onto the final flood susceptibility map for the LCRVR. An area surrounding and including the City of Middletown, Connecticut, was chosen for further scrutiny because of the presence of a large very high susceptibility zone (Figure 7). Several dams, bridges, and a large portion of the major routes and railroad in the Middletown vicinity are included within the high and very high susceptibility areas of 100-year flood inundation. It is also concluded that there are some areas identified as having medium to very high flood susceptibility to the 100-year flood that were not included in the FEMA 100-year SFHA. These differences exist primarily in an area on the west and south sides of Middletown—as can be seen in Figure 7 by the red and dark green shaded areas that are located outside of the hatched areas. These differences could have a major impact on the perceived vulnerability of critical infrastructure located in these areas.

4. Conclusions

The current study estimated flood susceptibility in the LCRVR attributable to nonclimatic factors using a method that involved performing a logistic regression for three subregions (urban, rural, and coastal) to determine the relations between several flood risk factors and flood inundation at the 100-year return period, which was defined by the FEMA 100-year SFHA, in each subregion. It was found that elevation and distance to water have the most influence on flood susceptibility in the urban and coastal subregions, while distance to water and surficial materials have the greatest influence in the rural subregion. It was also determined that urbanization has had the most influence on the contribution of land cover to 100-year flood susceptibility when compared to the rural subregion; development within the urban subregion has increased the contribution of *land use* by over 200%. The difference in the contribution of elevation to flood susceptibility between the urban and rural subregions was greater than that for land use, but it is assumed that this is likely not because of urbanization but rather attributable to natural differences in topographic features between the two subregions. Because there is still sufficient room for continued growth and development within the urban subregion, future significant increases in the effects of changing land cover on flood susceptibility in the area are possible.

The logistic regression equation was then used to create an overall flood susceptibility map for each subregion of the LCRVR onto which various types of critical infrastructure and regional existing land use and zoning data were overlaid. Differences between the 100-year susceptibility map developed here and the FEMA 100-year SFHA were observed. Most importantly, developed residential and commercial areas within the region fall within the medium to very high flood susceptibility (hot spot) areas beyond what is designated as the FEMA 100-year SFHA. Although the regional data is not at a scale large enough for local determinations, these hot spot areas warrant further consideration for future localized flood susceptibility mapping if future suitable data sets become available and further consideration at the municipal planning level.

One important disclaimer about the flood susceptibility map is that it was created for present-day conditions and is only to be used for planning purposes. There are several prominent factors that could affect the future flood susceptibility map: changes in impervious area (through urbanization), a higher sea level (for coastal areas), and changes in climatic factors (e.g., heavier precipitation). A future flood susceptibility map can be created by studying how each of these types of factors are expected to change. However, it is expected that the present-day flood susceptibility map provides an excellent relative foundation from which to consider future changes.

Acknowledgments

This work was funded by the U.S. Department of Housing and Urban Development (HUD) Community Development Block Grant—Disaster Recovery (CDBG-DR) Program—Federal grant B-13-DS-09-0001 and administered by the Connecticut Department of Housing (DOH)—grant 6202. Additional funding was obtained through a subaward agreement with the University of Connecticut’s (UConn) Institute for Resilience and Climate Adaption (CIRCA)—grant PO#43280 and the Connecticut Department of Energy and Environmental Protection (DEEP)—grant P5#2014-14249. The contents of this article are solely the responsibility of the authors and do not necessarily represent the official views of University of Connecticut or Connecticut Department of Energy and Environmental Protection. All data used in the current study can be found at the URLs provided in the tables and list of references.

References

Abbott, M. B., Bathrust, J. C., Cunge, J. A., O’Connell, P. E., & Rasmussen, J. (1986). An introduction to the European Hydrological System—Systeme Hydrologique Europeen, “SHE”, 2: Structure of a physically-based, distributed modeling system. *Journal of Hydrology*, *87*(1-2), 61–77. [https://doi.org/10.1016/0022-1694\(86\)90115-0](https://doi.org/10.1016/0022-1694(86)90115-0)

Allaire, M. C., Vogel, R. M., & Kroll, C. N. (2015). The hydromorphology of an urbanizing watershed using multivariate elasticity. *Advances in Water Resources*, *86*, 147–154. <https://doi.org/10.1016/j.advwatres.2015.09.022>

Blessing, R., Sebastian, A., & Brody, S. D. (2017). Flood risk delineation in the United States: How much loss are we capturing? *Natural Hazards Review*, *18*(3), 04017002. [https://doi.org/10.1061/\(ASCE\)NH.1527-6996.0000242](https://doi.org/10.1061/(ASCE)NH.1527-6996.0000242)

Center for Land Use Education and Research Land Cover, College of Agriculture and Natural Resources, University of Connecticut. (2010). Land cover 30-m data set. Location. Retrieved from <https://clear.uconn.edu/projects/landscapeLIS/landcover.htm>

Crawford, N. H., & Linsley, R. K. (1966). Digital simulation in hydrology: Stanford Watershed Model IV. (Tech. Rep. 39, p. 210). Stanford, CA: Department of Civil Engineering, Stanford University.

Connecticut Department of Energy and Environmental Protection. (1996). Connecticut GIS datasets. Location. Retrieved from https://www.ct.gov/deep/cwp/view.asp?a=2698&q=322898&deepNav_GID=1707

Connecticut Department of Energy and Environmental Protection. (2005). Connecticut GIS datasets. Location. Retrieved from https://www.ct.gov/deep/cwp/view.asp?a=2698&q=322898&deepNav_GID=1707

Connecticut Department of Energy and Environmental Protection. (2006). Connecticut GIS datasets. Location. Retrieved from https://www.ct.gov/deep/cwp/view.asp?a=2698&q=322898&deepNav_GID=1707

Dawson, C. W., & Wilby, R. L. (2001). Hydrological modelling using artificial neural networks. *Progress in Physical Geography: Earth and Environment*, *25*(1), 80–108. <https://doi.org/10.1177/030913330102500104>

Devi, G. K., Ganasri, B. P., & Dwarakish, G. S. (2015). A review on hydrological models. *Aquatic Procedia*, *4*, 1001–1007. <https://doi.org/10.1016/j.aapro.2015.02.126>

Doocy, S., Daniels, A., Murray, S., & Kirsch, T. D. (2013). The human impact of floods: A historical review of events 1980–2009 and systematic literature review. *PLOS Currents Disasters*, *1*, 29. <https://doi.org/10.1371/currents.dis.f4deb457904936b07c09daa98ee8171a>

Environmental Systems Research Institute. (2014). ArcGIS desktop: Release 10.2.2. Redlands, CA: Environmental Systems Research Institute.

Federal Emergency Management Agency. (2016). FEMA GeoPlatform, National Flood Hazard Layer (NFHL). Location. Retrieved from <https://fema.maps.arcgis.com/home/index.html>

FHWA (Federal Highway Administration). (2016). National Bridge Inventory (NBI) bridges dataset. Location. Retrieved from <https://www.arcgis.com/home/item.html?id=94c41e96db0d4b85b9eb622923e0a0e8>

Gassman, P. W., Reyes, M. R., Green, C. H., & Arnold, J. G. (2007). The soil and water assessment tool: Historical development, applications, and future research directions. *Transactions of the American Society of Agricultural and Biological Engineers*, *50*, 1211–1250.

Gogoi, S., & Chetia, B. C. (2011). Fuzzy rule-based flood forecasting model of Jialhal River basin, Dhemaji, Assam, India. *International Journal of Fuzzy Mathematical Systems*, *1*, 59–71.

Hosmer, D. W., Lemeshow, S., & Sturdivant, R. X. (2013). *Applied logistic regression*. New York: John Wiley. <https://doi.org/10.1002/9781118548387>

Hundecha, Y., Bardossy, A., & Theisen, H.-W. (2001). Development of a fuzzy logic-based rainfall-runoff model. *Journal des Sciences Hydrologiques*, *46*(3), 363–376. <https://doi.org/10.1080/02626660109492832>

Kia, M. B., Pirasteh, S., Pradhan, B., Mahmud, A. R., Sulaiman, W. N. A., & Moradi, A. (2012). An artificial neural network model for flood simulation using GIS: Johor River Basin, Malaysia. *Environmental Earth Sciences*, *67*(1), 251–264. <https://doi.org/10.1007/s12665-011-1504-z>

Kovacevic, M., Ivanisevic, N., Dasic, T., & Markovic, L. (2018). Application of artificial neural networks for hydrological modelling in karst. *Gradjevinar*, *70*(1), 1–10. <https://doi.org/10.14256/JCE.1594.2016>

Lawal, D., Matori, A., Hashim, A., Yusof, K., & Chandio, I. (2012). Detecting flood susceptible areas using GIS-based analytic hierarchy process. In *Proceedings of the International Conference on Future Environment and Energy* (Vol. 28, pp. 1–5). Singapore: IACSIT Press.

Lee, M. J., Kang, J. E., & Jeon, S. (2012). Application of frequency ratio model and validation for predictive flooded area susceptibility mapping using GIS. In *IEEE International Geoscience and Remote Sensing Symposium (IGARSS)* (pp. 895–898). Munich, Germany: Institute of Electrical and Electronics Engineers. <https://doi.org/10.1109/IGARSS.2012.6351414>

Li, H., Lei, X., Shang, Y., & Qin, T. (2018). Flash flood early warning research in China. *International Journal of Water Resources Development*, *34*(3), 369–385. <https://doi.org/10.1080/07900627.2018.1435409>

Lopez, M. G., Baldassarre, G. D., & Seibert, J. (2017). Impact of social preparedness on flood early warning systems. *Water Resources Research*, *53*, 522–534. <https://doi.org/10.1002/2016WR019387>

Mahmoud, S. H., & Gan, T. Y. (2018). Urbanization and climate change implications in flood risk management: Developing an efficient decision support system for flood susceptibility mapping. *Science of the Total Environment*, *636*, 152–167. <https://doi.org/10.1016/j.scitotenv.2018.04.282>

Matori, A. N., Lawal, D. U., Yusof, K. W., Hashim, M. A., & Balogun, A.-L. (2014). Spatial analytic hierarchy process model for flood forecasting: An integrated approach. *IOP Conference Series: Earth and Environmental Science*, *20*, 012029. <https://doi.org/10.1088/1755-1315/20/1/012029>

Miller, J. D., & Hutchins, M. (2017). The impacts of urbanisation and climate change on urban flooding and urban water quality: A review of the evidence concerning the United Kingdom. *Journal of Hydrology: Regional Studies*, *12*, 345–362. <https://doi.org/10.1016/j.ejrh.2017.06.006>

Moftakhari, H. R., Salvadori, G., AghaKouchak, A., Sanders, B. F., & Matthew, R. A. (2017). Compounding effects of sea level rise and fluvial flooding. *Proceedings of the National Academy of Sciences of the United States*, *114*, 9785–9790.

Papadopoulou-Vrynioti, K., Bathrellos, G. D., Skilodimou, H. D., Kaviris, G., & Makropoulos, K. (2013). Karst collapse susceptibility mapping considering peak ground acceleration in a rapidly growing urban area. *Engineering Geology*, *158*, 77–88. <https://doi.org/10.1016/j.enggeo.2013.02.009>

Park, S., Hamm, S.-Y., Jeon, H.-T., & Kim, J. (2017). Evaluation of logistic regression and multivariate adaptive regression spline models for groundwater potential mapping using R and GIS. *Sustainability*, *9*(7), 1157–1176. <https://doi.org/10.3390/su9071157>

Peterson, T. C., Heim, R. R. Jr., Hirsch, R. M., Kaiser, D. P., Brooks, H., Dickenbaugh, N. S., et al. (2013). Monitoring and understanding changes in heat waves, cold waves, floods and droughts in the United States: State of knowledge. *Bulletin of the American Meteorological Society*, *94*(6), 821–834. <https://doi.org/10.1175/BAMS-D-12-00066.2>

Pradhan, B., & Lee, S. (2010). Delineation of landslide hazard areas on Penang Island, Malaysia, by using frequency ratio, logistic regression, and artificial neural network models. *Environmental Earth Sciences*, *60*(5), 1037–1054. <https://doi.org/10.1007/s12665-009-0245-8>

- Qureshi, M., & Harrison, S. (2003). Application of the analytic hierarchy process to riparian revegetation policy options. *Small-Scale Forest Economics, Management and Policy*, 2(3), 441–458. <https://doi.org/10.1007/s11842-003-0030-6>
- R Development Core Team (2018). *R: A language and environment for statistical computing*. R Foundation for Statistical Computing, Vienna, Austria. Retrieved from <https://www.R-project.org/>
- Rahman, M. M., Goel, N. K., & Arya, D. S. (2013). Study of early flood warning dissemination system in Bangladesh. *Journal of Flood Risk Management*, 6(4), 290–301. <https://doi.org/10.1111/jfr3.12012>
- Richardson, C. P., & Amankwatia, K. (2018). GIS-based analytic hierarchy process approach to watershed vulnerability in Bernalillo County, New Mexico. *Journal of Hydrologic Engineering*, 23(5), 04018010. [https://doi.org/10.1061/\(ASCE\)HE.1943-5584.0001638](https://doi.org/10.1061/(ASCE)HE.1943-5584.0001638)
- RiverCOG (The Lower Connecticut River Valley Council of Governments). (2017). Lower Connecticut River Valley Region critical infrastructure dataset. Location. Retrieved from <https://www.rivercog.org>
- Saini, S. S., & Kaushik, S. P. (2012). Risk and vulnerability assessment of flood hazard in part of Ghaggar basin: A case study of Guhla block, Kaithal, Haryana, India. *International Journal of Geomatics and Geosciences*, 3, 10.
- Sen, Z., & Altunkaynak, A. (2004). Fuzzy awakening in rainfall-runoff modeling. *Hydrology Research*, 35(1), 31–43. <https://doi.org/10.2166/nh.2004.0003>
- Sharma, S. K., Gajbhiye, S., & Tignath, S. (2015). Application of principal component analysis in grouping geomorphic parameters of a watershed for hydrological modeling. *Applied Water Science*, 5(1), 89–96. <https://doi.org/10.1007/s13201-014-0170-1>
- Shortridge, J. E., Guikema, S. D., & Zaitchik, B. F. (2016). Machine learning methods for empirical streamflow simulation: A comparison of model accuracy, interpretability, and uncertainty in seasonal watersheds. *Hydrology and Earth System Sciences*, 20(7), 2611–2628. <https://doi.org/10.5194/hess-20-2611-2016>
- Siddayao, G. P., Valdez, S. E., & Fernandez, P. L. (2014). Analytic hierarchy process (AHP) in spatial modeling for floodplain risk assessment. *International Journal of Machine Learning and Computing*, 4(5), 450–457. <https://doi.org/10.7763/IJMLC.2014.V4.453>
- Singh, P. K., Kumar, V., Purohit, R. C., Kothari, M., & Dashora, P. K. (2009). Application of principal component analysis in grouping geomorphic parameters for hydrologic modeling. *Water Resources Management*, 23(2), 325–339. <https://doi.org/10.1007/s11269-008-9277-1>
- Sinha, R., Bapalu, G. V., Singh, L. K., & Rath, B. (2008). Flood risk analysis in the Kosi River Basin, North Bihar using multi-parametric approach of analytical hierarchy process (AHP). *Journal of the Indian Society of Remote Sensing*, 36(4), 335–349. <https://doi.org/10.1007/s12524-008-0034-y>
- Tehrany, M. S., Lee, M.-J., Pradhan, B., Jebur, M. N., & Lee, S. (2014). Flood susceptibility mapping using integrated bivariate and multivariate statistical models. *Environmental Earth Sciences*, 72(10), 4001–4015. <https://doi.org/10.1007/s12665-014-3289-3>
- Ullah, N., & Choudhury, P. (2013). Flood flow modeling in a river system using adaptive neuro-fuzzy inference system. *Environmental Management and Sustainable Development*, 2(2), 54–68. <https://doi.org/10.5296/emsd.v2i2.3738>
- Umar, Z., Pradhan, B., Ahmad, A., Jebur, M. N., & Tehrany, M. S. (2014). Earthquake induced landslide susceptibility mapping using an integrated ensemble frequency ratio and logistic regression models in West Sumatera Province, Indonesia. *Catena*, 118, 124–135. <https://doi.org/10.1016/j.catena.2014.02.005>
- United States Department of Agriculture-Natural Resources Conservation Service. (2017). Soil data access. Location. Retrieved from <https://sdmdataaccess.nrcs.usda.gov/>
- United States Department of Health and Human Services. (2012). Healthcare facilities dataset. Location. Retrieved from https://maps3.arcgisonline.com/ArcGIS/rest/services/A-16/HHS_IOM_Health_Resources/MapServer/
- University of Connecticut Libraries' Map And Geographic Information Center. (2010). Connecticut GIS data, Connecticut military installations. Location. Retrieved from https://magic.lib.uconn.edu/connecticut_data.html
- U.S. Geological Survey. (2011). National Land Cover Database (NLCD). Location. Retrieved from <https://www.mrlc.gov/>
- U.S. Geological Survey. (2014). EarthExplorer elevation dataset. Location. Retrieved from <https://earthexplorer.usgs.gov/>
- Wallis, J. R. (1965). Multivariate statistical methods in hydrology—A comparison using data of known functional relationship. *Water Resources Research*, 1(4), 447–461. <https://doi.org/10.1029/WR001i004p00447>
- Wing, O. E. J., Bates, P. D., Sampson, C. C., Smith, A. M., Johnson, K. A., & Erickson, T. A. (2017). Validation of a 30 m resolution flood hazard model of the conterminous United States. *Water Resources Research*, 53, 7968–7986. <https://doi.org/10.1002/2017WR020917>
- Yahaya, S., Ahmad, N., & Abdalla, R. F. (2010). Multicriteria analysis for flood vulnerable areas in Hadejia-Jama'are River Basin, Nigeria. *European Journal of Scientific Research*, 42, 71–83.
- Yaseen, Z. M., Ramal, M. M., Diop, L., Jaafar, O., Demir, V., & Kisi, O. (2018). Hybrid adaptive neuro-fuzzy models for water quality index estimation. *Water Resources Management*, 32(7), 2227–2245. <https://doi.org/10.1007/s11269-018-1915-7>
- Zhang, H., Zhang, J., & Han, J. (2005). The assessment and regionalization of flood/waterlogging disaster risk in middle and lower reaches of Liao River of Northeast China. In *Proceedings of the Fifth Annual IIASA-DPRI Forum on Integrated Disaster Risk Management* (pp. 103–118). Beijing, China: IIASA-DPRI.
- Zhu, T., Lund, J. R., Jenkins, M. W., Marques, G. F., & Ritzema, R. S. (2007). Climate change, urbanization, and optimal long-term floodplain protection. *Water Resources Research*, 43, W06421. <https://doi.org/10.1029/2004WR003516>
- Zounemat-Kermani, M., & Teshnehlab, M. (2008). Using adaptive neuro-fuzzy inference system for hydrological time series prediction. *Applied Soft Computing*, 8(2), 928–936. <https://doi.org/10.1016/j.asoc.2007.07.011>